# Oceana Gold NZ Limited

## FY2023 Hydrogeology Support for WUG

**December 12, 2024**

Prepared by:
FloSolutions S.A.S.
Calle La Pinta E5-38, Ed. Royal Pacific
Oficina 801
Quito, Pichincha

## Numerical Groundwater Model



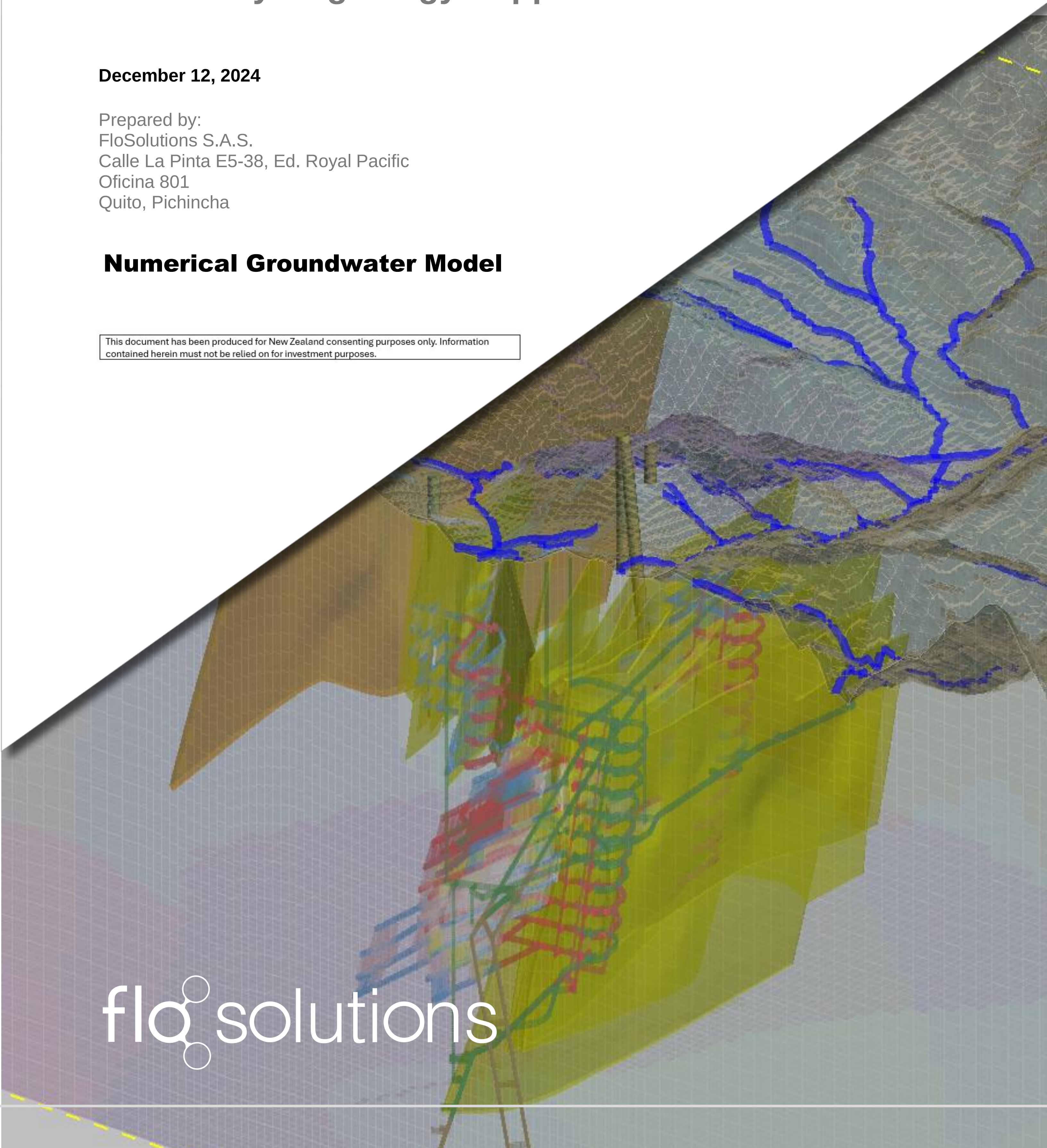

| | |
|---|---|
| Project: | Oceana Gold NZ Limited |
| Subject: | FY2023 Hydrogeology Support for WUG |
| Date: | December 12, 2024 |
| Document Ref. FS: | 1022310402-R-02 |

## Client

| Name | Title |
|---|---|
| Euan Leslie | Project Manager |
| | |
| | |

## FloSolutions

| Name | Title |
|---|---|
| John Fortuna | Principal Hydrogeologist / Project Manager |
| Jean Cho | Principal Groundwater Modeler |
| Frederico Lemos | Senior Hydrogeologist / Senior Groundwater Modeler |

## Revision Status

| Review | Date | Description | Prepared by: | Reviewed by: | Approved by: |
|---|---|---|---|---|---|
| A | Sept 6, 2023 | Internal review | F.Lemos / J.Cho | J.Fortuna | |
| B | Sept 18, 2023 | Issued to client | F.Lemos / J.Cho | J.Fortuna | J. Fortuna |
| 0 | November 16, 2023 | Issued to client | F.Lemos / J.Cho | J.Fortuna | J. Fortuna |
| 1 | March 05,2024 | Issued to client | F.L. / J.Cho / V.R. | J.Fortuna | J. Fortuna |
| 2 | December 12, 2024 | Revised | | J. Fortuna | J. Fortuna |

# TABLE OF CONTENTS

## List of Figures

## List of Tables

## Appendices

# 1. INTRODUCTION

FloSolutions Ecuador S.A.S. (FloSolutions) was contracted by OGNZL in early 2021 for hydrogeology support services for the OGC Waihi North project, including the proposed Wharekirauponga Underground (WUG) project development. FloSolutions was engaged to evaluate potential interactions between proposed underground mine development and shallow groundwater and surface water, and to assist the project with technical support and further studies to support project development.

Substantial hydrogeological project work has been undertaken since late 2021 by OGNZL, GWS Limited (GWS), FloSolutions, and others – including field work (drilling, hydraulic testing, water level measurements, water quality sampling, etc.), data analysis and evaluation, conceptualization, and analytical and 3D numerical groundwater flow modeling. This work was undertaken to support groundwater effects assessment and to assess the potential for underground mine development at Wharekirauponga to impact surface water streams in the overlying catchments. These studies have greatly improved site conceptualization and understanding of the groundwater system and potential surface water - groundwater dynamics. The results of these studies were summarized in a comprehensive, updated conceptual site model (CSM) report prepared by (FloSolutions, 1022310402-R-01 - Hydrogeological Conceptual Model Report, 2023).

The updated CSM forms the basis for numerical groundwater modelling. This report presents the description of the model construction, calibration, and simulations. An introductory section with general concepts used for the numerical is also included in this document. Further information is contained in the CSM report.,

## 1.1 Project overview

The proposed WUG project is located north of Waihi, New Zealand, in the Coromandel Ranges. The orebody and proposed mine is situated beneath land administered by the Department of Conservation (DOC). Site access is limited, and minimizing disturbance to the surface environment is a critical consideration in obtaining landowner and regulatory approvals. As a result, only a small number of drilling pads has been permitted to date, which restricts the amount of hydrogeologic (and other) data that can be collected.

The Wharekirauponga orebody is a high-grade gold deposit hosted in steeply dipping quartz veins that were emplaced along a northeast-trending regional-scale fault structure. OGNZL proposes to develop an underground mine (WUG) to access the orebody, with an AVOCA bottom-up mining method. Due to difficulties associated with obtaining an Access Arrangement (AA) to develop mine infrastructure on DOC lands, an underground tunnel will be developed to access the mineralized vein system. The tunnel portal would be established on farmland to the south of Wharekirauponga near Waihi (where OGNZL currently has its operations), and advanced northwards approximately 6 km to access the orebody from underground. If the project is developed, mined ore would be transported via the tunnel back to existing Waihi facilities for processing.

## 1.2 Study objectives

Project consenting and approvals are overseen by the Waikato Regional Council. A key part of the project understanding in support of approval relates to the potential effects of mining development on groundwater resources. The groundwater effects assessment must consider mine inflows, groundwater drawdown, deep recharge, potential effects on shallow groundwater, potential impacts to streams (baseflow reduction), and related effects. To properly assess and model these effects, a comprehensive understanding of the site groundwater system(s) is required.

The purpose of modelling is to develop a tool that can be used to understand changes in groundwater conditions in response to mining and related stresses.

The main objective of numerical groundwater modelling is to produce a model that is a simplified yet accurate representation of the CSM, and can reasonably reproduce site conditions and processes, including recharge-discharge processes, water levels, and transient water level fluctuations in response to stresses. Additional modelling objectives include effects of drawdown due to mine dewatering on aquifer and surface water system, and particularly to investigate the effects of uncertainties on those processes (considering data is limited due to access limitations and thus hydrogeological knowledge and understanding is limited). Uncertainty analysis is crucial to ensure that impacts are not underestimated (Middlemis & Peeters, 2018).

The objective of this report is to summarize the numerical modelling process into a document that covers the main information used, the modelling approach, assumptions, results, and limitations.

## 1.3 Report contents

A groundwater model is a simplified representation of a groundwater system. Groundwater models can be classified as physical or mathematical. While a physical model replicates physical processes on a smaller scale (e.g.: sand tank) a mathematical model describes the physical processes and boundaries of a groundwater system using one or more governing equations.

A numerical model divides space and/or time into discrete pieces. Features of the governing equations and boundary conditions can be specified as varying over space and time. This enables a more complex, and potentially more realistic, representation of a groundwater system than could be achieved with an analytical model. (Barnett, et al., 2012)

The current document covers the key elements of a groundwater numerical model, as shown in Figure 1.1.

Figure 1.1: Example final model report schedule - modified after (Barnett, et al., 2012)

| *Item* | *Title* | *Description* |
|---|---|---|
| 1 | Report title | The title should reflect the model and project objectives rather than just the study location. |
| 2 | Executive summary | The detailed model report includes a brief executive-style report to summarise the major findings of the study for non-technical audiences. |
| 3 | Model objectives | The objectives state how the groundwater model will be used to address the project objectives and the target confidence level. |
| 4 | Conceptualisation | This section describes the current level of understanding of the aquifer system and how this is translated into a conceptual model to address the model objectives.<br>Include reference to a data inventory. |
| 5 | Model design | The model design section specifies the model confidence level and the technical details of the groundwater model such as spatial and temporal discretisation, parameter distributions, implementation of stresses and boundary conditions, and model code and software. |
| 6 | Model calibration | Summary of how model parameters are changed within predefined constraints to match observations. This requires a clear description of the parameterisation, objective function and constraints as well as the calibration methodology and sensitivity analysis. |
| 7 | Predictive modelling | Description of the use of the model to address the model objectives by exploring aquifer behaviour under different stresses. |
| 8 | Uncertainty analysis | Presentation of the uncertainty associated with the predictions, based on, at least, heuristic descriptions of measurement uncertainty associated with parameters, stresses and calibration targets and structural model uncertainty, associated with the conceptual and mathematical model. |
| 9 | Model limitations | States the limitations of data and code, the reliability of different outcomes of the model and how further data collection or research may improve reliability. |
| 10 | Conclusions and recommendations | Summary of model findings and recommendations for further analysis. |
| 11 | References | Full references of cited literature and data sources. |
| 12 | Appendices | Maps, graphs and tables containing detailed information on the model that is important to fully document the model. |

# 2. PROJECT DESCRIPTION

## 2.1 Overall project description

The Waihi North Project expects to extend the current Waihi life of mine plan for 8 more years. The current life-of-mine (LOM) is until 2030, and the new expansions will extend this date until 2038. The Waihi North project will include development of a new open pit (the Gladstone Open Pit) close to the Waihi township operations, and a new underground mine (the Wharekirauponga Underground Mine as known as WUG) located approximately 11km northwest of the current Processing Plant (Figure 2.1).

The proposed Gladstone Open Pit (GOP) will be located primarily on Gladstone Hill and part of Winner Hill, adjacent to the current Processing Plant and Martha Pit conveyor as presented in the Figure 2.2. The surrounding land consists of rolling farmland, pastures, and a small pine plantation. The Ohinemuri River is situated about 300 meters southwest of the GOP (OceanaGold, 2021).

The GOP will cover an area of approximately 18.7 hectares, with a depth of 95 meters and dimensions of 375 meters wide and 625 meters long. Conventional open pit mining methods will be employed. The GOP will be mined for around six years, after which it will be converted into a tailings storage facility. It's important to note that no tailings will be discharged in the GOP until production from the Martha Underground operation has ceased (OceanaGold, 2021).

The Au and Ag deposits extracted close to the Waihi city in Martha mine and the coming GOP mine are typical low-sulphidation adularia-sericite epithermal quartz veins related to north and northeast faults. The medium to sheerly dipping veins are distinguished by a height around 170 to 700 m, 200 to 2000 in length and normally widths from 1 to 5 m, but it has been observed widths up to 30 m locally. The principal gold bearing minerals are electrum and silver sulphides stablished within quartz veins (OceanaGold, 2020). Unlike the WUG project, these veins are hosted in andesite volcanic flows.

The existing Waihi Processing Plant will be enhanced to process up to 2.25 millions of tons per annum (MTPA) from up to 1.25 MTPA produced at the moment, which involves building a new tailings storage facility (TSF3), a new rock stack at the Northern Stockpile area, upgrading the existing Water Treatment Plant, and modifying the existing overland and load out conveyors to allow waste rock loading and transport to the Northern Rock Stack (OceanaGold, 2021).

The Martha project, will keep working in parallel until 2030, and the Waihi North Project will use some of the existing infrastructure as tailings storage facilities, roads, entrance, parking area, existing core sheds and administration offices among others (OceanaGold, 2021).

Figure 2.1: Site arrangement and Wharekirauponga mine area (OceanaGold, 2021).

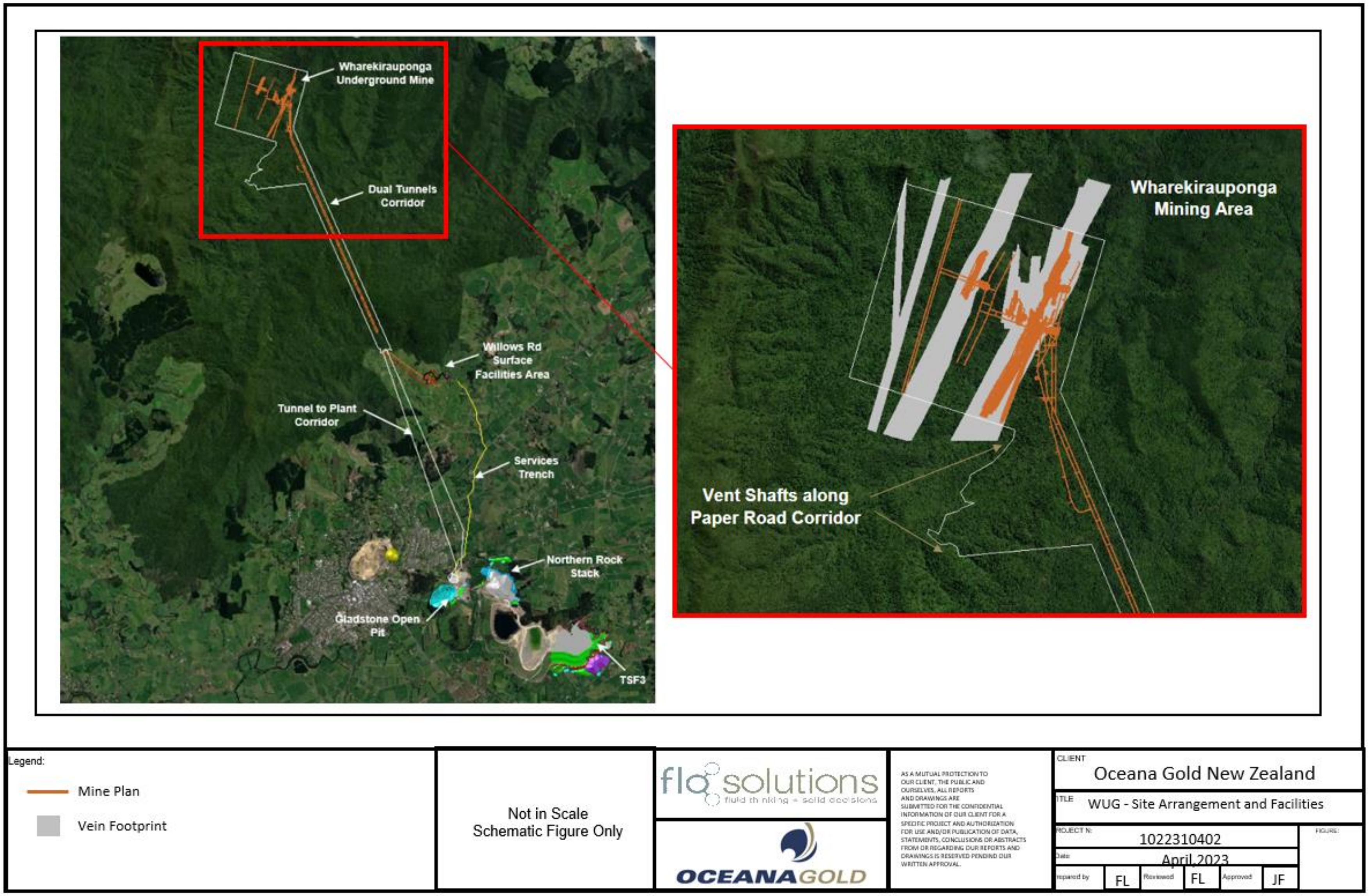

Figure 2.2: Gladstone Open Pit Project (OceanaGold, 2021)

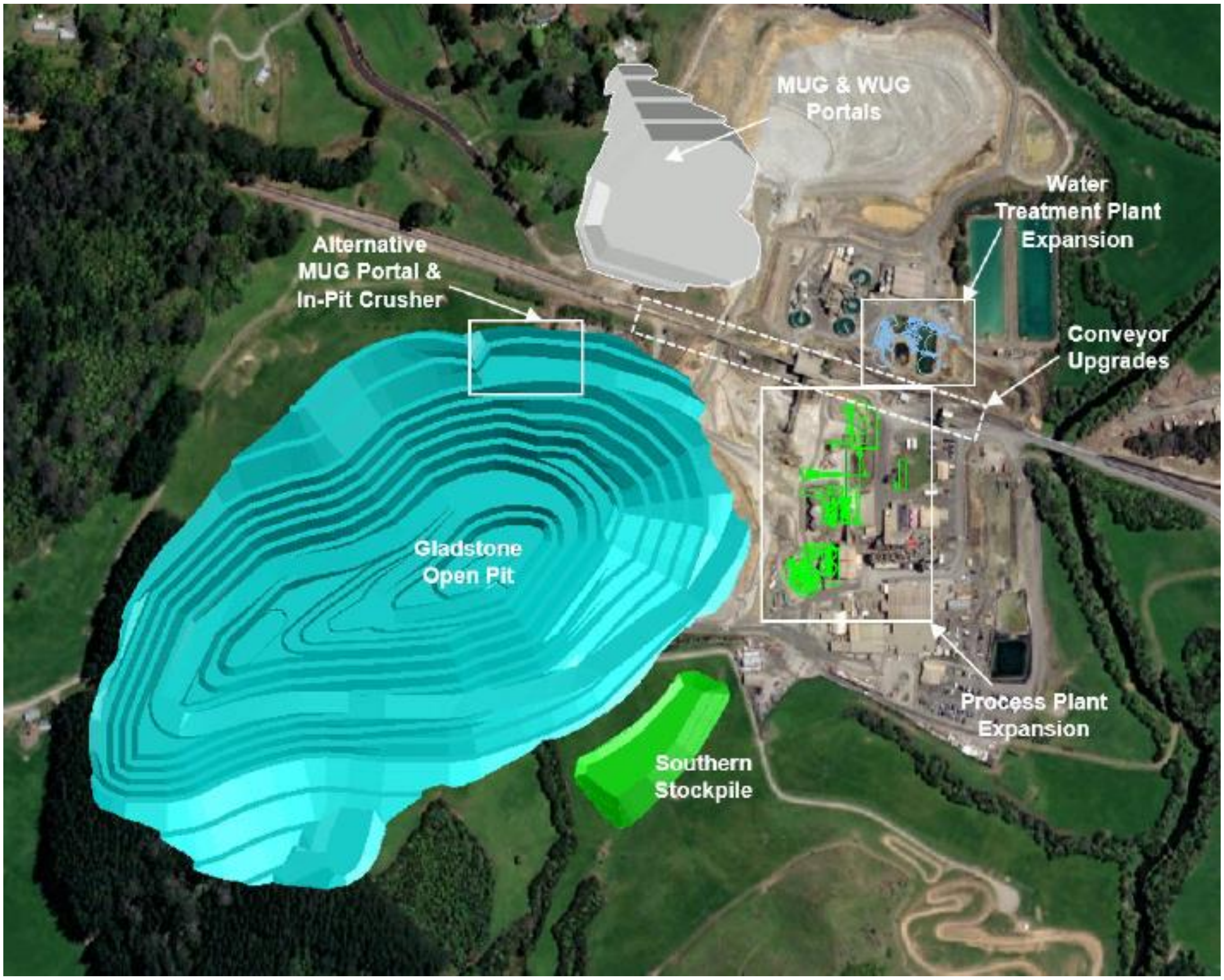


## 2.2 Local project description (WUG)

The WUG orebody is located 10 km north of Waihi town (Figure 2.1). Due to the sensitivity of the DOC lands two long tunnels have been planned by OGZNL to access the orebody. The tunnels will advance from the Willows Road Surface Facilities Area located outside of DOC lands and be used as the main access for the mine. The current design includes tunnels with dimensions of 6 m high and 5.8 m wide. A ventilation shaft located at the Willows Road property is planned to serve to remove exhaust during tunnel construction and later, as an air intake during mining operations. Additional ventilation shafts will be built inside the DOC lands and will have a small local footprint at surface (OceanaGold, 2021). Cross cuts will be constructed to provide a connection between the intake and the exhaust tunnels. An ore transfer tunnel, about 5 km long, will be built from Willows Road surface facilities area to the Processing Plant.

The mine will be supported by infrastructure situated on land located at the end of Willows Road, OGNZL property. The top of the mine and the mining activity will be over 65 m below the ground level to keep the surface effects at low levels.

## 2.3 Project development Plan

### 2.3.1 Underground mine plan

The current plan for development of the WUG will occur in two phases (OceanaGold, 2021):

- First phase (years 1-4): Pre-mining access tunnelling from Willows Farm to the orebody. This phase includes additional definition drilling of the resource and the respective trend extensions, as well as geotechnical drilling, within the mining permit area.
- Second phase (years 5-10): The second phase consists of mine development and ore extraction and will be carried out once the tunnel reaches the deposit and appropriate ventilation is established.

This is shown in Figure 2.3 below.

Development design profiles vary from 5.8mW x 6.0mH to 4.5mW x 4.5mH. All development was designed at a maximum 1:7 gradient. Declines and capital development requiring truck access were planned to be developed at a 5.0mW x 5.5mH. Development required for infrastructure includes sumps, pump/dewatering cuddies, crib rooms, electrical infrastructure, refuge chambers, underground workshop, and underground magazine (OceanaGold, 2021).

### 2.3.2 Lateral development

The development strategy for all underground operations involves mining of declines for access to stoping blocks. In this case, access drives will be excavated to develop drilling and loading levels, intersecting the orebodies centrally and the ore drives will be developed in both directions along strike from the access drives. These are shown as occurring during years 5 and 6 in Figure 2.3.

Figure 2.3: Mine development sequence by year.

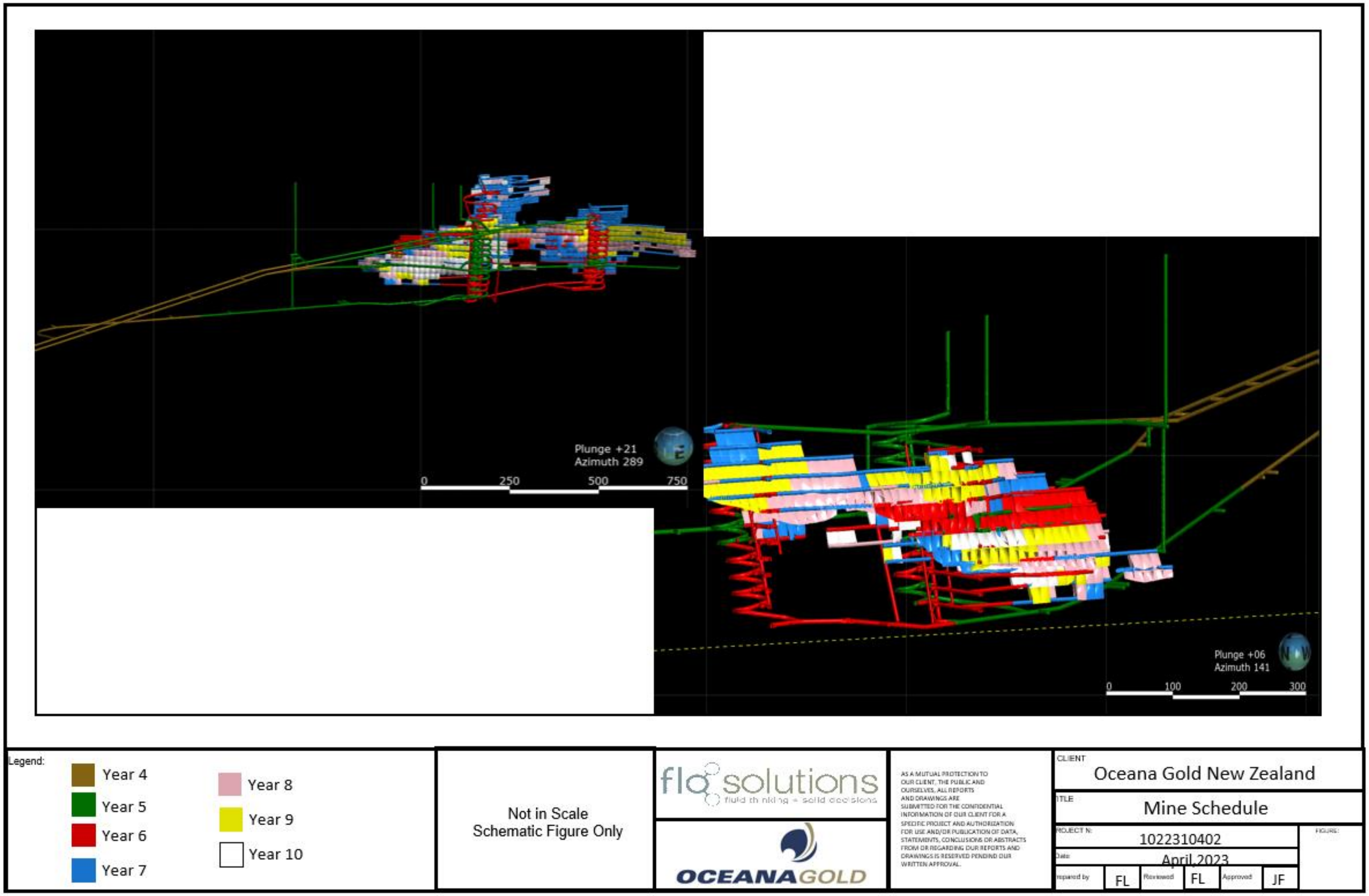

### 2.3.3 Stoping

For the mining of the Wharekirauponga deposit, the modified Avoca method has been selected.

During mining, holes will be drilled and loaded with explosives and the stope will be blasted, with broken material falling to the bottom drive for extraction. Remote controlled load haul dump machines will remove the blasted material from the stope. Stope structural support is provided through a combination of cable bolting and rock fill.

### 2.3.4 Vertical development

For vertical development the preferred method is Alimak, however there is more flexibility around methodology for any internal vertical development underground. Finger passes and longhole winzes that are generally short in length (i.e., up to 30m) will be drilled and blasted with a longhole production rig. Electrical holes, service holes and drain holes up to 30m in length can also be drilled with a longhole production rig. (OceanaGold, 2021)

Figure 2.4 shows the location of vertical development throughout the mine.

Figure 2.4: Wharekirauponga vertical development (highlighted red). From (OceanaGold, 2021).

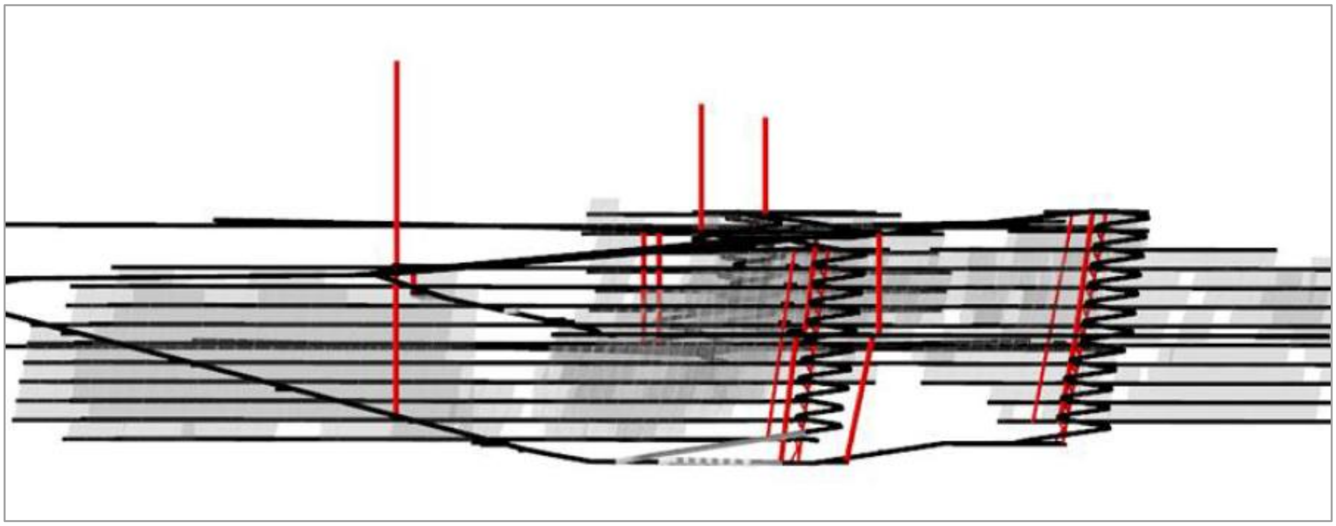

### 2.3.5 Primary and secondary pumping

The mine dewatering system has been designed to handle water inflows up to 30,000 m3/day, which is considered conservative due to current uncertainties regarding the hydraulic characteristics of the vein system (OceanaGold, 2021).

The management of total water inflows into the mine will consist of three primary pumping stations and five interim pumping stations. Due to the length of tunnel development and head difference to reach the portal, a combination of centrifugal horizontal slurry pumps and vertical pumps will be required to dewater the mine.

A secondary pumping strategy will be to pump or, in most cases, gravity feed water to sumps located in the level access development. This water is then gravity fed through drain holes linking level sumps and pumped or directed to the primary pumping stations.

# 3. CONCEPTUALIZATION

This section is a summary of the conceptualization presented in the Conceptual Model Report (FloSolutions, 1022310402-R-01 - Hydrogeological Conceptual Model Report, 2023). Additional details and information are contained in the CSM report.

## 3.1 Site setting

- The WUG project is located in the Coromandel peninsula in northeastern New Zealand, approximately 10 km north of the township of Waihi and 6 km west of Whiritoa. The Wharekirauponga orebody lies beneath the Coromandel Forest Park in the land managed by the Department of Conservation (DOC).
- The Coromandel Forest Park includes the Waihi Ecological District, an area of approximately 43,700 ha located at the southern end of the Coromandel Range and northern end of the Kaimai Range, with the Ohinemuri River catchment between and includes the east coast between Whangamatā and Waihi Beach (Environment Waikato , 2010).
- The area of the project is in the Wharekirauponga Valley, characterized by higher elevations in the southwest – around 600 meters above mean sea level (mamsl) – that gradually decrease towards the northeast. The topography forms a catchment aligned in the SW-NE direction, following the course of the Wharekirauponga River.
- The project's main area of interest, where mineralized veins are found, is situated in the central part of the catchment. This region spans approximately 1 $km^2$ and has elevations ranging from 260 to 110 mamsl. The slope gradients vary, with steep slopes in the SW and NW portions and flatter regions in the NE, averaging around 22 degrees with some slopes reaching up to 60 degrees.

## 3.2 Climate and hydrology

- The region is characterized by a sub-tropical climate with rainy and warm summers and gentle winters with higher precipitation. Annual average precipitation (AAP) in the project area usually ranges around 2000 mm. In a very rainy year, the precipitation may be observed to be above 3000mm (at Waitekauri River Station). Winter is the rainiest season, with peak rainfall in June and July. During the rainy season maximum precipitation rates can reach up to 480mm per month. The driest season is usually distributed between the months of January and February with rainfall rates ranging around 50mm/month.
- The catchment of the Wharekirauponga Stream covers an area of 14.5 $km^2$.
    - The Wharekirauponga Stream is fed by tributaries distributed in the higher portions of the catchment like Adams Stream, Teawaotemutu Stream, Edmonds Stream and Thompson Stream. The Wharekirauponga Stream then flows in the NE direction as a major tributary of the Otahu River (which flows to the sea).

- Surface water flow rates have been gauged on a number of occasions and are fully presented in the conceptual model. For the modelling purposes, the continuous gauging stations will be listed: WKP01, WKP02, WKP03, T-Stream E and T-Stream W. Flow rates are listed in the table below.

Table 3.1 Flow measurements in key gauging stations (Liters per second) (modified from (GWS, 2021))

| Location | Jan-19 | Jun-19 | Sep-19 | Jan-20 | May-20 | Aug-20 | Dec-20 | May-21 | Dec-21 | Mar-22 | Aug-22 |
|---|---|---|---|---|---|---|---|---|---|---|---|
| **T-Stream West** | 44 | 61 | 253 | 29 | 24 | 144 | 56 | 51 | 108 | 90 | 255 |
| **T-Stream East** | 60 | 53 | 245 | 33 | 26 | 142 | 74 | 52 | 109 | 97 | 276 |
| **WKP3** | 80 | 86 | 425 | 53 | 37 | 267 | 95 | 84 | 181 | 158 | 442 |
| **WKP2** | 146 | 91 | 426 | 70 | 49 | - | 121 | 105 | 196 | 185 | 477 |
| **WKP1** | - | - | - | 91 | 68 | - | 164 | 143 | 255 | 248 | 669 |

Figure 3.1 Gauging stations – Spatial Distribution

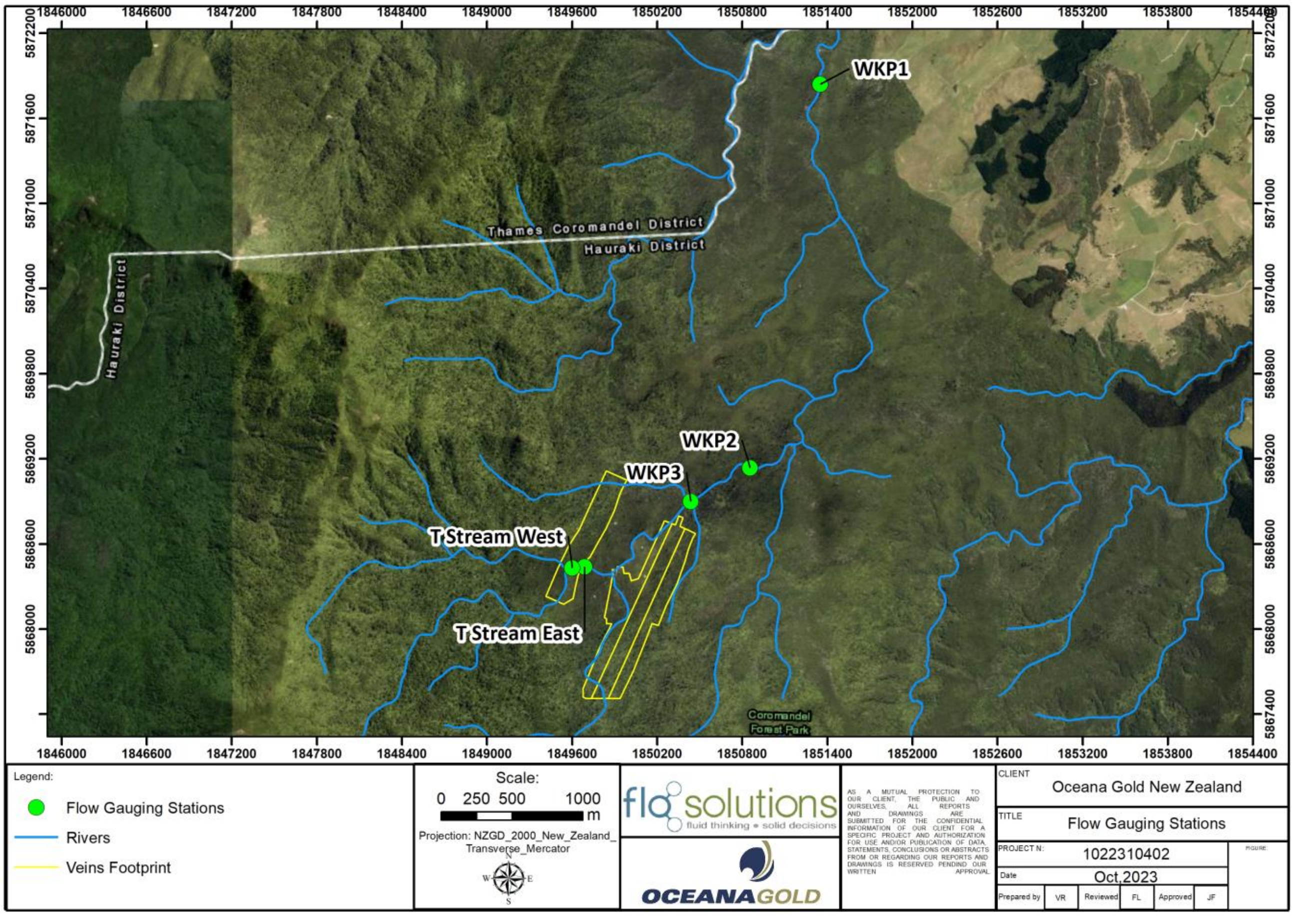

## 3.3 Geology

- Local geology is quite complex and has been studied by various authors. The Coromandel Volcanic Zone (CVZ) is an extinct volcanic arc that is within the Coromandel Peninsula of the North Island, New Zealand. Most of the deposits in the southern part of the Hauraki district, including the Waihi district, are hosted by andesite flows of the Waipupu Formation which are interlayered with volcaniclastic and tuffaceous materials. Wharekirauponga, however, is hosted by an extensive area of flow banded rhyolite and felsic lithic tuff. NE and NNE trends to vein systems are associated with extensional and oblique extensional faults which imply structural controls to emplacement and formation of the vein systems.
- The oldest unit of the geological sequence in the project area is early andesite flows, possibly part of the Waipupu Formation or the Whiritoa Andesite.
- Dome-like intrusive bodies are found within the tuff sequence. These domes usually host the majority of the EG-Vein (Figure 3.2).
- Apart from the rhyolite bodies, the only other significant intrusion that has been intersected by drilling is an NNE trending and steeply WNW dipping andesitic dike in the northwestern portion of the area.

Figure 3.2: Domes hosting the Vein System

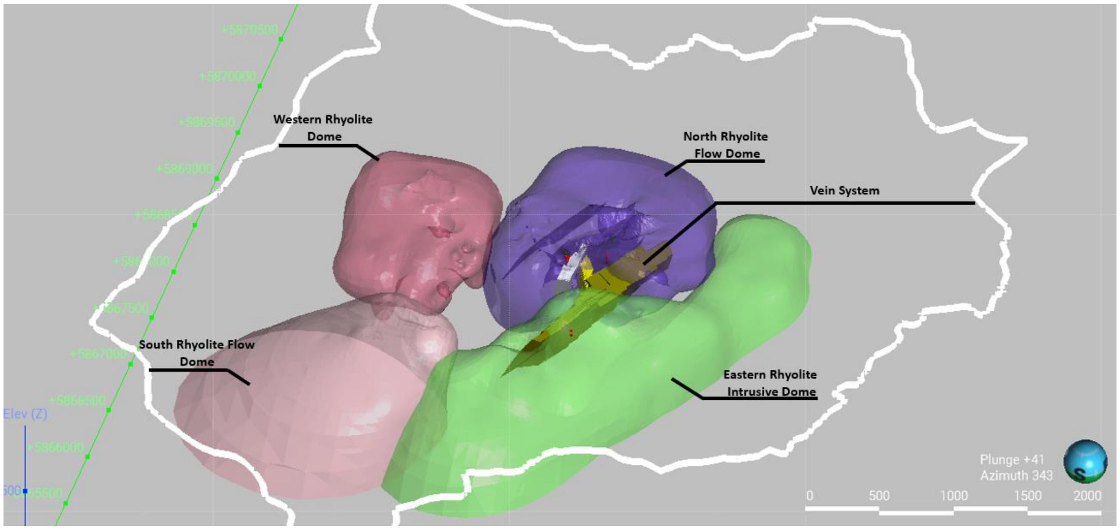


- There are three main vein sets onsite; called “Eastern Graben” or EG veins, T-Stream veins, and the Western vein. The veins are related to north-east trending, moderately dipping (60-65°) extensional step faults that relate to graben development and are up to 10 m wide. Secondary veins are developed between, or adjacent to, the main veins that are oriented northerly to north easterly, are moderately to steeply dipping and are up to 1 m wide. The vein zones are 90-95% quartz and are highly brittle in nature.

- Geophysics and surface mapping has shown extensive hydrothermal alteration of the host rock mass during the mineralization phase of the deposit's formation. The alteration largely consists of moderate to strong clay alteration with a zone of silicification centred around the vein system (based on outcrop analysis). In March 2023, FloSolutions undertook a study to evaluate the lateral extent of the clay alteration layer, based on available data, to assess if it should be extended beyond the mapped alteration zone in the mine domain during numerical modelling. This assessment resulted in the development of extended surfaces of the clay alteration zone (FloSolutions, 2023).
- The process of rock weathering in an environment with approximately 2000 mm/yr of rainfall can be accelerated, especially under dense vegetation and complex stream channel distribution found on WUG project. The March 2023 study by FloSolutions (FloSolutions, 2023) described four levels of rock zone alteration: the clay alteration zone (a result of hydrothermal alteration), a weathered zone, a slightly to moderately weathered zone, and un-weathered zone (fresh rock). Evaluation of available hydraulic testing data indicates that the degree of alteration and weathering has impacts on host rock hydraulic conductivity. These zones were modelled on Leapfrog and incorporated into the numerical model.
- During the site visit in February 2023, FloSolutions reviewed core logs from recent exploration, and identified the presence of a strongly silicified zone at the contact between a rhyolite flow dome and the rhyolite volcaniclastic units that they intruded. The silicified contacts are (presumed to be) much lower in permeability than the host rocks due to porosity occlusion and may restrict groundwater flow to the mine during development. These contacts were mapped in 3D and plotted on Leapfrog to be further used in development of 3D numerical groundwater flow models. Further details can be found on the Conceptual Model Report (FloSolutions, 1022310402-R-01 - Hydrogeological Conceptual Model Report, 2023).
- Edmonds Fault:
  - As previously described by various authors, the site exhibits strong NW-SE and NE-SW trends, which correspond to significant geological structures that facilitated the formation of the veining system. Lidar information has revealed several lineaments, particularly oriented in the NW-SE, NE-SW, and E-W directions.
  - The GNS database has indicated the presence of major structural NNE-SSW lines intersecting the vein footprint. In the numerical model, the major NE-SW fault has been incorporated, following the dip of a locally mapped dike at approximately 70 degrees. Considering that the fault doesn't outcrop at site (nor represented in shallow model layers), the observed flat hydraulic gradient in the deep piezometers suggests that the structure has high permeability allowing for deep groundwater pressures to be released along its strike.

## 3.4 Hydrostratigraphic Units:

- Shallow fractured zone: This hydrostratigraphic unit includes the upper, near surface zone (upper few meters) where flow processes are dominated by interflow. The shallow fractured zone is considered a type of variably or intermittently saturated zone and may be dry during parts of the year. As such, it is neither an 'aquifer' nor 'aquitard' by standard definition. Some very shallow hydraulic tests have resulted in very low K in this zone, probably because the zone was not fully saturated when tested.
- Clay alteration zone: The clay alteration zone is a zone of hydrothermal alteration, as previously described. Based on the core and geophysical review carried out by FloSolutions in March 2023 (FloSolutions, 2023), this zone is expected to be low permeability, acting as a natural flow barrier between the shallow groundwater system and the deeper groundwater system. This hydrostratigraphic unit is an important local aquitard. Strong water level fluctuations in the shallow aquifer in response to rainfall, and the lack of these responses in the deeper aquifer are attributed, in part, to the presence of this layer and its role in limiting connections between them.
- EG-Vein: The west-dipping EG-Vein is the largest vein structure at Wharekirauponga. Because exploration drilling has explicitly targeted the EG-Vein, there is more information on the geologic and hydrogeologic properties of this unit than other hydrostratigraphic units. Drilling information and hydraulic testing show an important fracturing grade and regular existence of voids (both related to strong secondary porosity development). However, while hydraulic testing and water levels in the EG-Vein aquifer suggest a single aquifer system, the scale and degree of the hydraulic connections along strike in this aquifer have not been established. Despite lacking a long-term pumping test in this aquifer – to improve the understanding about how a hydraulic stress would propagate along and across the vein strike – available information including hydraulic tests suggests that the vein zone hosts the deep aquifer at the site (major capacity to store and transmit a significant amount of groundwater in the deep aquifer system).
- T-Stream Vein: The T-Stream vein has been investigated, but not to the same extent as the EG-Vein. Review of core logs indicates intermittent oxidation and staining in the vein at depth (hundreds of meters), suggesting variable saturation, but VWPs installed in and around the vein system are dry – or show pressure heads equivalent to the VWP elevation. The T-Stream vein does not appear to be in hydraulic connection with the overlying T-Stream. The role of this unit in the site groundwater flow system is not clear, but it is not expected to be significant.
- Intrusive Domes: The Eastern rhyolite intrusive dome, North and South Rhyolite flow domes, and Western Rhyolite Dome are dome-shaped intrusive igneous bodies that were intruded into the tuff sequence at WUG. Primary porosity of these intrusions is low, but may be locally enhanced due to alteration and fracturing (secondary porosity). Since the porosity (secondary porosity) would be expected to be limited to the zones where fracturing systems are more prominent, these zones are considered aquitards surrounding the main aquifer system. However, the North Rhyolite Flow Dome hosts a significant part of the EG vein system and has been subject to more significant fracturing and hydrothermal alteration than other units. As a result, it exhibits higher permeability than other intrusive domes (discussed below) and is likely connected hydraulically to the EG vein system, at least locally.

- Rhyolite Volcaniclastics: The Rhyolite volcaniclastics (RV) unit is one of the main geological units forming the lithological framework of the site. The RV unit is the host rock for the majority of the domes, veins and dykes identified onsite, and based on its massive nature is assumed to extend beyond the immediate project area. Based on the overall conditions of the unit (massive, sometimes banded, low to mid fracturing) it is expected for this unit to act as an aquitard, with local variations. The widest range of K values has been identified in this unit – ranging over 4 orders of magnitude – due primarily to post-emplacement alteration and fracturing.

## 3.5 Hydraulic properties

- A hydraulic testing program was implemented in 2021 and continued in 2022. In general, two types of tests have been conducted 1) packer tests in open exploration boreholes and 2) falling head tests in constructed piezometers. There are, in total, 57 test results (47 Packer Tests and 10 Falling Head Tests)
- Tests results were organized according to the hydrostratigraphic unit, as presented in the table below.

Table 3.2: Summary of hydraulic parameters by hydrostratigraphic unit.

| Hydrostratigraphic Unit | | Type | Number of Tests | Average K (m/s) | Geomean K (m/s) | Max K (m/s) | Min K (m/s) |
|---|---|---|---|---|---|---|---|
| Shallow fractured zone | | Variable | 3 | 6.4E-08 | 1.5E-08 | 1.3E-07 | 4.6E-10 |
| Shallow groundwater system | | Aquifer | 11 | 4.8E-07 | 2.9E-08 | 3.3E-06 | 3.7E-10 |
| Clay alteration zone | | Aquiclude | 0 | - | | | |
| EG-Vein | | Aquifer | 12 | 4.8E-06 | 1.7E-06 | 3.1E-05 | 2.8E-07 |
| T-Stream Vein | | Aquitard | 0 | - | | | |
| Intrusive Domes | Eastern Rhyolite Intrusive Dome | Aquitard | 9 | 1.9E-06 | 1.4E-07 | 7.6E-06 | 3.8E-10 |
| | North Rhyolite Flow Dome | Aquitard* | 12 | 3.1E-06 | 3.5E-06 | 9.1E-06 | 9.8E-08 |
| | South Rhyolite Flow Dome | Aquitard | 0 | - | | | |
| | Western Rhyolite Dome | Aquitard | 0 | - | | | |
| Rhyolite Volcaniclastics | | Aquitard* | 4 | 1.3E-06 | 4.8E-08 | 3.8E-06 | 3.9E-10 |

*Locally an aquifer with higher hydraulic conductivity close to the EG Vein system

- **<u>Shallow fractured zone:</u>** There is very little information in the shallow fractured zone. A few standpipe piezometers are interpreted to be installed along this unit, where falling head tests have been completed (WKP-01S, WKP-08 S/D). Hydraulic conductivity is usually low (around 1E-8 m/s), probably due to the influence of the unsaturated zone on test results.
- **<u>Shallow groundwater system:</u>** Most of the tests completed in the shallow aquifer are at depths of 35 to 60m below ground surface. Hydraulic conductivity can be quite variable, ranging from 3E-6 to 1E-8 m/s.

- **Clay alteration zone:** There is no direct information of hydraulic parameters of the clay alteration zone. Considering the composition of the unit, it's expected to be low permeability.
- **EG-Vein:** Tests in the EG-Vein form the most comprehensive dataset of hydraulic testing. This unit has the narrowest range in permeability, with relatively high K values of approximately 3E-05 to 3E-07 m/s. Considering that this unit is highly fractured, this is expected.
- **T-Stream Vein:** From the dataset analysed, there is not much information in the zone of the EG-Vein, as previously mentioned. Of the 4 packer tests completed in the zone of the T-Stream, none has been completed in the Vein itself. The closest test is around 25m away from the vein and has resulted in a K value of 1.1E-7 m/s.
- **Intrusive Domes:** In total 21 tests were performed in domes. These were restricted to the North Rhyolite Flow Dome and Eastern Rhyolite Intrusive Dome. Hydraulic conductivities can be quite low in these units where they are intact and unfractured, with tests as low as 3.8E-10 m/s. However, where fractured near the EG vein system, K values are orders of magnitude higher, resulting in values close to the EG vein aquifer geomean values. By extension, the South and Western rhyolite flow domes, which do not host the EG vein system, are expected to be low permeability.
- **Rhyolite Volcaniclastics:** Hydraulic conductivity of the RV unit can be quite variable depending on where the test has been completed. The test completed in the tunnel area, for example, has shown a very low K (2.4E-9 m/s), while tests completed in the region of VWP-09 have resulted in high hydraulic conductivities around 1E-6 m/s. This difference is probably related to the difference of fracturing near the EG vein, where it is more fractured and permeable, relative to rock quality outside the vein area (less fractured and permeable).

- The water balance was initially assessed by (GWS, 2021), which considered that an average of 7% of the rainfall should reach the aquifers (recharge calculated through mass balance – further details can be obtained on the referred report GWS,2021). (Ling, 2003) (The Groundwater Regime of the Waihi Basin, North Island, New Zealand) has presented a modelled recharge in the order of 1% of the annual average precipitation (AAP). This value was coherent to the recharge values reported by (Waihi Gold Company, 1985a).
  - For this current analysis, an initial recharge of 7% of AAP (2000mm) will be defined and further calibration / analysis will be carried out during the modelling process.

## 3.6 Water levels

- In terms of water level data, the WUG project groundwater monitoring system started in 2019 with some localized standpipe piezometers and later (2021) improved with the installation of additional VWPs. Currently, there are a total of 29 VWPs and piezometers installed at site, which in general have been monitored since their installation.

- In general, water levels within the site can be quite variable in the shallow groundwater system (from 250 mamsl to 140 mamsl), while the deep groundwater system usually shows a regular distribution, especially in the EG-Vein (levels ranging around 110 to 120 mamsl). The graph below shows the piezometric head distribution based on the number of piezometers (shallow instruments are usually installed between elevations 225 mamsl to 130 mamsl, while deep instruments are installed from 130 mamsl to -120 mamsl).

Figure 3.3: Average piezometric heads (m)

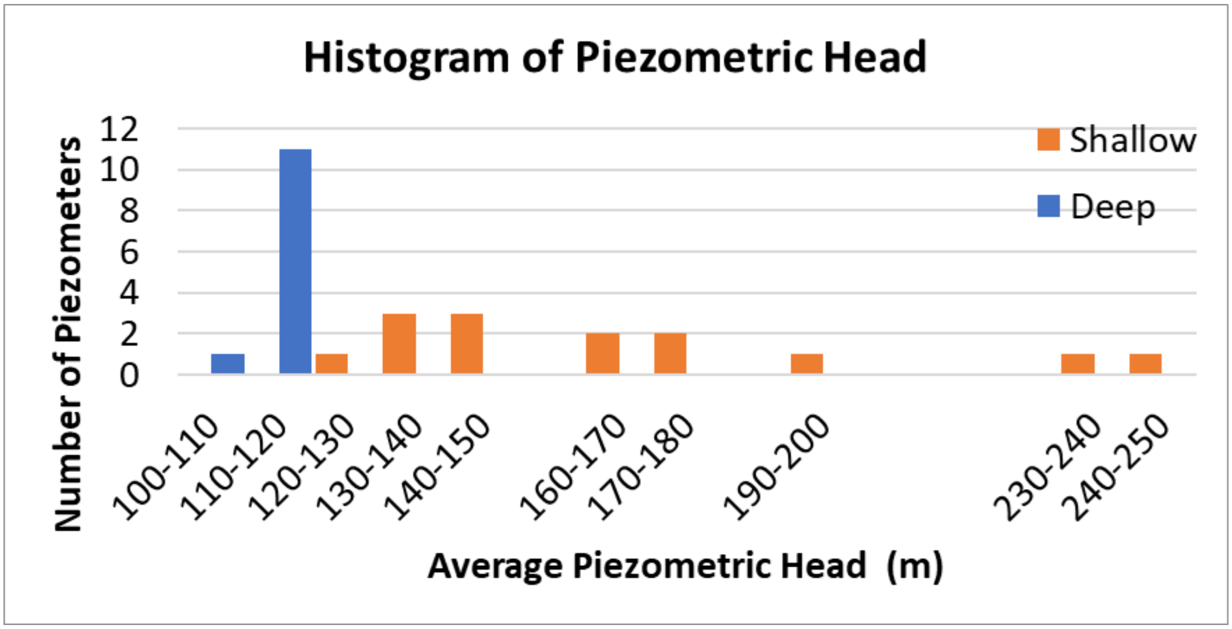

# 4. NUMERICAL MODEL

Based on the information presented in previous topics, this section will detail the groundwater model construction, calibration, simulations, and sensitive analysis.

## 4.1 Model Objectives

As discussed in Section 1.2 the main objective is to produce a model that is a simplified yet accurate representation of the CSM and can reasonably reproduce site conditions and processes. Based on the project scope and intended model use, the following specific objectives can be listed for this current groundwater numerical model:

- Reproduce numerically underground flow patterns.
- Simulate and evaluate underground mine water inflows and associated drawdown.
- Simulate and evaluate the impacts of the underground workings on loss of stream baseflow.
- Assessment of mitigation options and evaluation of results.
- Simulation of post-mining water level recovery, flow paths, and travel times.

## 4.2 Modelling Code

The code selected for the current numerical simulation was MODFLOW USG (Panday, Langevin, Niswonger, Ibaraki, & Hughes, 2013) developed by the USGS (United States Geological Survey). MODFLOW USG was developed to support a wide variety of structured and unstructured grid types. The code is based on an underlying control volume finite difference (CVFD) formulation in which a cell can be connected to an arbitrary number of adjacent cells.

MODFLOW–USG also contains an optional Newton-Raphson formulation, based on the formulation in MODFLOW–NWT, for improving solution convergence and avoiding problems with the drying and rewetting of cells.

Groundwater Vistas 8 was used as the MODFLOW pre- and post-processor for the project model.

## 4.3 Model Construction

### 4.3.1 Model Domain and Mesh

The model domain is usually defined based on hydrological and/or geological features. The conditions along the boundaries of the conceptual model determine the mathematical boundary conditions of the numerical model. Boundaries can include hydraulic features such as groundwater divides and physical features such as bodies of surface water and relatively impermeable rock (Anderson, Woessner, & Hunt, 2015).

The WUG numerical model was defined to completely encompass the upper portion of the Wharekirauponga catchment, where the vein system (T-Stream and EG-Veins) is located. The model domain includes a total area of 22.1 Km2 (4.5 Km in the N-S axis and 5Km in the E-W axis). The model is limited in the north portion by the Lignite Stream, and in the south by the Waiharakeke Stream. Both east and west portions are limited by higher elevations in topography (limits of the Wharekirauponga catchment).

Vertical boundaries have been defined based on the available topography, the geological model provided by OGNZL, and based on the mining plan. The lower limit of the model was set to the elevation -500m. The maximum elevation ranges around 750m (coincident to the higher portions of the Whakamoehau peak and surrounding areas).

Model mesh consists of a total of 294 rows and 200 columns. Initial mesh size was defined as 35m x 35m (regular finite difference grid), and later refined in the portion of the vein area to a more detailed mesh (15m x 15m). For the vertical discretization, layers of 15m (average) were used from the top of the model (reflection from the topographic elevation) to the bottom of the underground workings (around -150m). In total 38 layers have been used. The table below summarises the elevations based on a cell in the location of the WKP-01.

Table 4.1: Layer elevations (vein area – WKP-01)

| Layer | From (m) | To (m) | Layer | From (m) | To (m) |
|---|---|---|---|---|---|
| 1 | 183 | 168 | 20 | -94 | -109 |
| 2 | 168 | 154 | 21 | -109 | -123 |
| 3 | 154 | 139 | 22 | -123 | -138 |
| 4 | 139 | 124 | 23 | -138 | -152 |
| 5 | 124 | 110 | 24 | -152 | -167 |
| 6 | 110 | 95 | 25 | -167 | -181 |
| 7 | 95 | 81 | 26 | -181 | -196 |
| 8 | 81 | 66 | 27 | -196 | -211 |
| 9 | 66 | 52 | 28 | -211 | -225 |
| 10 | 52 | 37 | 29 | -225 | -240 |
| 11 | 37 | 22 | 30 | -240 | -254 |
| 12 | 22 | 8 | 31 | -254 | -269 |
| 13 | 8 | -7 | 32 | -269 | -283 |
| 14 | -7 | -21 | 33 | -283 | -298 |
| 15 | -21 | -36 | 34 | -298 | -313 |
| 16 | -36 | -50 | 35 | -313 | -327 |
| 17 | -50 | -65 | 36 | -327 | -342 |
| 18 | -65 | -79 | 37 | -342 | -356 |
| 19 | -79 | -94 | 38 | -356 | -400 |

### 4.3.2 Geology in MODFLOW

The representation of the geology in MODFLOW was completed using the following items:

- Geological model provided by OGNZL geology team.
    - The original exploration model, which covers a smaller area, was extended to the edges of the numerical model domain by the OGNZL geology team
    - The vein solids defined by OGNZL were grouped into three different zones. This approach was mostly based on hydraulic testing results and considering a uniform head distribution along the deeper vein system. Figure 4.1 shows the EG-Vein zones.
- Geological assessment in the shallow zone: weathered zone, clay alteration zone and silicified contacts) - (details previously discussed on topic 3. ).
- Definition of regional fault structure – Edmonds Fault (based on GNS database).

The Figure 4.1 shows the geological model in Groundwater Vistas for the first 10 layers. All figures presenting the geology from Layer 1 to Layer 38 are compiled in Appendix A.

Figure 4.1: Vein system – modeled zones

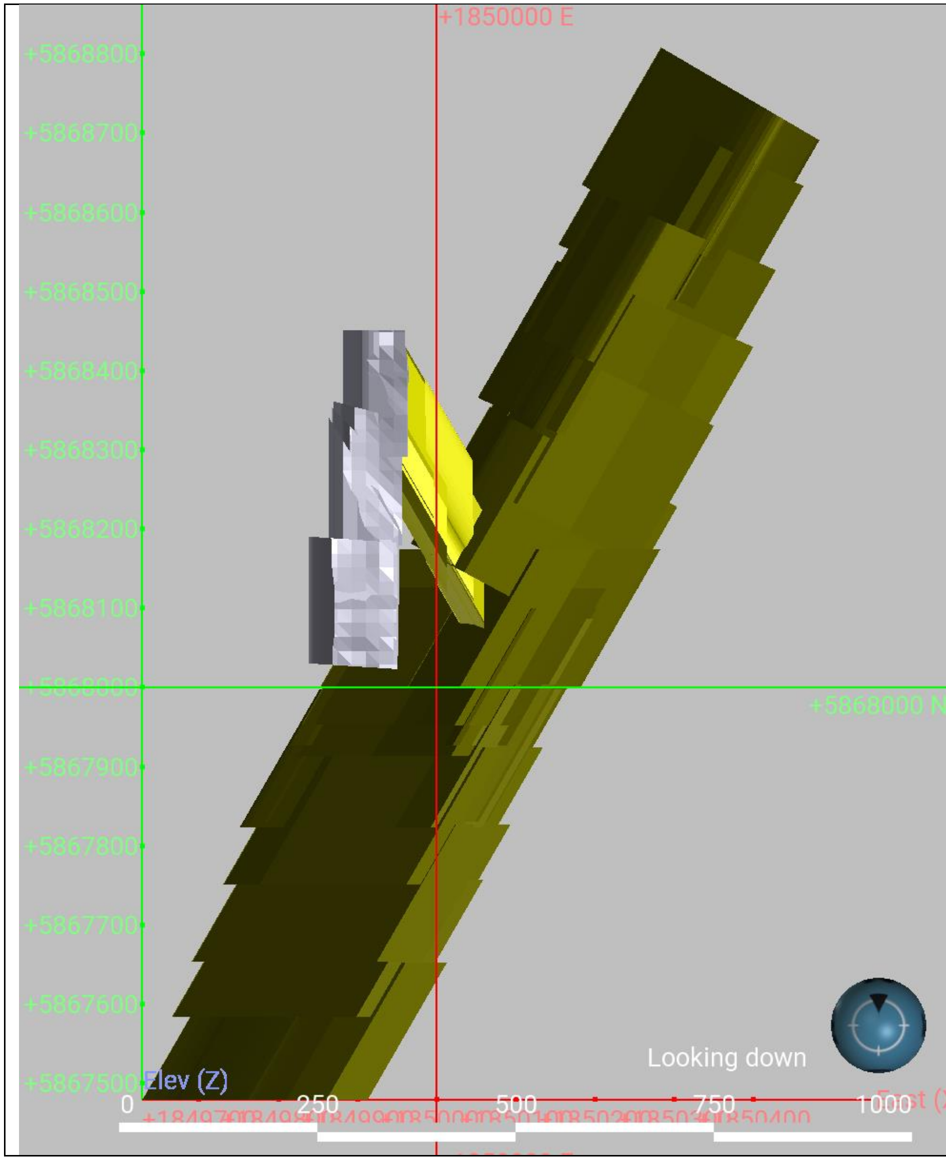


EG-1: Most to the west and shallower zone (gray).
EG-2: The intermediate portion (central) of the vein system (light yellow).
EG-3: The bigger zone, comprehending the deeper and longer section aligned to the NE-SW structure (dark yellow).

Figure 4.2: Modflow geology (Layer 1 to Layer 10)

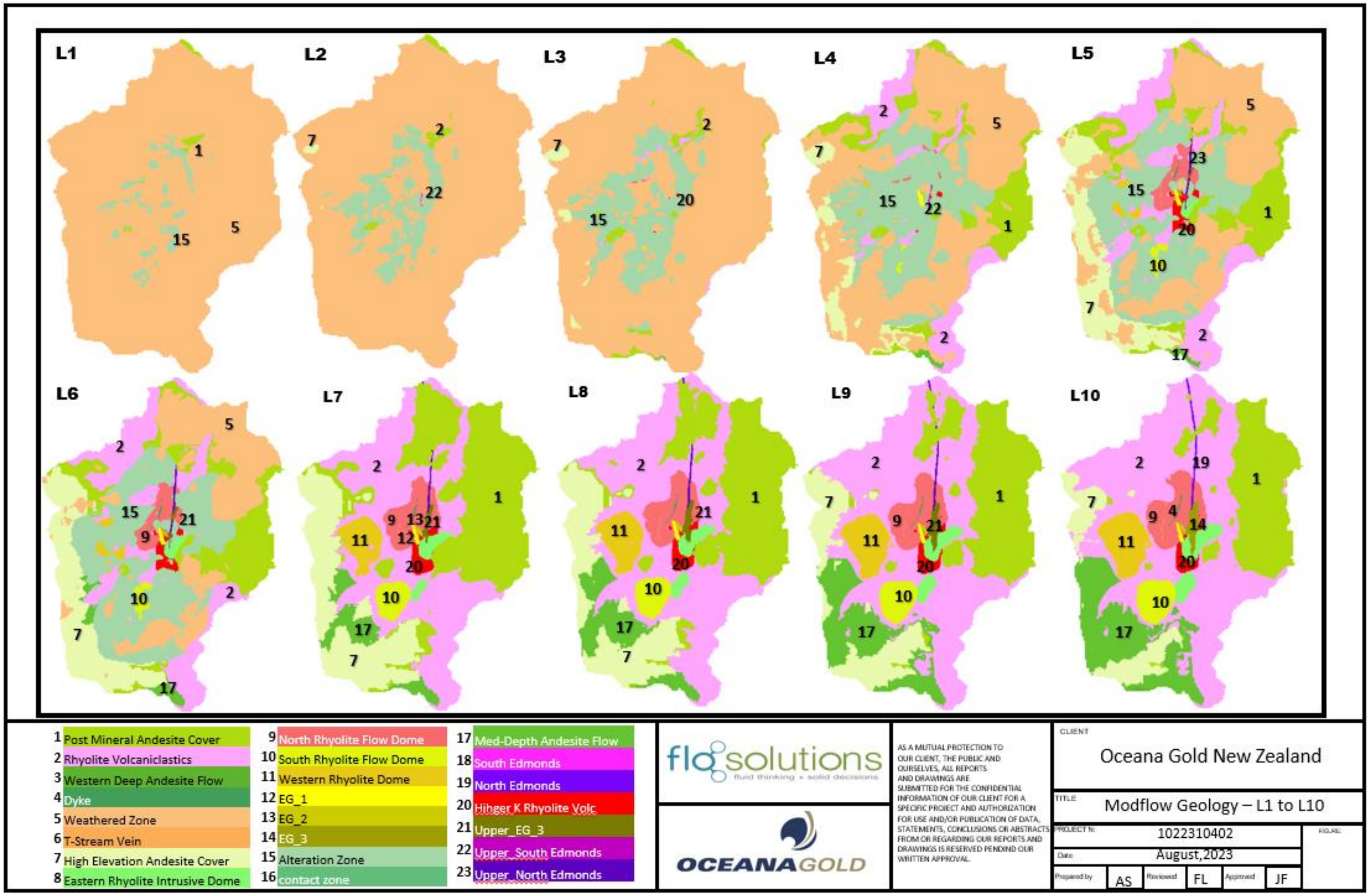

### 4.3.3 Boundary Conditions

Boundary conditions (BCs) are used to refer to hydraulic conditions external and internal to the problem domain. For this current model, the following BCs have been applied: No Flow Boundary, Recharge, Rivers Drains and General Head Boundary.

#### 4.3.3.1 No Flow boundaries

The no flow boundaries correspond to the topographic catchment limits of the active area of the model, where there is assumed to be no groundwater inflow into the model or outflow from the model. Considering the low hydraulic conductivity of the rock mass and that deep flows should be negligible, No Flow BCs have also been applied to the bottom of the model -500m.

#### 4.3.3.2 Recharge boundaries

Recharge represents the fraction of the rainfall which infiltrates in the soil and reaches the aquifer. The recharge boundary applied to the top of this model was initially based on the average recharge calculated by GWS and briefly described in section 3. The distribution of the recharge within the model domain usually can be difficult to estimate since a wide range of factors will likely affect how recharge occurs in each portion of the area (for example: vegetation, slopes, soils, geology).

During the model construction, some zonation adjustments were necessary to better represent the recharge distribution in the catchment and conceptually represent the distribution of fluxes and heads. In total, 8 (eight) recharge zones were defined:

- Recharge is generally higher at higher elevations.
  - Recharge from 250m to higher than 400m were assigned to be 256 mm/yr
- The central portion of the model, where a clay alteration zone was identified during the site visit, was assigned to have a recharge rate of 12 mm/yr. This zone has been observed to be restricted to main portion of the area – as described in the Site Visit Technical Memorandum (FloSolutions, 2023)
- Zones below 250m covering a significant extension of the model domain were assigned a value of 110 mm/yr.
- Recharge is ~0 on northwest corner of model in Lignite River catchment, where shallow water tables are consistently simulated.

Recharge zones (total recharge) are illustrated in the Figure 4.4.

#### 4.3.3.3 Rivers

Rivers in the model domain have been represented in the model by the MODFLOW river package (McDonald & Harbaugh, 1988).

Stream – aquifer flux exchange is usually parameterized with a river conductance (CRIV) using a head-dependent flux (Cauchy-type) boundary condition (e.g., (Furman, 2008); (Ebel, Mirus, Heppner, VanderKwaak, & Loague, 2009); (Goderniaux, 2009); (Flipo, 2014)) such as implemented in the MODFLOW river package ( (McDonald & Harbaugh, 1988); (Furman, 2008)). The stream-aquifer exchange flow is calculated as the product of CRIV by the head difference between the stream and the cell where the Cauchy-type boundary condition is applied.

When (Prickett, 1971) introduced the concept of river conductance, they considered a simplified conceptual model where stream-aquifer flux exchange is controlled by the thickness and vertical hydraulic conductivity of streambed deposits. This widely used approach is described in the MODFLOW river package.

River conductances were applied following the parameters as shown in the figure below. Whenever overall river geometries were available (like in the main mining area – zones 5, 6, 7, 8, 9 - (Boffa Miskell, 2021) ) these values have been used to calculate model river parameters. Outside the mine area, where information is limited to inexistent, river parameters were assumed based on the best conceptual judgement from the modeler (bigger rivers limiting the model domain in the zone 2 and 4) and river geometry following the river channel upwards in zone 10.

Figure 4.3 River parameters – Approach for the conductance calculation

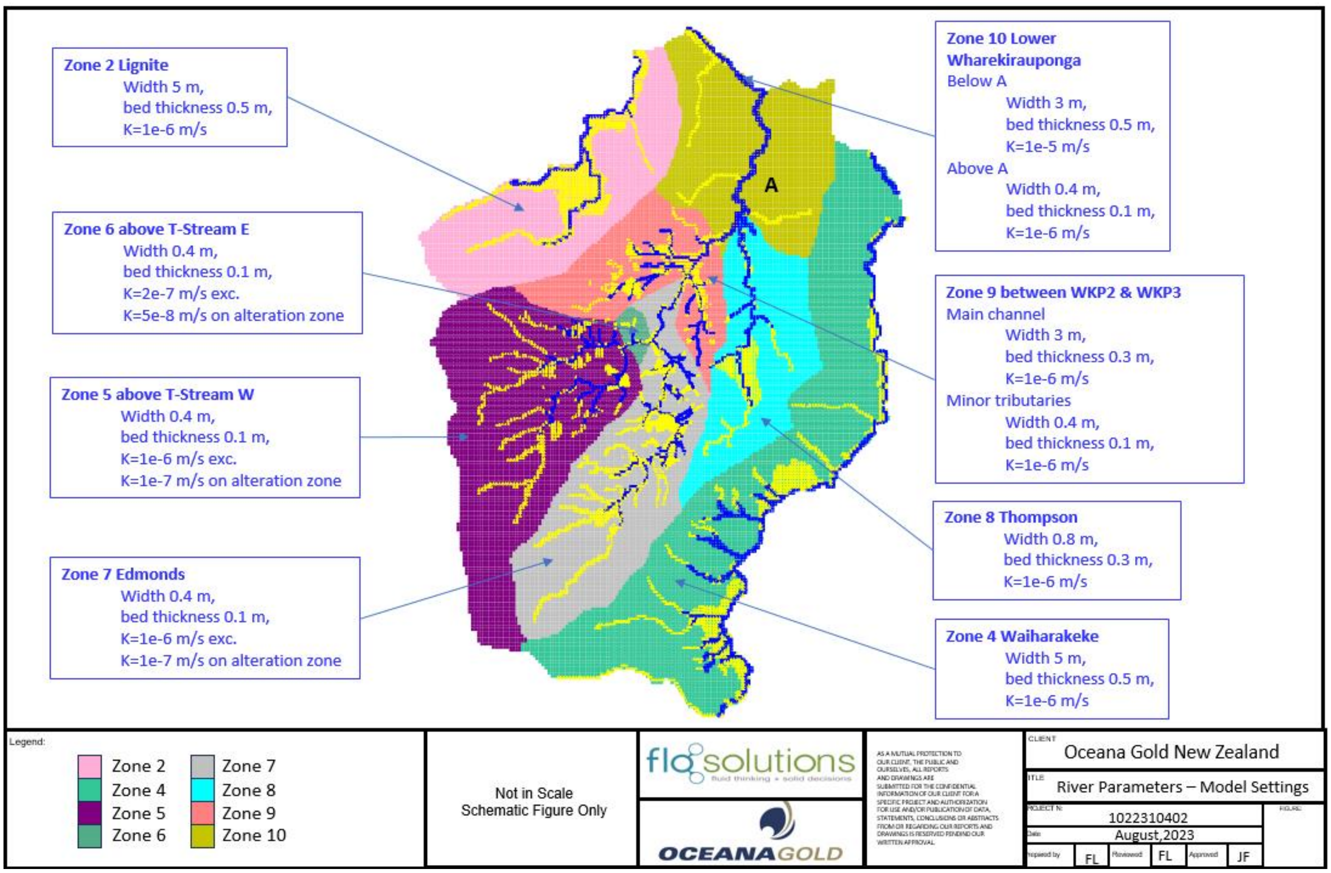

#### 4.3.3.4 Drains

Drains are usually inserted in the model to represent those boundaries that can only remove water from the system based on the conductance and head elevation around this specific BC. For this model, Drains were added during the simulation of the underground workings and to represent some sections of streams.

Additional drains were added to areas where the water table is shallow during the transient calibration. The reason for this is that, in some areas, the high recharge applied in 2022 and 2023 resulted in ponding at ground surface.

The distribution of drains is presented in the Figure 4.4.

#### 4.3.3.5 General Head Boundary

The general head boundary condition (GHB) allows head-dependent normal flux into or out of the model, depending on the modelled head at the boundary.  Boundary conditions like this are sometimes called 3rd type. For this current model, GHBs were implemented as a deep groundwater outlet from the catchment at the Edmonds Fault, from Layer 7 to 32. Considering that no groundwater information is currently available in the northern / northeastern portion of the area, the boundary reference head was set to 53.6 masl, equal to the lowest river elevation on the northern boundary – assuming that rivers at lower portions of the catchment behave as gaining streams, consistent with the conceptual model. The conductance was set to 880 m2/d.

The need for an outlet was identified during the initial model calibration, where significantly lower hydraulic heads needed to be simulated in deeper piezometers. Figure 4.4 presents the boundary conditions applied to the model.

Figure 4.4 Boundary Conditions projected on Layer 1

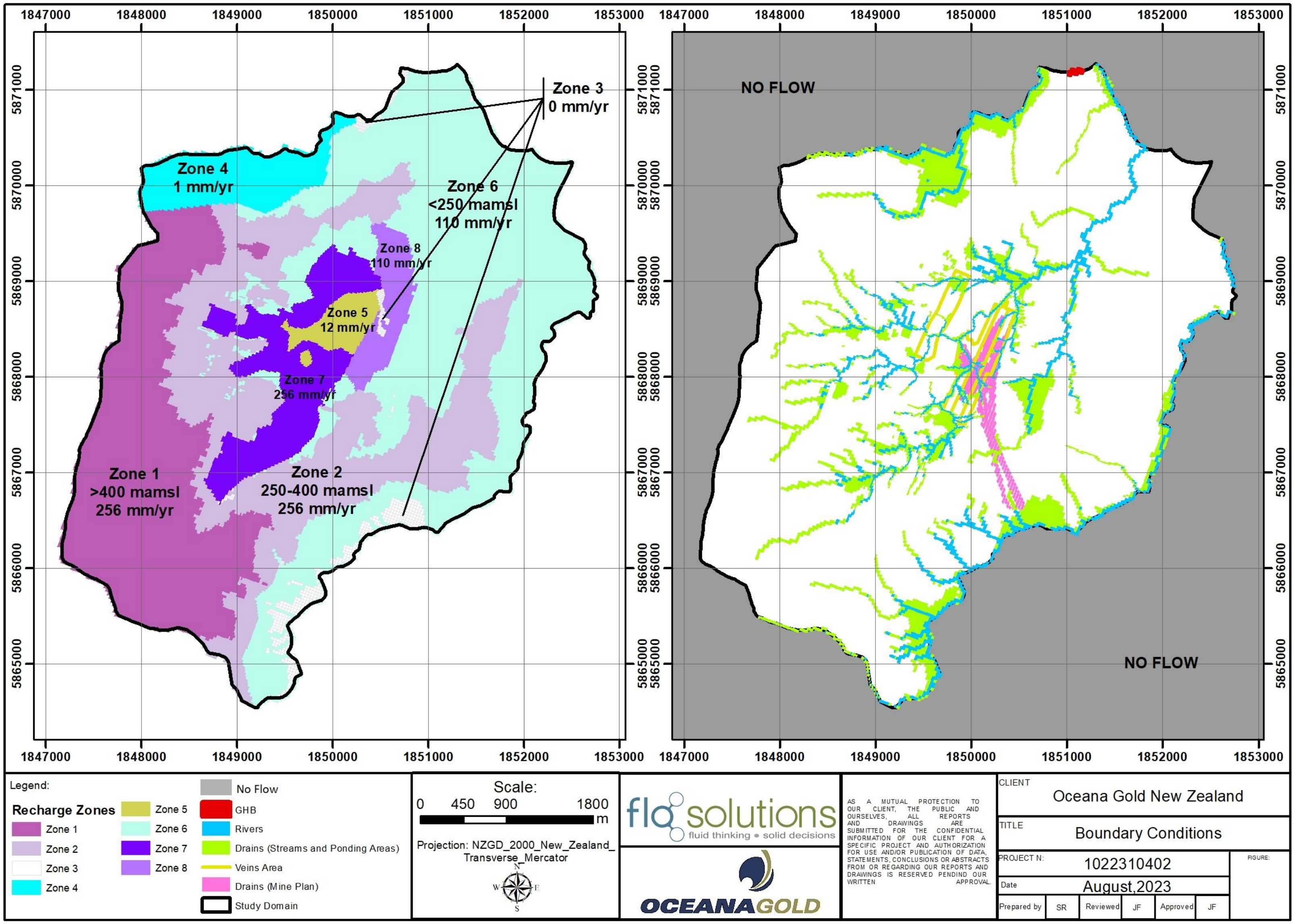

## 4.4 Steady State Model Calibration

Model calibration involves the adjustment of model input parameters to attempt to match real-world conditions. Typically, calibration targets include measured water levels (from piezometers and VWPs) and flows (where known).

### 4.4.1 Steady state calibration targets

The model calibration undertook a reasonable amount of effort and time to achieve an acceptable history match and representation of heads and fluxes. Initial model parameters were mostly based on real field data (whenever available) in composition to literature values for the units outside the mine domain (where testing was not completed).

The trial-and-error calibration processes was initially applied in order to get a sense on general parameters and model response, followed by PEST (Doherty & Hunt, 2010) automated calibration process. Adjustments on hydraulic properties were needed specially in the vein system and surrounding units (North Rhyolite Flow Dome, Eastern Intrusive Dome and Rhyolite Volcaniclastics). PEST calibrations were limited by field dataset (constraining hydraulic conductivity variation). The following sections present the targets and model parameters.

#### Heads

For this current model calibration, heads from VWPs and Standpipe piezometers have been used according to the table below.

Table 4.2: Calibration Targets – Steady State Model

| Name | X | Y | Target (Head m) | Name | X | Y | Target (Head m) |
|---|---|---|---|---|---|---|---|
| WKP_01D | 1849835 | 5868326 | 139.3 | WKP04D_M | 1850221 | 5868497 | 104.0 |
| WKP_01S | 1849837 | 5868326 | 171.7 | WKP04D_S | 1850120 | 5868560 | 139.0 |
| WKP_02D | 1850116 | 5868370 | 173.5 | WKP05D_S | 1850126 | 5867507 | 241.4 |
| WKP_02S | 1850115 | 5868370 | 190.7 | WKP09D_D | 1850095 | 5868125 | 112.0 |
| WKP_06D | 1849837 | 5868334 | 110.5 | WKP09D_M | 1849952 | 5868232 | 126.5 |
| WKP_06S | 1849837 | 5868324 | 112.0 | WKP09D_S | 1849905 | 5868266 | 149.0 |
| WKP_07D | 1850116 | 5868359 | 110.2 | WKP10D_D | 1849929 | 5868059 | 110.5 |
| WKP_08D | 1850095 | 5868559 | 144.8 | WKP10D_M | 1849894 | 5868090 | 111.7 |
| WKP_08S | 1850095 | 5868559 | 164.7 | WKP10D_S | 1849836 | 5868142 | 143.8 |
| WKP03D_D | 1849693 | 5868585 | 112.2 | WKP11D_D | 1850026 | 5867971 | 114.4 |
| WKP03D_M | 1849675 | 5868625 | 163.3 | WKP11D_M1 | 1849907 | 5868185 | 112.1 |
| WKP03D_S | 1849653 | 5868673 | 234.2 | WKP11D_M2 | 1849969 | 5868070 | 113.2 |
| WKP04D_D | 1850267 | 5868467 | 117.3 | WKP11D_S | 1849881 | 5868238 | 135.1 |

### Stream Baseflow

In addition to the head targets, some stream baseflows have been assigned as calibration targets. Although baseflow assessment is not fully complete, May, 2020, is the driest month among the historical dataset, and it has been assumed that the gauged flow in May, 2020 was equivalent to baseflow for calibration purposes. The table below summarizes the applied recharge values compared to baseflows. Recharge is usually higher than baseflows as part of the recharge will be converted to baseflow and part will feed the groundwater system.

Table 4.3: Baseflow Targets

| Gauge | May/2020<br>Q (L/s) | Applied Recharge<br>(L/s) |
|---|---|---|
| T-Stream W | 24 | 33 |
| T-Stream E | 30 | 34 |
| WKP3 | 40 | 57 |
| WKP2 | 50 | 67 |

## 4.4.2 Steady state final parameters

The table below summarizes the calibrated model parameters, model details and boundary conditions.

Table 4.4 Model details and main parameters

| Model Components | Description | | |
|---|---|---|---|
| **Model Mesh** | | | |
| Total Area | 22.1 Km² – Aprox 5.5 km x 4.0 km | | |
| Mesh discretization | 294 rows and 200 columns, 38 layers - Total: 2234400 cells. | | |
| **Hydrogeological Parameters (SS320)** | **Kx (m/s)** | **Ky (m/s)** | **Kz (m/s)** |
| Post Mineral Andesite Cover | 2.1E-07 | 2.1E-07 | 4.2E-08 |
| Rhyolite Volcaniclastics | 1.0E-09 | 1.0E-09 | 1.0E-10 |
| Western Deep Andesite Flow | 5.0E-10 | 5.0E-10 | 2.0E-10 |
| Dyke | 5.0E-10 | 5.0E-10 | 5.0E-10 |
| Weathered Zone | 1.5E-06 | 1.5E-06 | 8.2E-06 |
| T-Stream Vein | 7.8E-07 | 7.8E-07 | 1.6E-08 |
| South Colluvium | 5.0E-10 | 5.0E-10 | 1.5E-10 |
| Eastern Rhyolite Intrusive Dome | 2.1E-08 | 2.1E-08 | 1.3E-08 |
| North Rhyolite Flow Dome | 7.7E-07 | 7.7E-07 | 3.6E-10 |
| South Rhyolite Flow Dome | 5.0E-10 | 5.0E-10 | 5.0E-10 |
| Western Rhyolite Dome | 5.0E-10 | 5.0E-10 | 6.9E-11 |
| EG_1 | 4.8E-07 | 4.8E-07 | 9.6E-09 |
| EG_2 | 1.3E-08 | 1.3E-08 | 7.8E-09 |
| EG_3 | 1.0E-05 | 1.0E-05 | 2.1E-07 |
| Alteration Zone | 1.1E-08 | 1.1E-08 | 1.5E-09 |
| contact zone | 5.0E-08 | 5.0E-08 | 5.0E-08 |
| Med-Depth Andesite Flow | 5.0E-10 | 5.0E-10 | 2.0E-10 |
| South Edmonds | 2.0E-05 | 2.0E-05 | 3.7E-08 |
| North Edmonds | 3.0E-05 | 3.0E-05 | 3.7E-08 |
| Hihger K Rhyolite Volc | 1.2E-08 | 1.2E-08 | 1.2E-09 |
| Upper_EG_3 | 1.0E-10 | 1.0E-10 | 2.1E-10 |
| Upper_South Edmonds | 2.0E-10 | 2.0E-10 | 3.7E-10 |
| Upper_North Edmonds | 3.0E-10 | 3.0E-10 | 3.7E-10 |
| **Boundary Conditions** | | | |
| No Flow | Model boundaries (except by the Edmonds Fault limit to the NE) | | |
| Drains | Used to simulate the underground workings, to simulate some and to improve calibration by avoid ponding in Transient Calibration. | | |
| General Head Boundary | Applied as a deep groundwater outlet at the Edmonds Fault from layers 7 to 32 (35 mamsl to -280 mamsl). Spatial distribution (plan view) can be found in Figure 4.4. | | |
| River | Applied to most of the drainage system existent in the site – River parameters are presented in Figure 4.3. River elevations have been obtained from OGNZL Lidar survey. | | |
| Recharge | **Zone** | **m/d** | **mm/yr** |
| | Zone 1 | 0.0007 | 256 |
| | Zone 2 | 0.0007 | 256 |
| | Zone 3 | 0 | 0 |
| | Zone 4 | 0.000004 | 1 |
| | Zone 5 | 0.0000340 | 12 |
| | Zone 6 | 0.0003 | 110 |
| | Zone 7 | 0.0007 | 256 |
| | Zone 8 | 0.0003 | 110 |

### 4.4.3 Steady state calibration

#### Heads

The steady-state model calibration was assessed both quantitatively and qualitatively. Quantitatively, global statistical measures of steady state model performance with respect to simulated head levels are provided in Table 4.5. Model calibration is generally considered appropriate where the normalized root mean square error (NRMSE) is less than 10%, indicating a reasonable history matching (Barnett, et al., 2012). Reported residuals are calculated as follows:

*Residual = Observed Value – Simulated Value*
*where positive (+) residuals indicate underprediction and negative values (-) indicate overprediction.*

Table 4.5 Steady-state model statistics

| Statistics – Steady State Calibration | |
|---|---|
| Residual Mean | 3.5 |
| Absolute Residual Mean | 20.3 |
| Residual Std. Deviation | 23.5 |
| Sum of Squares | 14685.5 |
| RMS Error | 23.8 |
| Min. Residual | -39.2 |
| Max. Residual | 37.8 |
| Number of Observations | 26 |
| Range in Observations | 137.5 |
| Scaled Residual Std. Deviation | 0.171 |
| Scaled Absolute Residual Mean | 0.148 |
| Scaled RMS Error | 17.3% |
| Scaled Residual Mean | 0.026 |

As can be observed from the table above, calibration reached NRMSE of 17.3%. This is expected due to the nature of fractured media, the small number of calibration points, and the restrictions in their spatial distribution close to the mine domain. Figure 4.6 shows the calibration graph with targets distribution, while the map from Figure 4.7 presents the spatial distribution of residuals. Figure 4.5 shows the steady state water budget. Water balance error is close to 0% (0.0001%).

Calibration was further assessed during the Latin Hypercube analysis (presented later in this report).

Figure 4.5: Steady State Model – Mass Balance (L/s)

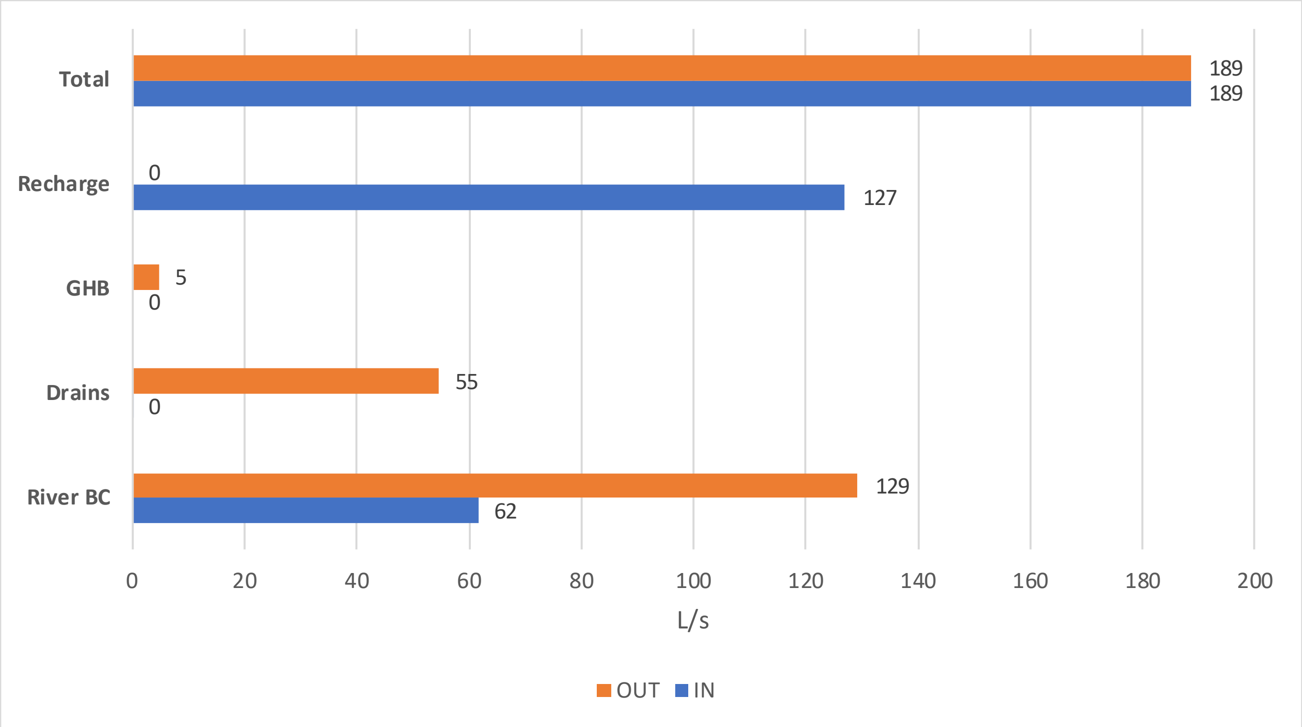


## Baseflow

Simulated baseflows were reasonably close to the targets defined from May-2020. The table below shows the comparison between the modelled values and target values.

Table 4.6: Baseflows (Target versus Calculated)

| Stream Gauge | Baseflow (L/s) | |
|---|---|---|
| | Target | Simulated |
| T-Stream W | 24 | 30 |
| T-Stream E | 26 | 32 |
| WKP3 | 37 | 55 |
| WKP2 | 49 | 64 |

Figure 4.6: Steady-state calibration – Calibration points distribution

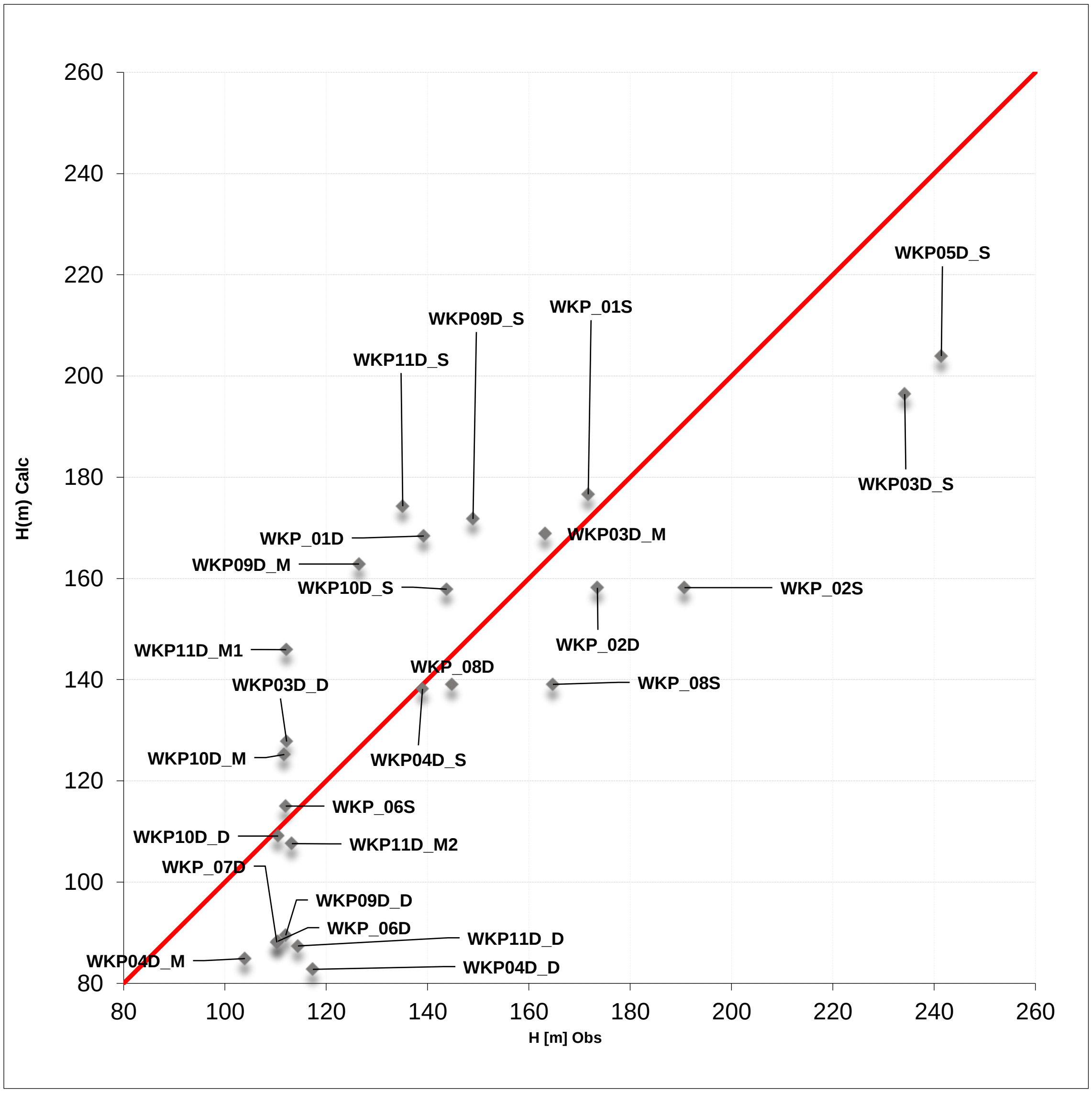

Figure 4.7 Steady-state targets and calibration

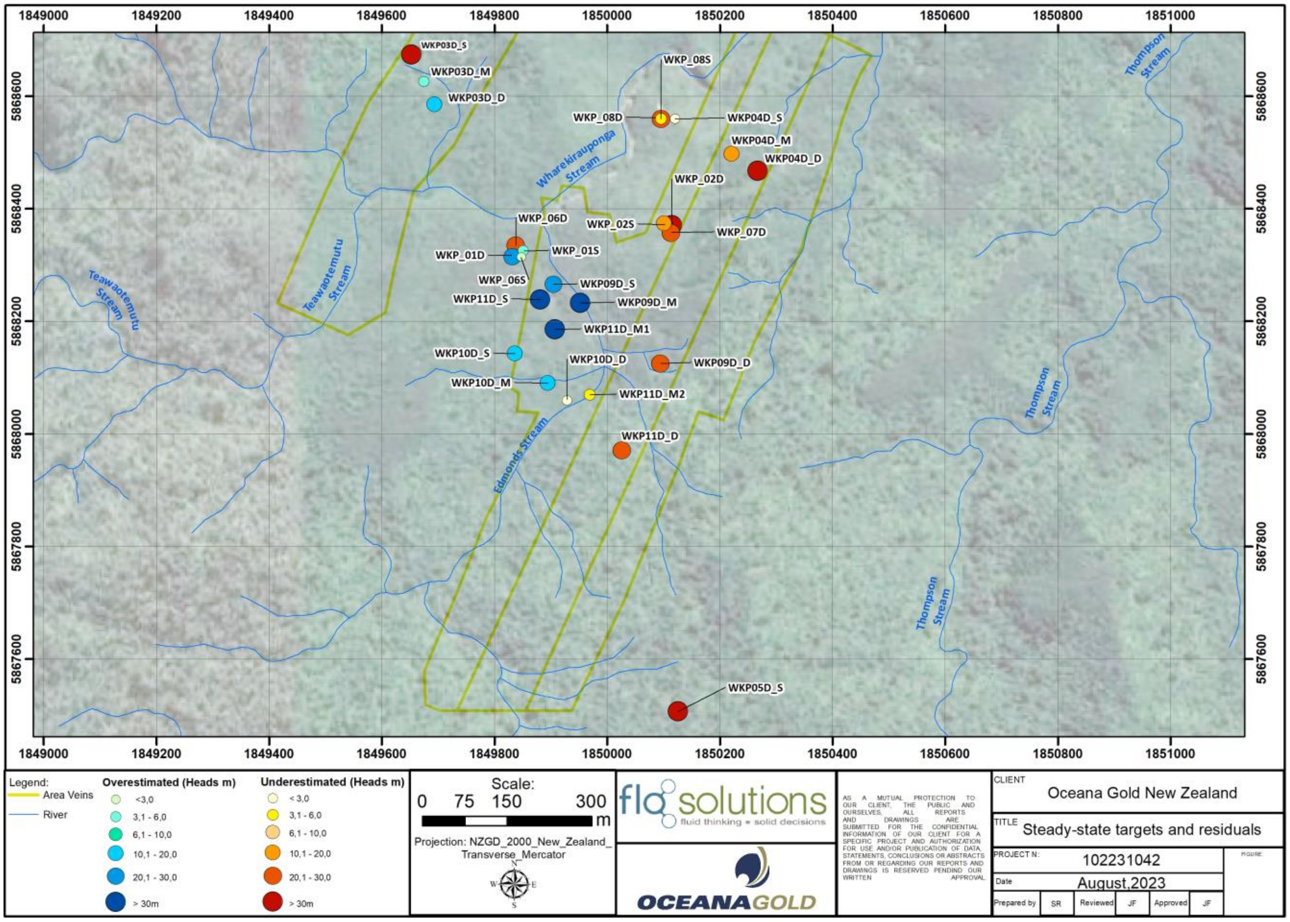


## 4.5 Transient Model

The Transient Calibration Model (TR) was constructed to simulate and calibrate model response to the hydraulic stresses imposed on the hydrogeologic system attributed to operations at WUG mine.

### 4.5.1 Transient Settings

The transient model is set up with 53 model stress periods between December 2018 to April 2023 - Table 4.7. Stress periods are associated with calendar months and defined in terms of total days as such.

Table 4.7 Transient calibration model stress period setup

| SP | Type | Length [d] | Cumulative [d] | Start Date | End Date | SP | Type | Length [d] | Cumulative [d] | Start Date | End Date |
|---|---|---|---|---|---|---|---|---|---|---|---|
| 1 | TR | 1 | 1 | 1/12/2018 | 2/12/2018 | 28 | TR | 28 | 821 | 1/02/2021 | 1/03/2021 |
| 2 | TR | 30 | 31 | 2/12/2018 | 1/01/2019 | 29 | TR | 31 | 852 | 1/03/2021 | 1/04/2021 |

| SP | Type | Length [d] | Cumulative [d] | Start Date | End Date | SP | Type | Length [d] | Cumulative [d] | Start Date | End Date |
|---|---|---|---|---|---|---|---|---|---|---|---|
| 3 | TR | 31 | 62 | 1/01/2019 | 1/02/2019 | 30 | TR | 30 | 882 | 1/04/2021 | 1/05/2021 |
| 4 | TR | 28 | 90 | 1/02/2019 | 1/03/2019 | 31 | TR | 31 | 913 | 1/05/2021 | 1/06/2021 |
| 5 | TR | 31 | 121 | 1/03/2019 | 1/04/2019 | 32 | TR | 30 | 943 | 1/06/2021 | 1/07/2021 |
| 6 | TR | 30 | 151 | 1/04/2019 | 1/05/2019 | 33 | TR | 31 | 974 | 1/07/2021 | 1/08/2021 |
| 7 | TR | 31 | 182 | 1/05/2019 | 1/06/2019 | 34 | TR | 31 | 1005 | 1/08/2021 | 1/09/2021 |
| 8 | TR | 30 | 212 | 1/06/2019 | 1/07/2019 | 35 | TR | 30 | 1035 | 1/09/2021 | 1/10/2021 |
| 9 | TR | 31 | 243 | 1/07/2019 | 1/08/2019 | 36 | TR | 31 | 1066 | 1/10/2021 | 1/11/2021 |
| 10 | TR | 31 | 274 | 1/08/2019 | 1/09/2019 | 37 | TR | 30 | 1096 | 1/11/2021 | 1/12/2021 |
| 11 | TR | 30 | 304 | 1/09/2019 | 1/10/2019 | 38 | TR | 31 | 1127 | 1/12/2021 | 1/01/2022 |
| 12 | TR | 31 | 335 | 1/10/2019 | 1/11/2019 | 39 | TR | 31 | 1158 | 1/01/2022 | 1/02/2022 |
| 13 | TR | 30 | 365 | 1/11/2019 | 1/12/2019 | 40 | TR | 28 | 1186 | 1/02/2022 | 1/03/2022 |
| 14 | TR | 31 | 396 | 1/12/2019 | 1/01/2020 | 41 | TR | 31 | 1217 | 1/03/2022 | 1/04/2022 |
| 15 | TR | 31 | 427 | 1/01/2020 | 1/02/2020 | 42 | TR | 30 | 1247 | 1/04/2022 | 1/05/2022 |
| 16 | TR | 29 | 456 | 1/02/2020 | 1/03/2020 | 43 | TR | 31 | 1278 | 1/05/2022 | 1/06/2022 |
| 17 | TR | 31 | 487 | 1/03/2020 | 1/04/2020 | 44 | TR | 30 | 1308 | 1/06/2022 | 1/07/2022 |
| 18 | TR | 30 | 517 | 1/04/2020 | 1/05/2020 | 45 | TR | 31 | 1339 | 1/07/2022 | 1/08/2022 |
| 19 | TR | 31 | 548 | 1/05/2020 | 1/06/2020 | 46 | TR | 31 | 1370 | 1/08/2022 | 1/09/2022 |
| 20 | TR | 30 | 578 | 1/06/2020 | 1/07/2020 | 47 | TR | 30 | 1400 | 1/09/2022 | 1/10/2022 |
| 21 | TR | 31 | 609 | 1/07/2020 | 1/08/2020 | 48 | TR | 31 | 1431 | 1/10/2022 | 1/11/2022 |
| 22 | TR | 31 | 640 | 1/08/2020 | 1/09/2020 | 49 | TR | 30 | 1461 | 1/11/2022 | 1/12/2022 |
| 23 | TR | 30 | 670 | 1/09/2020 | 1/10/2020 | 50 | TR | 31 | 1492 | 1/12/2022 | 1/01/2023 |
| 24 | TR | 31 | 701 | 1/10/2020 | 1/11/2020 | 51 | TR | 31 | 1523 | 1/01/2023 | 1/02/2023 |
| 25 | TR | 30 | 731 | 1/11/2020 | 1/12/2020 | 52 | TR | 28 | 1551 | 1/02/2023 | 1/03/2023 |
| 26 | TR | 31 | 762 | 1/12/2020 | 1/01/2021 | 53 | TR | 31 | 1582 | 1/03/2023 | 1/04/2023 |
| 27 | TR | 31 | 793 | 1/01/2021 | 1/02/2021 | | | | | | |

Boundary conditions in the transient model remained constant throughout the simulation. The recharge was set to vary according to the rainfall.

- The annual average value used to compute the factors is 2460mm, based on climate notations from niwa.co.nz, which notes that:
  - 2019 & 2020 were dry years, with rainfall in most places between 50% and 79% of normal values.
  - 2021 was an average year, though the mine gauge has recorded values similar to 2019 & 2020.
  - 2022 was a wet year, with rainfall in most places between 120% and 149% of normal values.

Figure 4.8: Recharge distribution – Transient Model

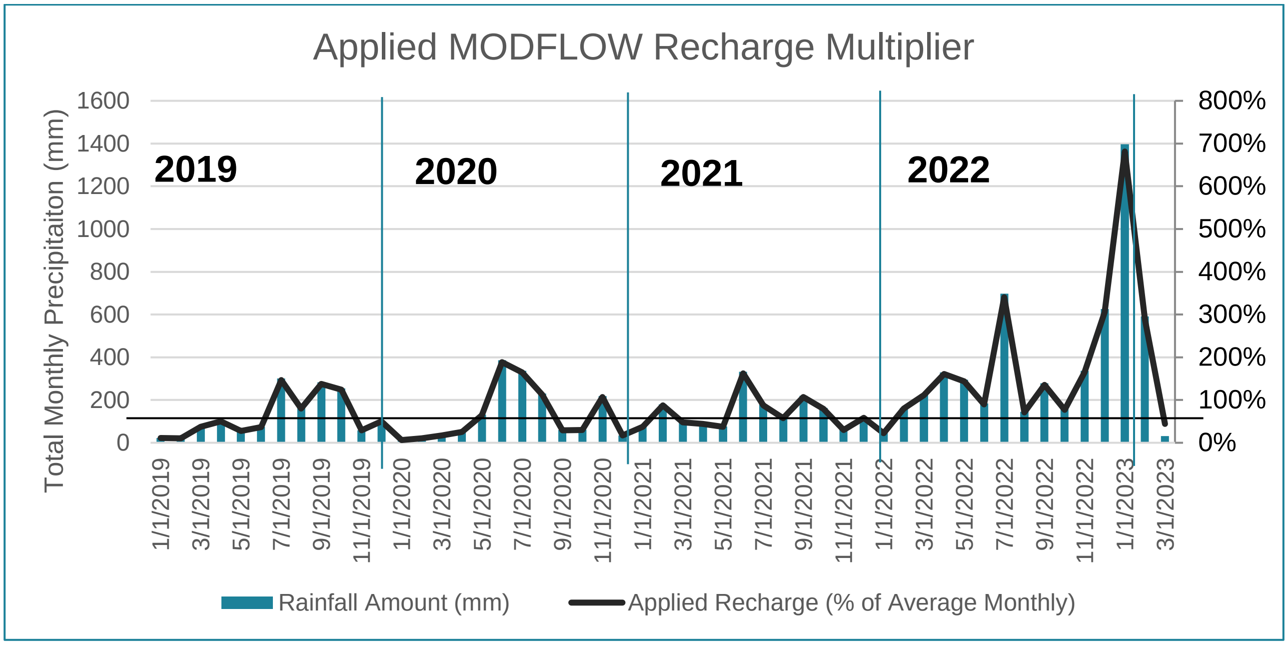


## 4.5.2 Transient Parameters

The following table summarizes the hydraulic parameters used for the transient calibration. It's important to emphasize that initial values based on literature have been applied to the model and then further adjusted using PEST. Up to the current date there are no transient parameters available for the site. References for Specific Yield (Sy) and Specific Storage (Ss) can be found on the following studies: (Domenico, 1965), (Heath, 1983), (Morris, 1967), (USGS, 1967).

Table 4.8 Transient state calibrated parameters

| Hydrogeological Parameters – Transient State Model | Ss | Sy |
|---|---|---|
| Post Mineral Andesite Cover | 5.0E-06 | 2.0% |
| Rhyolite Volcaniclastics | 5.0E-06 | 4.0% |
| Western Deep Andesite Flow | 5.0E-06 | 2.0% |
| Dyke | 5.0E-06 | 1.5% |
| Weathered Zone | 1.0E-05 | 8.0% |
| T-Stream Vein | 5.0E-06 | 3.5% |
| South Colluvium | 5.0E-06 | 2.0% |
| Eastern Rhyolite Intrusive Dome | 5.0E-06 | 2.0% |
| North Rhyolite Flow Dome | 5.0E-06 | 2.0% |
| South Rhyolite Flow Dome | 5.0E-06 | 2.0% |
| Western Rhyolite Dome | 5.0E-06 | 2.0% |
| EG_1 | 5.0E-06 | 3.5% |
| EG_2 | 5.0E-06 | 3.5% |
| EG_3 | 5.0E-06 | 3.5% |
| Alteration Zone | 5.0E-06 | 3.0% |
| contact zone | 5.0E-06 | 3.0% |
| Med-Depth Andesite Flow | 5.0E-06 | 2.0% |
| South Edmonds | 5.0E-06 | 2.0% |
| North Edmonds | 5.0E-06 | 2.0% |
| Hihger K Rhyolite Volc | 5.0E-06 | 6.0% |
| Upper_EG_3 | 5.0E-06 | 3.5% |
| Upper_South Edmonds | 5.0E-06 | 2.0% |
| Upper_North Edmonds | 5.0E-06 | 2.0% |

### 4.5.3 Transient Calibration Performance

Performance of the Transient Calibration Model is assessed on replication of measured head levels and response to natural environmental fluctuations (rainfall variation). As discussed in the Australian Groundwater Modelling Guidelines (Barnett, et al., 2012), guiding principle 5.2, “The calibration process should be used to find model parameters that prepare a model for use during predictions of future behaviour, rather than finding model parameters that explain past behaviour.”

To be useful for predictions, the model must be able to simulate observed fluctuations in water levels in response to rain events, which is more important than matching past head levels precisely (the NRSME value). Particular attention was directed at matching fluctuation in the shallow groundwater system.

All calibration graphs can be found on Appendix B. General comments related to the transient calibration (some graph examples can be found in Figure 4.11):

- Transient calibration, despite model limitations related to transient hydraulic parameters (Specific Storage and Specific Yield), can be considered sufficiently well calibrated for use in predictive simulations. Simulation curves match reasonably well the calibration targets.
  - The model predicts the minimum (but non-zero) change in head due to seasonal recharge in the piezometers in the EG vein.
  - The model simulates a decline in water level during the dry years of 2019 and 2020, followed by a water level increase due to the wet years of 2022 and early 2023.
  - The increase in head observed in the Eastern Rhyolite Intrusive Dome is slightly underestimated.
  - Trends in shallow monitoring points (such as WKP-03S, WKP-08S, WKP-02S) are well captured by the model.

Baseflows simulated by the model are quite responsive to rainfall events. As can be seen in the Figure 4.12 below, no restriction in monthly recharge was imposed for the extremely wet months at the end of 2022 and early 2023 – the groundwater discharge to streams during those months is correspondingly high.

The model is considered a high “Class 2” model based on the AGMG (Barnett, et al., 2012), as it lacks some elements required to achieve Class 3, specifically:

- Groundwater head observations and bore log are available but are limited to the central part of the model domain.
- Calibration statistics are reasonable but suggest errors in parts of the model domain.
- Short temporal record of water levels used in calibration (generally less than 2 years).
- Transient calibration over a short time frame compared to that of predictions.

Figure 4.9 Transient water balance – Main TR components

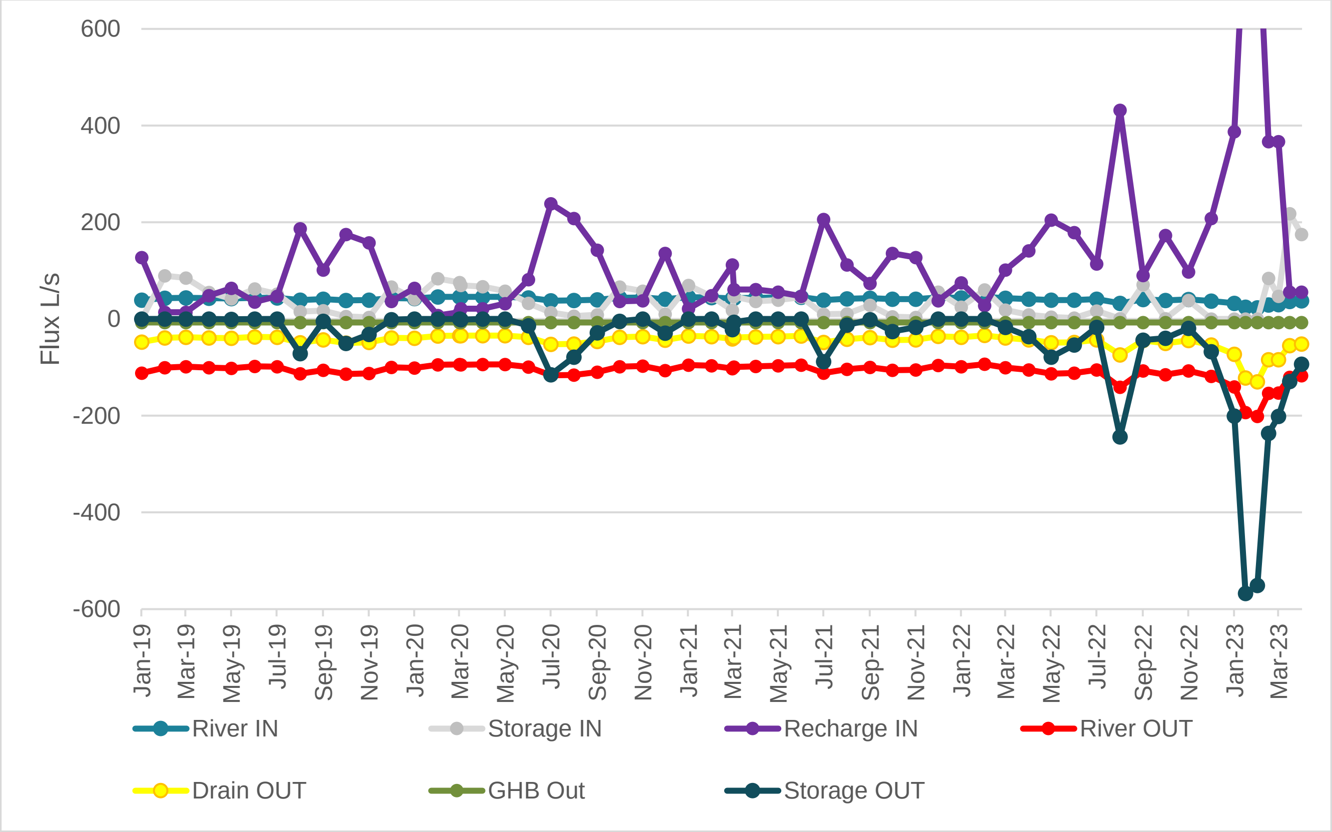


Figure 4.10 Transient Total IN versus Total OUT

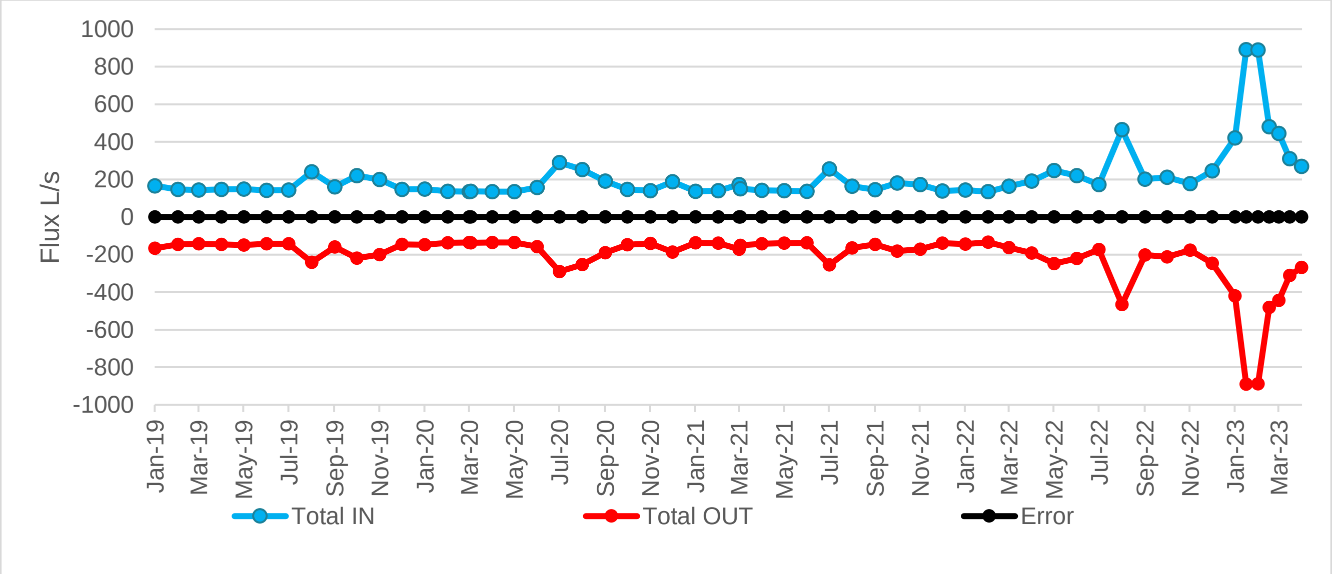

Figure 4.11: Transient calibration graphs.

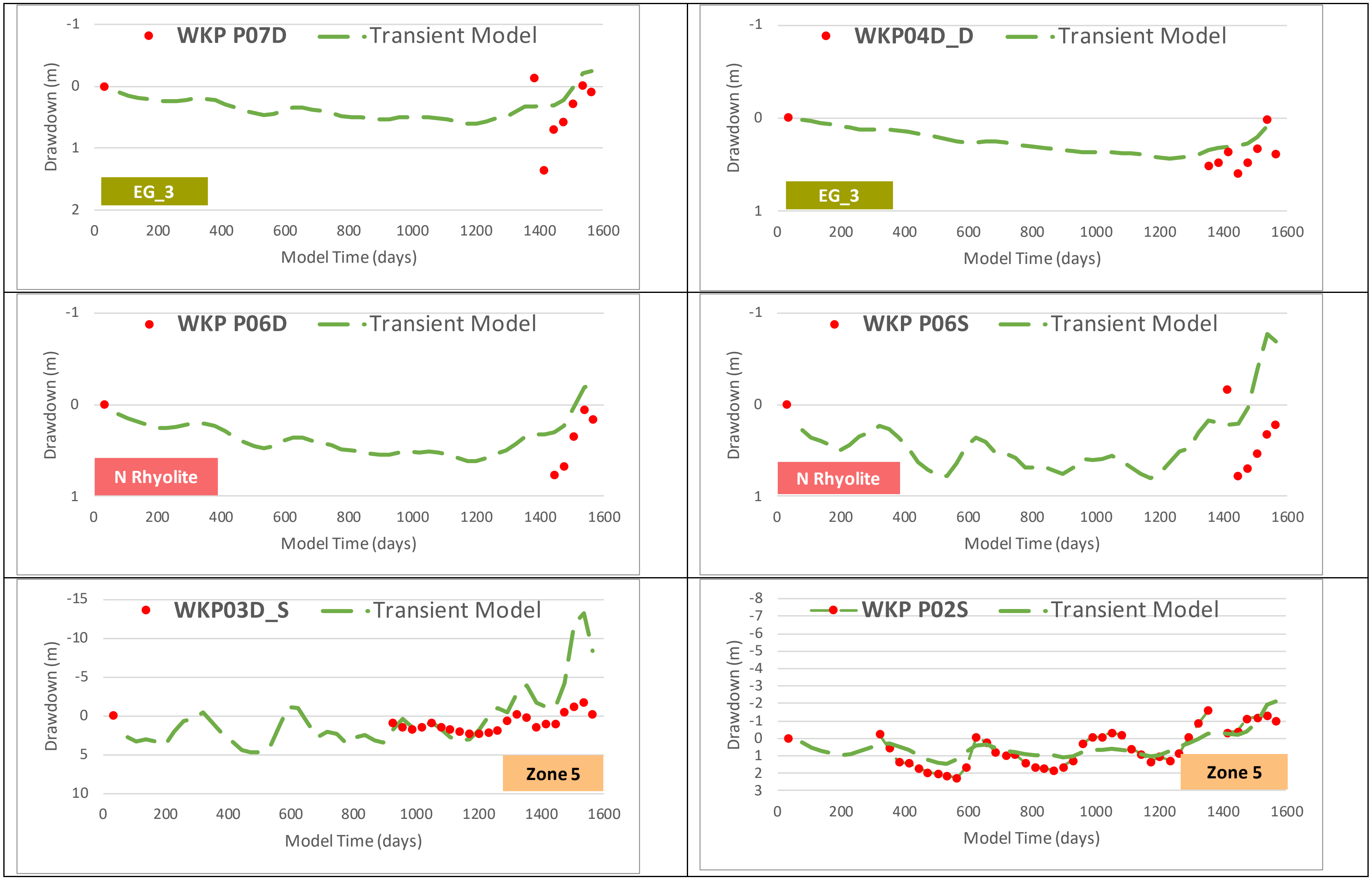

Figure 4.12: Baseflow simulation

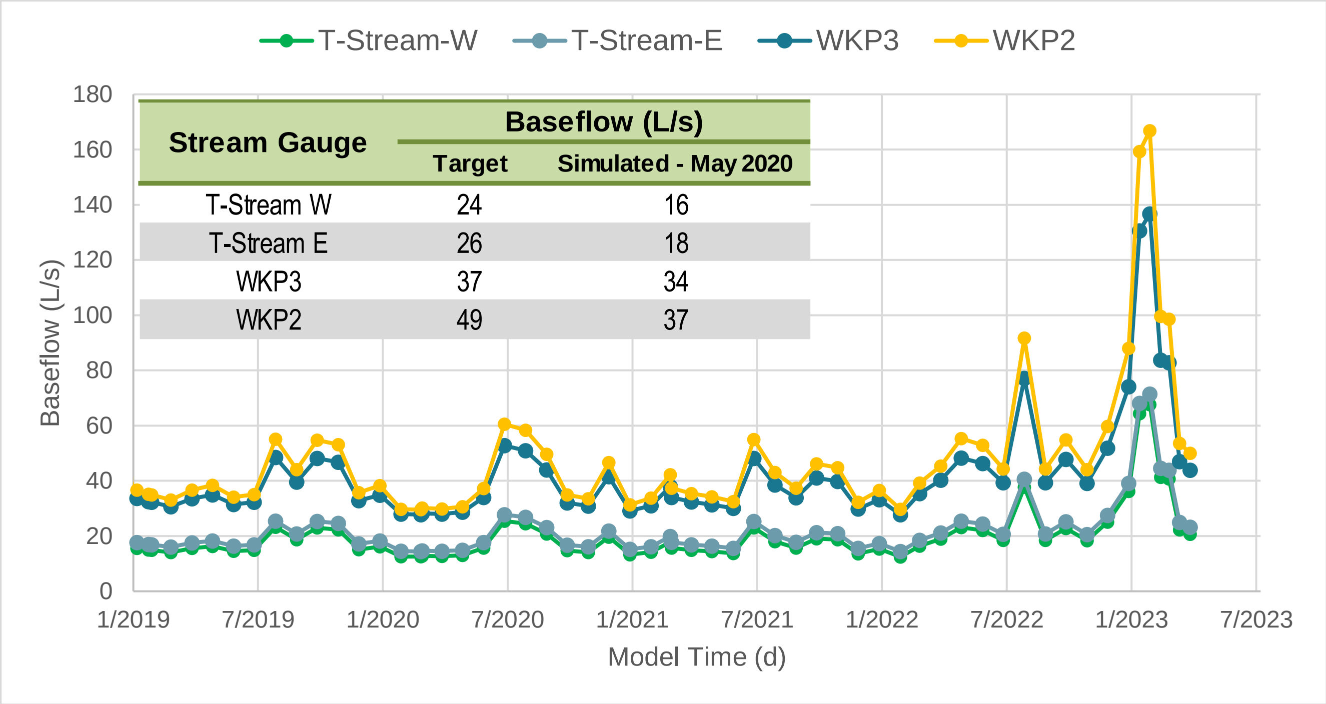


| Stream Gauge | Baseflow (L/s) | |
|---|---|---|
| | Target | Simulated - May 2020 |
| T-Stream W | 24 | 16 |
| T-Stream E | 26 | 18 |
| WKP3 | 37 | 34 |
| WKP2 | 49 | 37 |

## 4.6 Simulation

### 4.6.1 Mine Plan Implementation

OGNZL plans to implement mining over an approximate 10-year period. As a matter of model scheduling, mining has been simulated from Jan/2023 to Dec/2034 on a 6-month basis. The recharge was not modified during the simulation – parameters applied in the steady state model have been applied to model simulation.

The mine plan was converted from DXF to a cloud of points file with elevations and scheduling. Each point represents a drain cell implemented in the model to simulate voids in the subsurface created by mining (Figure 4.13).

Drains were represented with nominal widths of 5m and thicknesses (for conductance computation) of 1m. Drain conductance was computed using drain hydraulic conductivity equal to the MODFLOW cell hydraulic conductivity. When activating drains in the model, each drain remains active until the end of mining operations (in the model simulation).

The early years of the mine plan (2024, 2025 and 2026) are focusing on tunnel development from Willows farm to the mine domain, and will be completed outside of the model domain. Simulation in the groundwater model domain starts in 2027 (Figure 4.14 and Figure 4.15).

Figure 4.13 Mine plan and drain cells.

| Mine Plan | Number of drain cells |
|---|---|
| 2027 | 220 |
| 2028 | 1176 |
| 2029 | 835 |
| 2030 | 833 |
| 2031 | 500 |
| 2032 | 466 |
| 2033 | 359 |

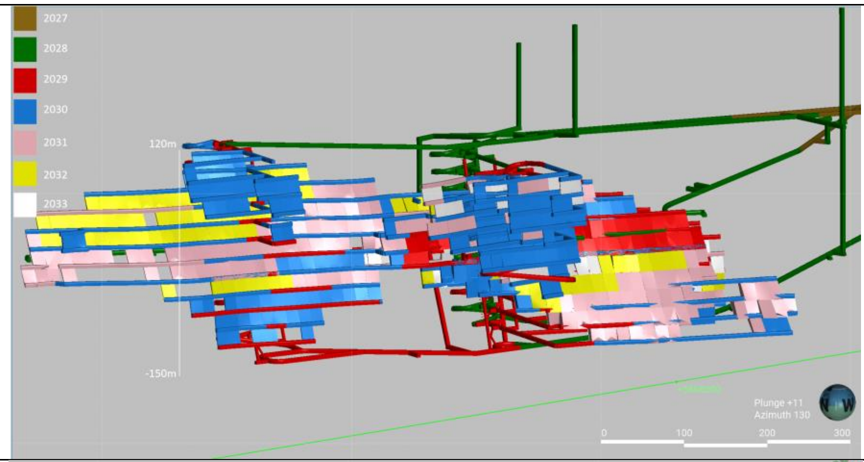


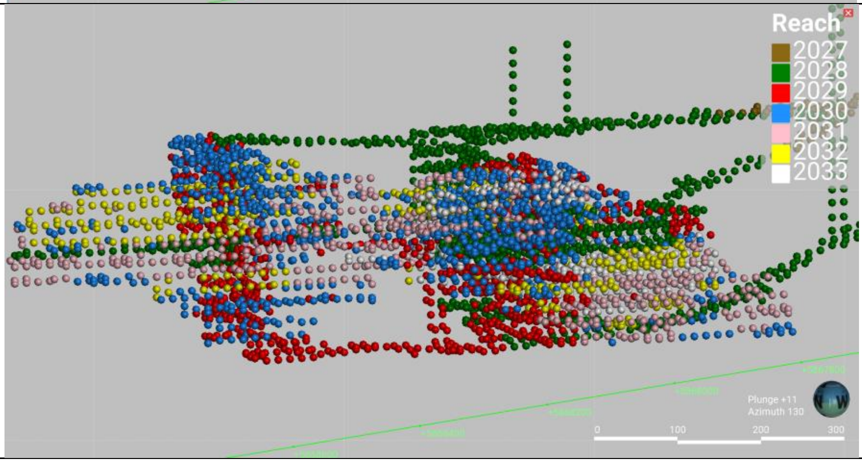

Figure 4.14 Mine Plan – Access tunnel (2024, 2025 and 2026)

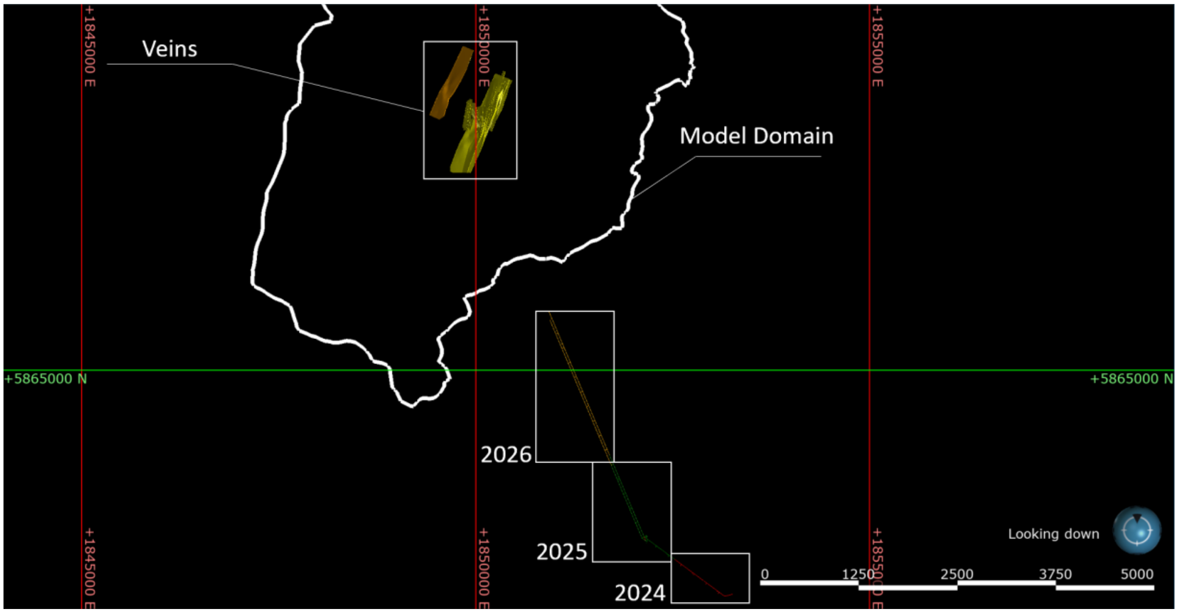


Figure 4.15 Mine Plan – Development per year – General overview

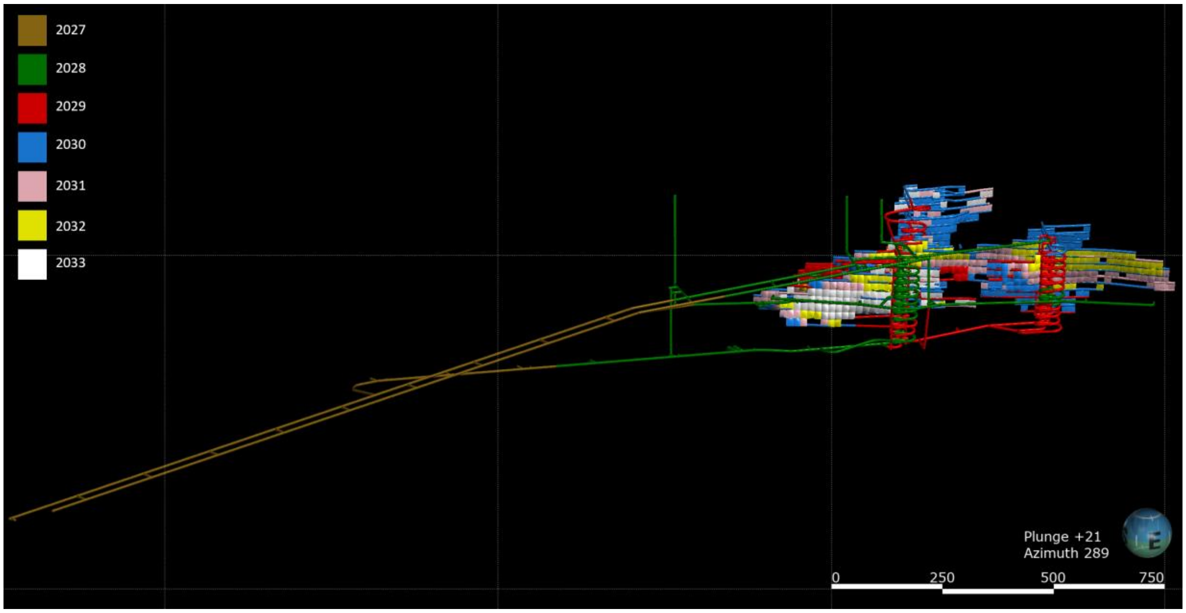

Figure 4.16 Mine Plan – Development per year – Cross section

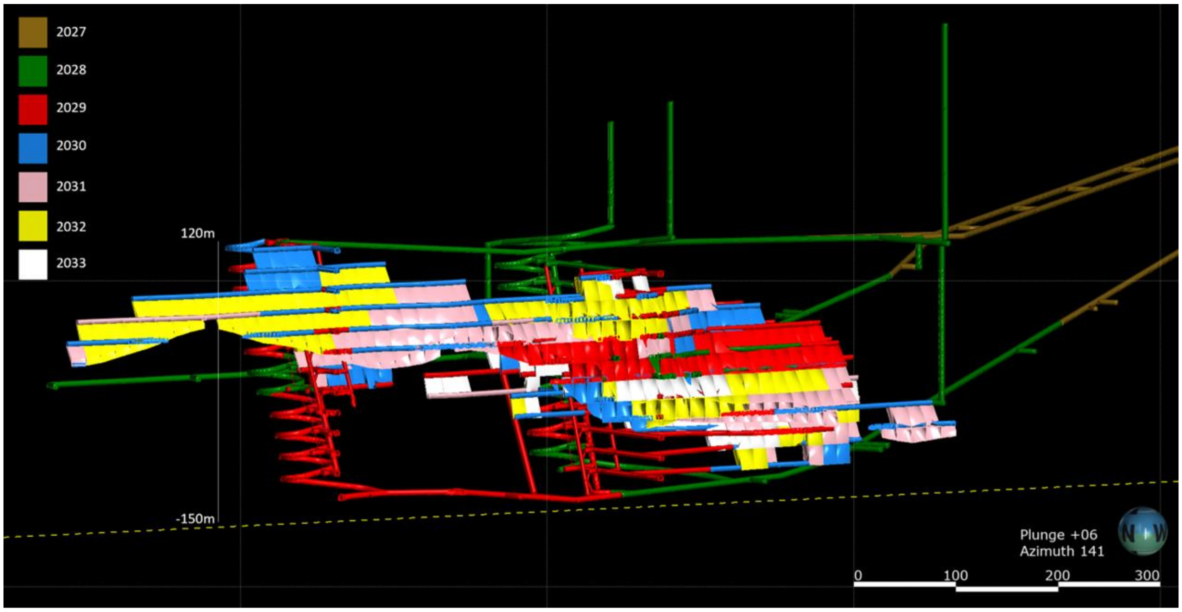


## 4.6.2 Simulation of mining

The mining simulation is run by progressively turning on the drain cells in the appropriate time period when mining reaches that area.

Table 4.9 presents the model schedule for the mine plan simulation, which consists of 24 nearly uniform periods of approximately 6 months each. The model was initially set to run by 6 months periods to allow for variable recharge (high rainfall season and low rainfall season). After initial model runs and initial results, it was defined that the best technical approach would be a conservative and constant recharge throughout the model simulation since high peaks of recharge could bias water recovery therefore affecting impact predictions.

Table 4.9 Simulation model schedule

| Simulation Period | Length [d] | Cumulative [d] | Start Date | End Date |
|---|---|---|---|---|
| 1 | 181 | 181 | 1/01/2023 | 1/07/2023 |
| 2 | 184 | 365 | 1/07/2023 | 1/01/2024 |
| 3 | 182 | 547 | 1/01/2024 | 1/07/2024 |
| 4 | 184 | 731 | 1/07/2024 | 1/01/2025 |
| 5 | 181 | 912 | 1/01/2025 | 1/07/2025 |
| 6 | 184 | 1096 | 1/07/2025 | 1/01/2026 |
| 7 | 181 | 1277 | 1/01/2026 | 1/07/2026 |
| 8 | 184 | 1461 | 1/07/2026 | 1/01/2027 |
| 9 | 181 | 1642 | 1/01/2027 | 1/07/2027 |
| 10 | 184 | 1826 | 1/07/2027 | 1/01/2028 |
| 11 | 182 | 2008 | 1/01/2028 | 1/07/2028 |
| 12 | 184 | 2192 | 1/07/2028 | 1/01/2029 |
| 13 | 181 | 2373 | 1/01/2029 | 1/07/2029 |
| 14 | 184 | 2557 | 1/07/2029 | 1/01/2030 |
| 15 | 181 | 2738 | 1/01/2030 | 1/07/2030 |
| 16 | 184 | 2922 | 1/07/2030 | 1/01/2031 |
| 17 | 181 | 3103 | 1/01/2031 | 1/07/2031 |
| 18 | 184 | 3287 | 1/07/2031 | 1/01/2032 |
| 19 | 182 | 3469 | 1/01/2032 | 1/07/2032 |
| 20 | 184 | 3653 | 1/07/2032 | 1/01/2033 |
| 21 | 181 | 3834 | 1/01/2033 | 1/07/2033 |
| 22 | 184 | 4018 | 1/07/2033 | 1/01/2034 |
| 23 | 181 | 4199 | 1/01/2034 | 1/07/2034 |
| 24 | 184 | 4383 | 1/07/2034 | 1/01/2035 |

### 4.6.3 Simulation Results

The simulation results report the following:

- Simulated water levels and water level trends for the shallow and deep groundwater systems.
- Water balance obtained from simulation.
- Estimated mine inflows / required dewatering flow rates.
- Baseflow Reduction
- Spatial (plan-view) responses to simulated stresses.

## Simulated Water Levels

Maximum water level reductions in the groundwater system generally occur near the end of mining. Water level reductions during the mining simulation relative to observation point depths are shown in Figure 4.17. Appendix C presents all the simulation graphs.

- Water levels decrease in the shallow groundwater system between 0.2m (WKP-03S) to a maximum of 15m (WKP-01D).
    - The lower reduction at WKP-03S is probably because this observation point is situated in the T-Stream Vein, outside the mining area so not really affected by the mine operation.
    - In general drawdown in the shallow groundwater system is averaging around 3m.
- Reductions in water levels in the deep groundwater system, which is strongly affected by the mining operations, can reach up to 190m (WKP-04D).
- There is a clear correlation between instrument depth and simulated drawdown. Figure 4.17 shows this correlation.

Figure 4.17: Observation points depth compared to calculated drawdown.

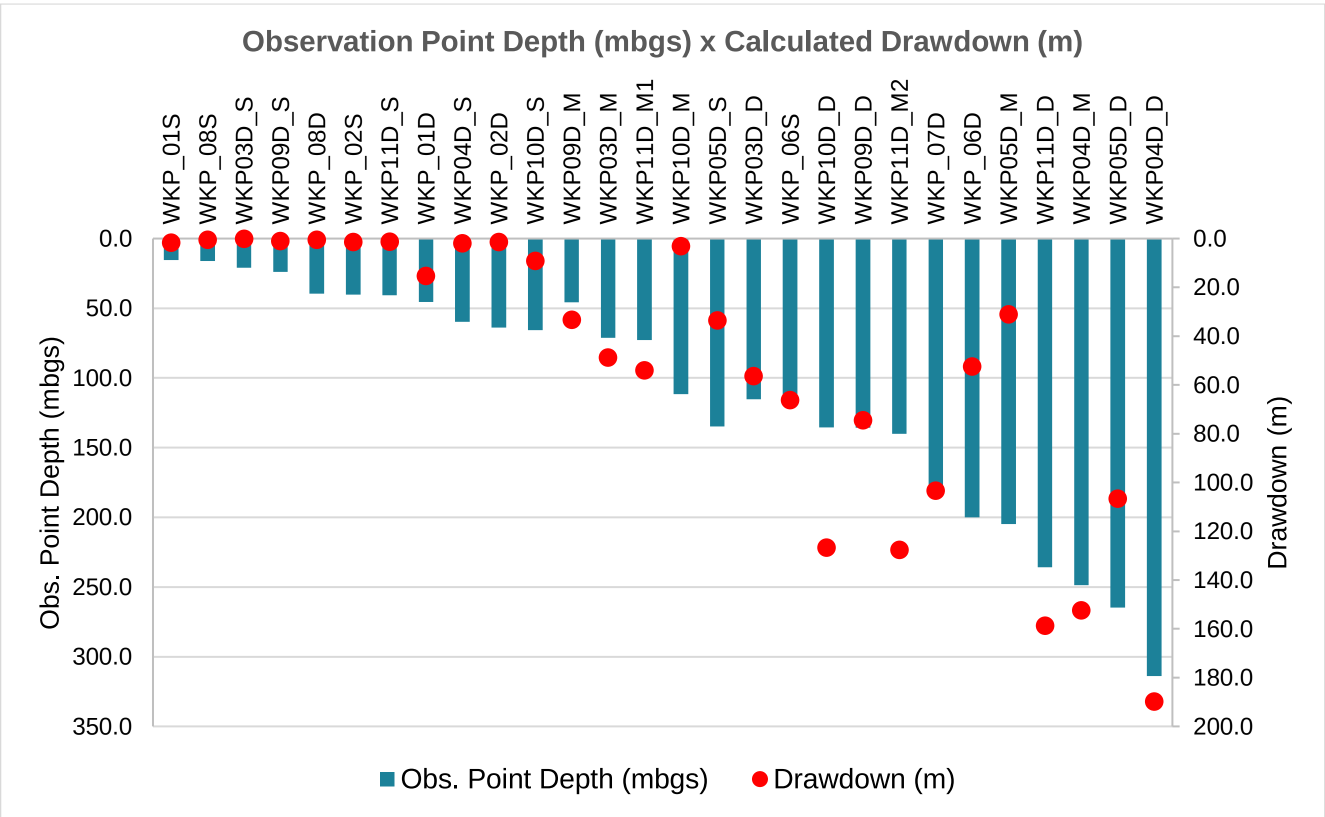

## Water Balance – Simulation

Simulation water balance has been exported from numerical model for the entire model domain. As it can be seen below, when the underground mine activates, there is an immediate response from the geological framework providing water from storage, therefore depleting water levels specially in the deep groundwater system.

Figure 4.18 Simulation water balance

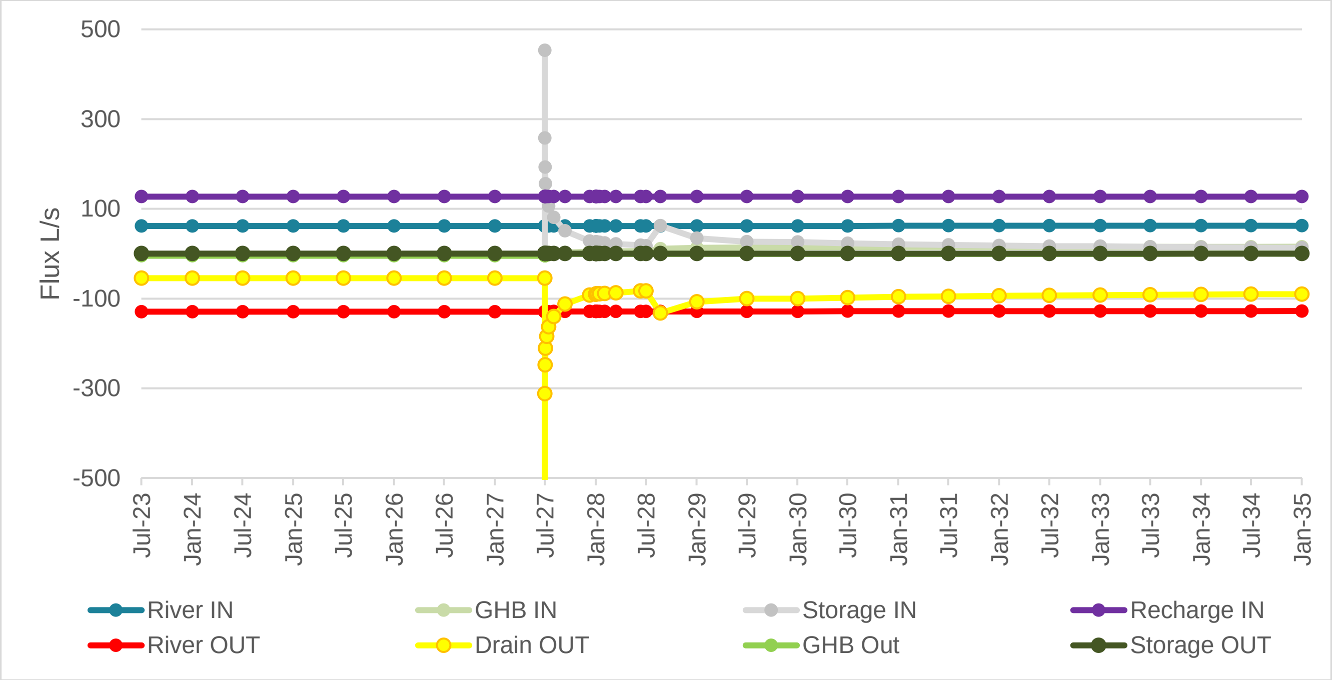

Figure 4.19 Simulation Total IN versus Total OUT

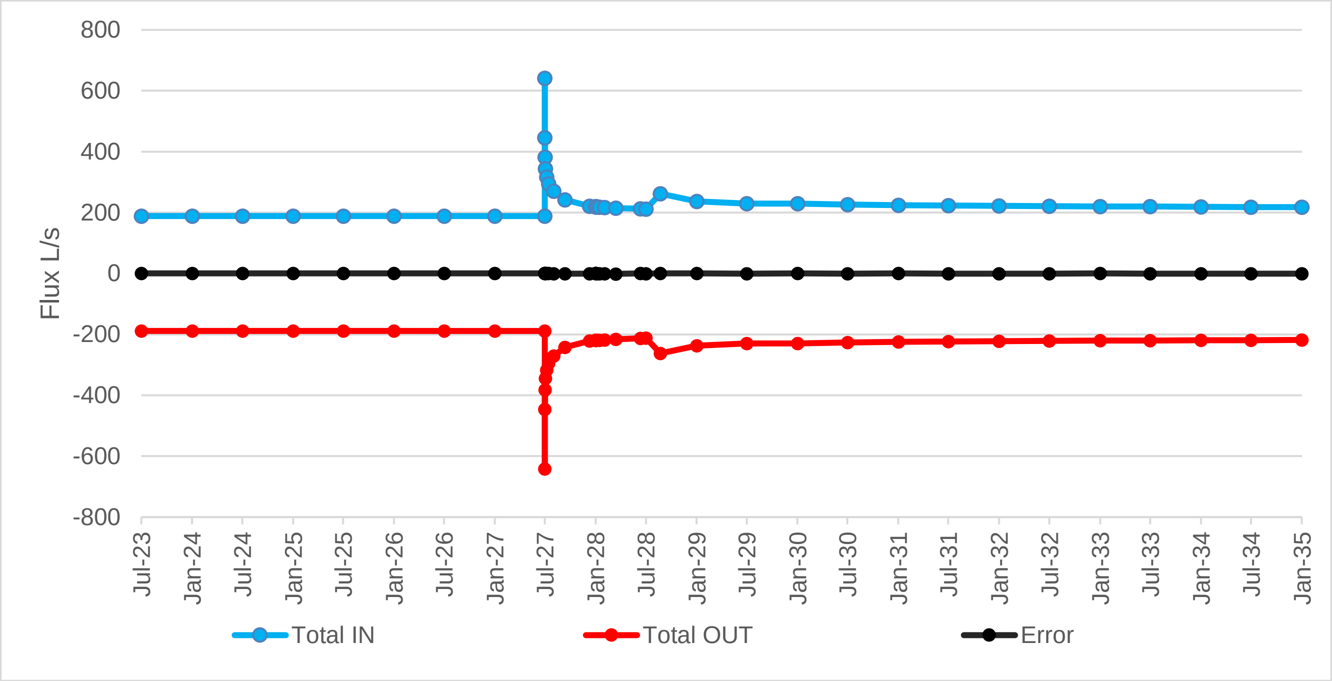


Figure 4.20 Simulation final water balance – Pre Mining versus Post Mining

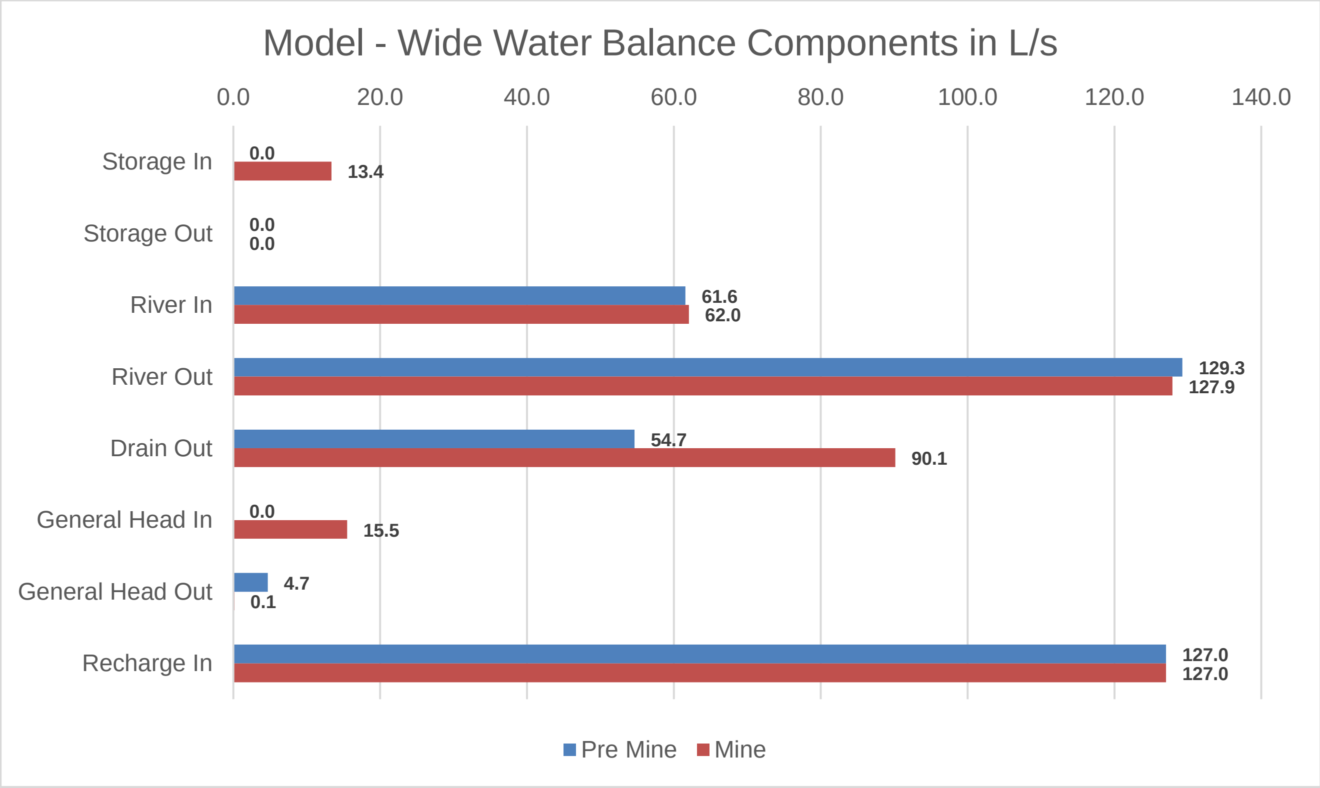

## Simulated Mine Inflows

Simulated mine inflows are in the range of 40 to 60 L/s with peak inflows during the early stress periods when drains are initially activated, and the vertical gradients between the deep aquifer static water levels and the drain cells are the greater.

For computational efficiency, all tunnels, ramps, and stopes to be dewatered during a given year were activated as drains at the beginning of the year. Consequently, large initial inflows are evident in July 2027, when tunnel construction is simulated to begin and again in July 2028, when the lower ramps are constructed. These two periods correspond to times when a relatively large volume of bedrock will be influenced by mining for the first time.

Figure 4.21 presents the simulated mine inflows until the end of mine (2033 to 2035). However, due to the use of “sudden” drain cell activation, the modelling method likely overestimates the peak flows.

Figure 4.21: Mine Inflows

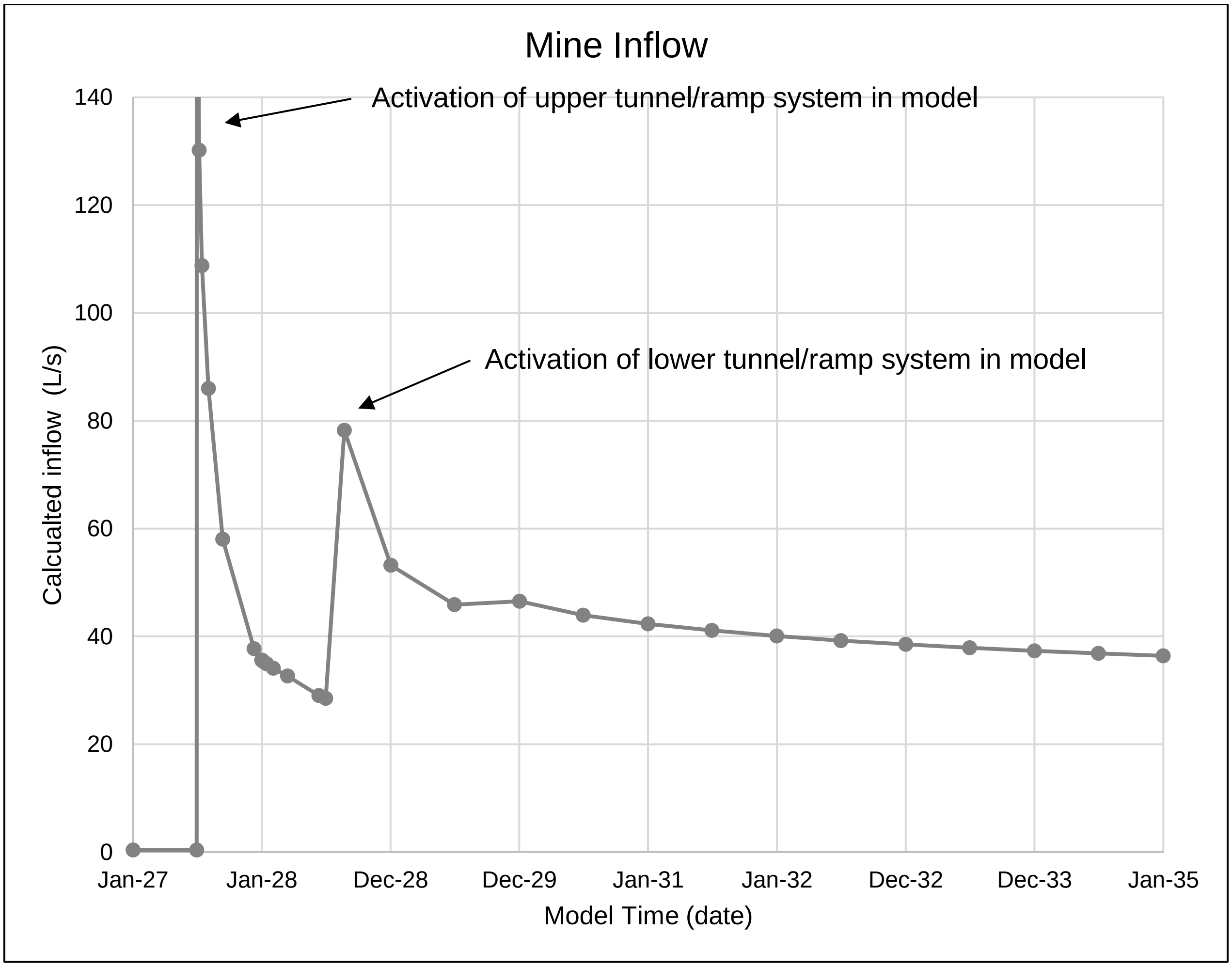

## Stream baseflow reductions

Baseflow reductions were calculated using hydrostratigraphic units (HSUs). The concept of an HSU provides a way of grouping property zones into a single unit. The model cells of the first layer of the numerical model were grouped according to its sub-catchment and using major gauging stations to define some segments within sub-catchments (WKP-3, WKP-2, T-Stream W and T-Stream E). The sub-catchments of the Wharekirauponga Stream (calculation zones) are presented in Figure 4.22. Using this calculation approach, model mass balance can be exported by each zone, therefore assessing, and comparing with real field data (as river flow gauging).

- Baseflow reduction in the sub-catchments is variable ranging from 0.3% to 7.1%
  - The highest reduction was observed in Zone 8 – 7.1% (Thompson - immediately east of mine)
  - Lowest reduction was calculated in zone 4, outside the main mining area.

Figure 4.22: Zone budgets and baseflow reductions.

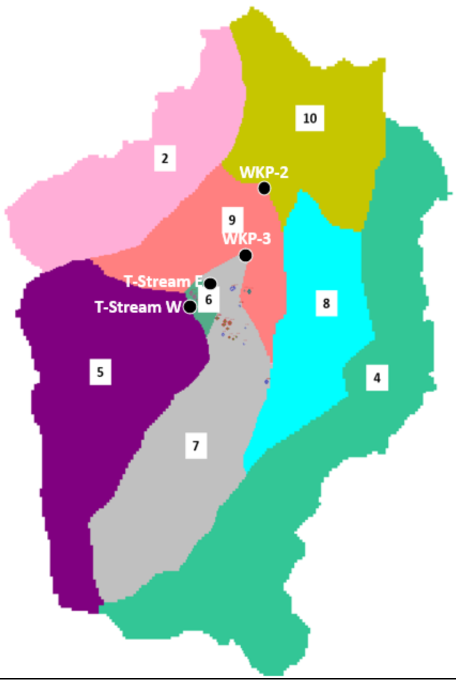


| Zones | Reduction | |
|---|---|---|
| | % | L/s |
| Zone 2 | 2.9% | -0.21 |
| Zone 4 | 0.3% | -0.14 |
| Zone 5 | 0.7% | -0.16 |
| Zone 6 | 4.0% | -0.09 |
| Zone 7 | 3.1% | -0.65 |
| Zone 8 | 7.1% | -0.48 |
| Zone 9 | 4.8% | -0.27 |
| Zone 10 | 2.6% | -0.41 |
| T-Stream W | 0.7% | -0.16 |
| T-Stream E | 1.1% | -0.25 |
| WKP-3 | 2.0% | -0.90 |
| WKP-2 | 2.3% | -1.18 |

## Drawdown (Spatial distribution)

The drawdown (DDN) cone will be more significant in the main mining area and along the Edmonds Fault (to the NE portion of the model). Some drawdown will also be observed in the tunnel area, where drain cells are placed from layer 9 to layer 19 mostly in the Rhyolite Volcaniclastics.

In general, the first layer of the model shows a maximum drawdown in the order of 2.5m, increasing to 15m in the third layer. The following figures show the DDN distribution from L1 to L9. Drawdown geometries from layer 9 forward are quite similar.

Figure 4.23: Drawdown L1 to L3

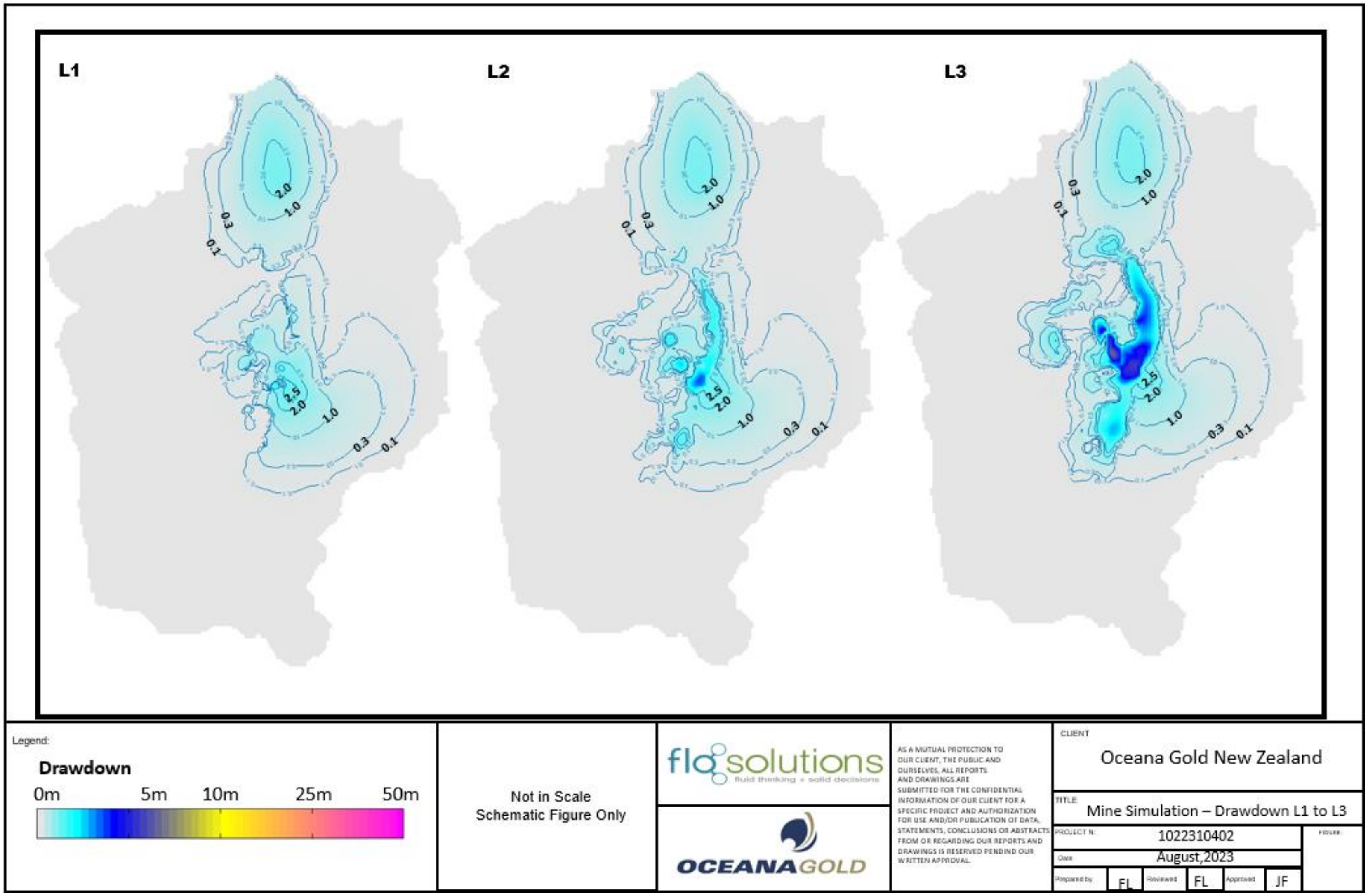

Figure 4.24: Drawdown L4 to L6

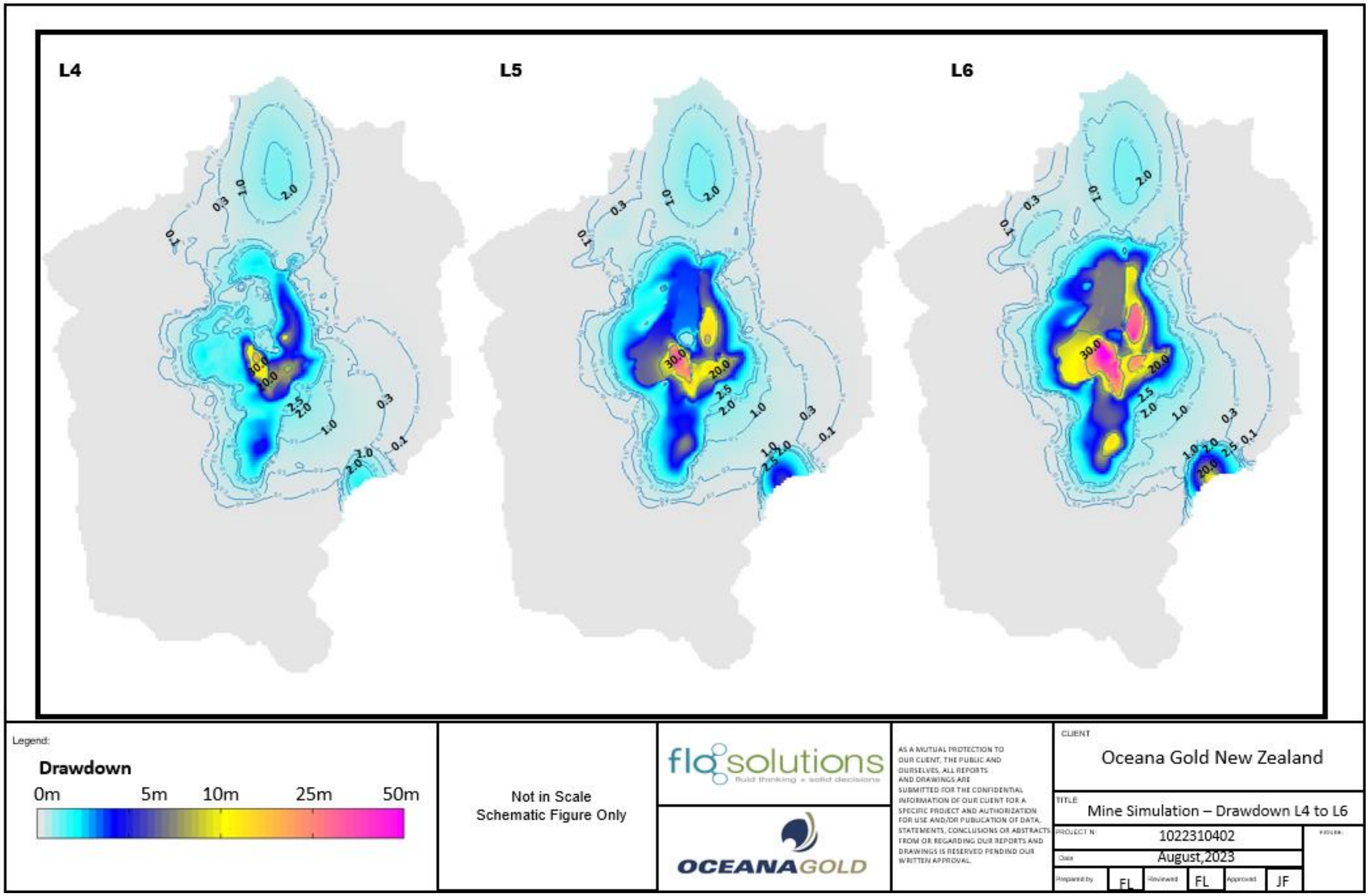

Figure 4.25: Drawdown L7 to L9

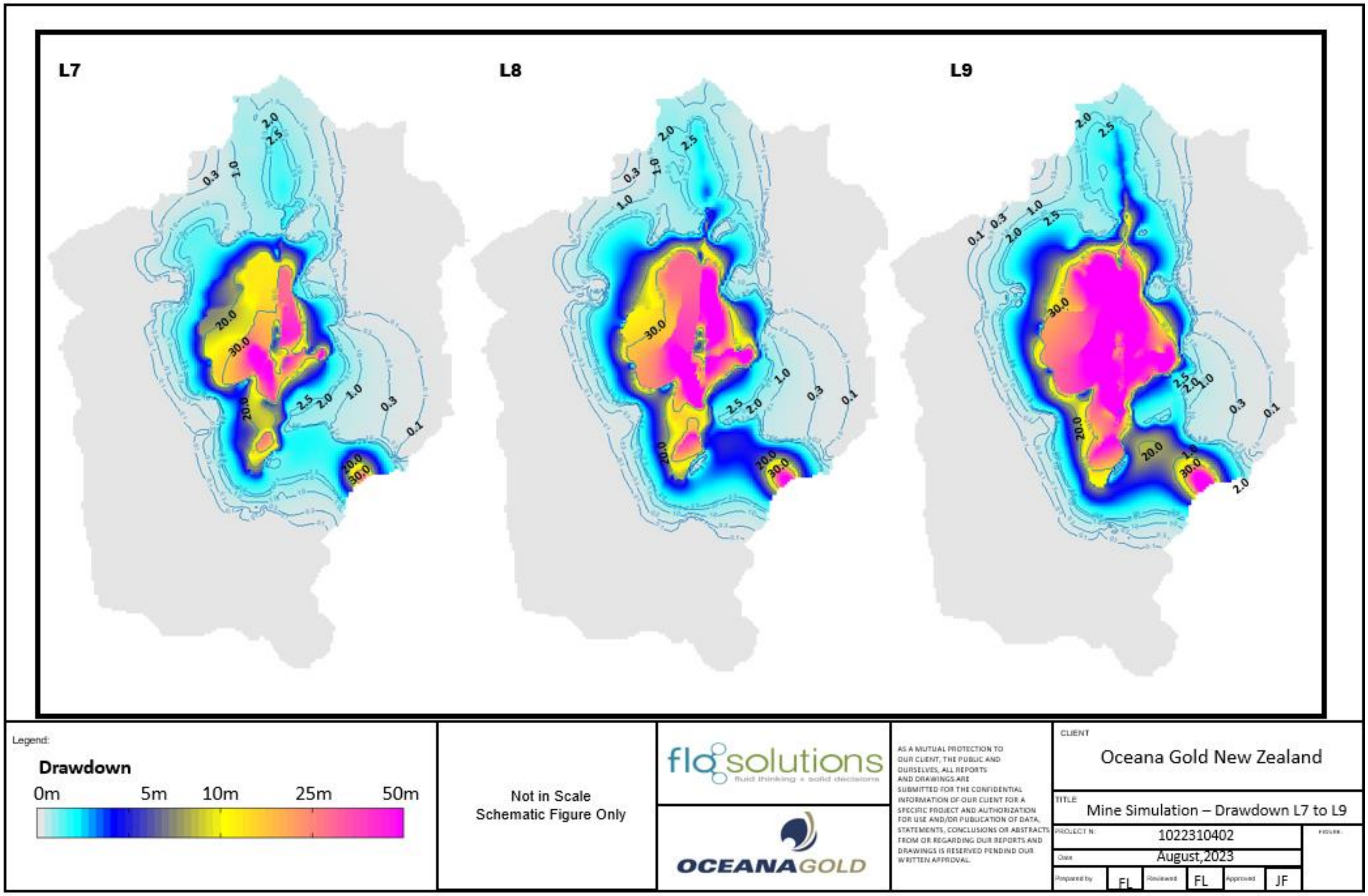

## 4.7 Sensitivity Analysis

Model sensitivity describes the changes in predicted groundwater responses to changes in model inputs. Sensitivity analyses is typically undertaken to assess the importance of various parameters on model behaviour (predictive capability).

Sensitivity analysis involves changing a model parameter by a small amount to establish how model predictions are affected by that change. Sensitivity analyses usually focuses on model input parameters that have a direct and noticeable effect on model behaviour, which may include hydraulic properties such as hydraulic conductivity and storage. Other input parameters, including boundary conditions (recharge, rivers, GHB or any other applicable boundary condition) may also be tested, although typically these have less influence on model performance.

During the model calibration (trial-and-error calibration), it was found that some units were more sensitive to changes when compared to others (for example the vein system itself and surrounding intrusive domes). Changing the K of these units resulted in a quite different model-predicted hydraulic heads and baseflow variations. Changes made to recharge were usually less significant to model results while changes to river conductance in general resulted in strong model instability and running times due to the unsaturated conditions (neither of these scenarios will be presented in the current sensitivity analysis section).

For these reasons, initial sensitivity analyses focused on changes to the hydraulic conductivity of various units.

### 4.7.1 Scenarios settings

For the current analysis, the parameters more relevant for the calibration (identified during the calibration phase), were modified by 10 (multiplying or dividing).

The baseflow variations for each scenario have been compiled for each sub-catchment. The main purpose for the current sensitivity analysis is to present a further assessment on how K variations could affect model predictions in terms of impacts on rivers (it’s important to emphasize that further and more robust analysis will be presented in the Latin Hypercube Section). Table 4.10 lists the scenarios tested.

Table 4.10 Sensitivity analysis run summary.

| Scenario | Zone | Unit | Base Case (m/s) | | | Change | Scenario Value (m/s) | | |
|---|---|---|---|---|---|---|---|---|---|
| | | | Kx | Ky | Kz | | Kx | Ky | Kz |
| SA1 | 2 | Rhyolite Volcanoclastics | 1.0E-09 | 1.0E-09 | 1.0E-10 | /10 | 1.0E-10 | 1.0E-10 | 1.0E-11 |
| SA2 | 2 | Rhyolite Volcanoclastics | 1.0E-09 | 1.0E-09 | 1.0E-10 | x10 | 1.0E-08 | 1.0E-08 | 1.0E-09 |
| SA3 | 5 | Weathered Zone | 1.5E-06 | 1.5E-06 | 8.2E-06 | /10 | 1.5E-07 | 1.5E-07 | 8.2E-07 |
| SA4 | 5 | Weathered Zone | 1.5E-06 | 1.5E-06 | 8.2E-06 | x10 | 1.5E-05 | 1.5E-05 | 8.2E-05 |
| SA5 | 8 | Eastern Rhyolite Intrusive Dome | 2.1E-08 | 2.1E-08 | 1.3E-08 | /10 | 2.1E-09 | 2.1E-09 | 1.3E-09 |
| SA6 | 8 | Eastern Rhyolite Intrusive Dome | 2.1E-08 | 2.1E-08 | 1.3E-08 | x10 | 2.1E-07 | 2.1E-07 | 1.3E-07 |

| Scenario | Zone | Unit | Base Case (m/s) | | | Change | Scenario Value (m/s) | | |
|---|---|---|---|---|---|---|---|---|---|
| | | | Kx | Ky | Kz | | Kx | Ky | Kz |
| SA7 | 9 | North Rhyolite Flow Dome | 7.7E-07 | 7.7E-07 | 3.6E-10 | /10 | 7.7E-08 | 7.7E-08 | 3.6E-11 |
| SA8 | 9 | North Rhyolite Flow Dome | 7.7E-07 | 7.7E-07 | 3.6E-10 | x10 | 7.7E-06 | 7.7E-06 | 3.6E-09 |
| SA9 | 12 | EG_1 | 4.8E-07 | 4.8E-07 | 9.6E-09 | /10 | 4.8E-08 | 4.8E-08 | 9.6E-10 |
| | 13 | EG_2 | 1.3E-08 | 1.3E-08 | 7.8E-09 | | 1.3E-09 | 1.3E-09 | 7.8E-10 |
| | 14 | EG_3 | 1.0E-05 | 1.0E-05 | 2.1E-07 | | 1.0E-06 | 1.0E-06 | 2.1E-08 |
| SA10 | 12 | EG_1 | 4.8E-07 | 4.8E-07 | 9.6E-09 | x10 | 4.8E-06 | 4.8E-06 | 9.6E-08 |
| | 13 | EG_2 | 1.3E-08 | 1.3E-08 | 7.8E-09 | | 1.3E-07 | 1.3E-07 | 7.8E-08 |
| | 14 | EG_3 | 1.0E-05 | 1.0E-05 | 2.1E-07 | | 1.0E-04 | 1.0E-04 | 2.1E-06 |
| SA11 | 15 | Alteration Zone | 1.1E-08 | 1.1E-08 | 1.5E-09 | /10 | 1.1E-09 | 1.1E-09 | 1.5E-10 |
| SA12 | 15 | Alteration Zone | 1.1E-08 | 1.1E-08 | 1.5E-09 | x10 | 1.1E-07 | 1.1E-07 | 1.5E-08 |
| SA13 | 18 | South Edmonds | 2.0E-05 | 2.0E-05 | 3.7E-08 | /10 | 2.0E-06 | 2.0E-06 | 3.7E-09 |
| | 19 | North Edmonds | 3.0E-05 | 3.0E-05 | 3.7E-08 | | 3.0E-06 | 3.0E-06 | 3.7E-09 |
| SA14 | 18 | South Edmonds | 2.0E-05 | 2.0E-05 | 3.7E-08 | x10 | 2.0E-04 | 2.0E-04 | 3.7E-07 |
| | 19 | North Edmonds | 3.0E-05 | 3.0E-05 | 3.7E-08 | | 3.0E-04 | 3.0E-04 | 3.7E-07 |

### 4.7.2 Baseflow variations

In total, 8 zones (sub-catchments) were defined in the catchment of the Wharekirauponga Stream (as previously discussed in section 4.6.3 ). Sensitivity analyses runs resulted in changes to predicted stream baseflow reductions relative to those predicted by the base case model. Table 4.11 presents the baseflow reduction results for the scenarios with the highest baseflow reductions in each subcatchment. Table 4.12 presents results for the scenarios with the lowest baseflow reductions in each subcatchment. Detailed results are presented in Appendix D.

Table 4.11: Calculated reductions per sub-catchment (Highest Reductions)

| Zone | Base Case Reduction | Highest Reduction | Reduction (l/s) | Scenario |
|---|---|---|---|---|
| Zone 2 | 2.9% | 18.4% | -0.23 | SA4 |
| Zone 4 | 0.3% | 2.2% | -0.94 | SA2 |
| Zone 5 | 0.7% | 2.8% | -0.59 | SA12 |
| Zone 6 | 4.0% | 18.2% | -0.38 | SA10 |
| Zone 7 | 3.1% | 11.2% | -2.37 | SA12 |
| Zone 8 | 7.1% | 21.3% | -1.38 | SA2 |
| Zone 9 | 4.8% | 18.7% | -0.89 | SA12 |
| Zone 10 | 2.6% | 7.0% | -1.09 | SA2 |
| T-Stream W | 0.7% | 2.8% | -0.59 | SA12 |
| T-Stream E | 1.1% | 4.0% | -0.93 | SA12 |
| WKP-3 | 2.0% | 7.4% | -3.29 | SA12 |
| WKP-2 | 2.3% | 8.5% | -4.19 | SA12 |

Table 4.12: Calculated reductions per sub-catchment (Lowest Reductions)

| Zone | Base Case Reduction | Lowest Reduction | Reduction (l/s) | Scenario |
|---|---|---|---|---|
| Zone 2 | 2.9% | 0.8% | -0.06 | SA3 |
| Zone 4 | 0.3% | 0.1% | -0.04 | SA3 |
| Zone 5 | 0.7% | -0.7% | 0.16 | SA4 |
| Zone 6 | 4.0% | 1.1% | -0.02 | SA11 |
| Zone 7 | 3.1% | 0.4% | -0.09 | SA11 |
| Zone 8 | 7.1% | -2.2% | 0.09 | SA4 |
| Zone 9 | 4.8% | 1.7% | -0.10 | SA11 |
| Zone 10 | 2.6% | 0.9% | -0.41 | SA4 |
| T-Stream W | 0.7% | -0.7% | 0.16 | SA4 |
| T-Stream E | 1.1% | -2.2% | 0.35 | SA4 |
| WKP-3 | 2.0% | 0.3% | -0.15 | SA11 |
| WKP-2 | 2.3% | 0.5% | -0.25 | SA11 |

Based on the results presented in Table 4.11 and Table 4.12, the following observations can be made:

- Highest baseflow reductions are usually associated with scenario SA12 (increasing the K of the Alteration Zone by 10), indicating that the Alteration Zone plays an important role in limiting interactions between the deeper groundwater zone and shallow groundwater. Increasing the K of this unit results in enhance interaction between the shallow and deep groundwater systems.
- Increasing the K of Rhyolite Volcaniclastics (Scenario SA2) also changes the way the shallow and deep groundwater system interacts, especially in the downstream area and the eastern portion of the model (Zones 8 and 10), that are underlain by this geological unit.
- The lowest baseflow reductions or baseflow increase are associated with 2 main scenarios, Scenario SA4 and Scenario SA11
  - Scenario SA4 simulates a higher K value in the weathered zone. Under a higher K, the weathered zone, which is the shallowest geological unit, can absorb more water from recharge therefore baseflows increase in some zones.
  - Scenario SA11 simulates a lower K at the alteration zone (opposite condition of scenario SA12), which results in decreased interaction between the shallow and deeper groundwater systems. Simulated water levels and water level trends for the deep groundwater system have less effect on shallow groundwater and baseflows.

## 4.8 Post mining flow analysis

Post-mining assessment is typically undertaken to simulate long-term conditions, including recovery of the water table, after mining is completed. These simulations are usually developed in the numerical model after the model is properly calibrated, as part of the predictive simulations. This is done by increasing the predictive model simulation period by several years or decades after completion of mining, to allow for the groundwater heads to fully recover. Under these conditions, further assessment on heads and groundwater fluxes post-mining can be made.

The post-mining model was initially developed to assess groundwater level recover time and residual impacts (if any). Simulations were later enhanced to support geochemical modelling and predictions of water quality currently being carried out separately by AECOM, including particle tracking, and additional zone budget analysis.

Post mining analysis is focused on:

- Identify main mine inflows and outflows after drain cells are deactivated.
- Calculate particle travel times from mine galleries and assess trajectory.
- Recovery Time

### 4.8.1 Mine and Decline Inflows / Outflows

Assessment of mine inflows were made using Zone Budgets (or HSUs) – as previously discussed, this tool allows for grouping or dividing geological units based on the scenario that needs to be assessed. For the current assessment, the groundwater inflows to the mine (areas of former workings as well as decline to access the workings) and groundwater outflows needed to be assessed.

The numerical model grid cells containing the mine workings and decline ramps were grouped into one HSU (Mine), and geological units above the Mine HSU were grouped into another HSU (Shallow Rock) to distinguish groundwater entering the mine workings and decline areas from above from inflows derived from deeper groundwater.

Calculations were made considering the steady state models and assuming that the underground mine will be backfilled to permeabilities similar to the pre-mining Ks. An alternative testing was completed with backfilling material 10 times greater in hydraulic conductivity, but no real variation has been observed. For the current analysis, the base case scenario is presented to give a range of mine inflow sources.

As can be seen on graphs below, the vast majority (90%) of mine inflow (i.e., groundwater flow into the Mine HSU) will come from the EG3 (47%) plus direct recharge + shallow rock (43%).

Figure 4.26: Main mine inflows (L/s and % of total)

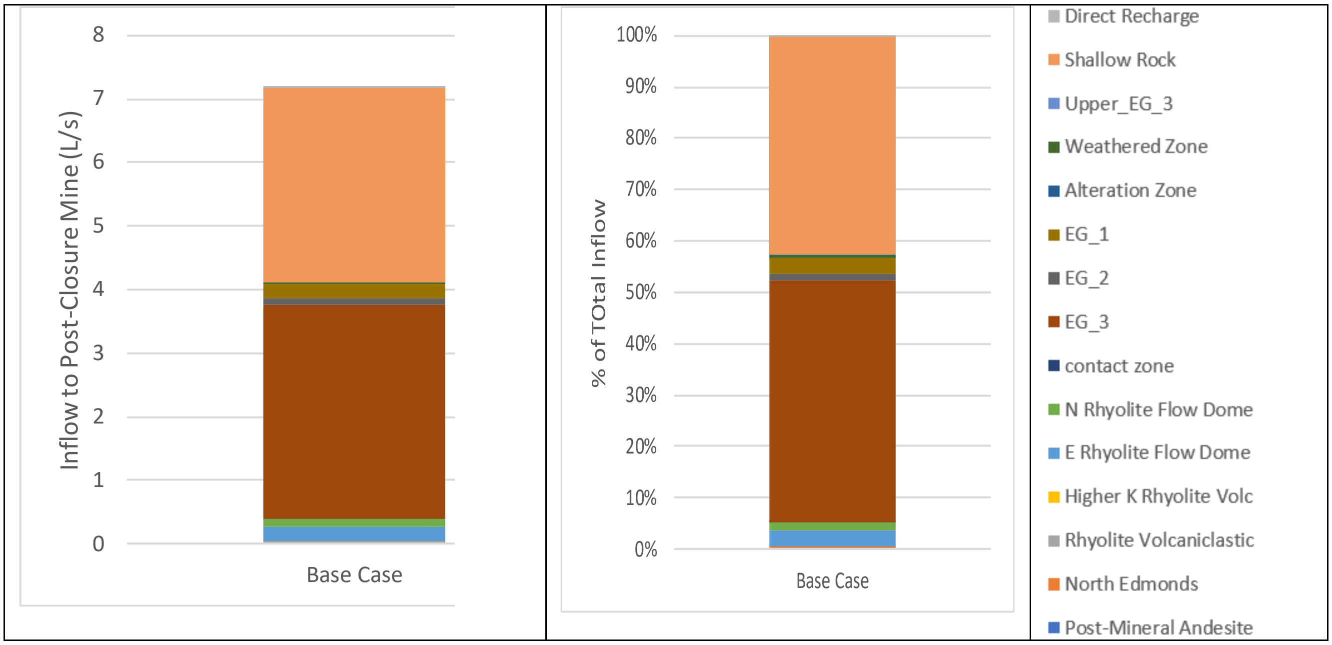


In terms of mine outflows, most of outflows will pass through the EG3 (almost 75%), while the second most common outflows will pass through the EG1 (around 9%).

Figure 4.27: Main mine outflows

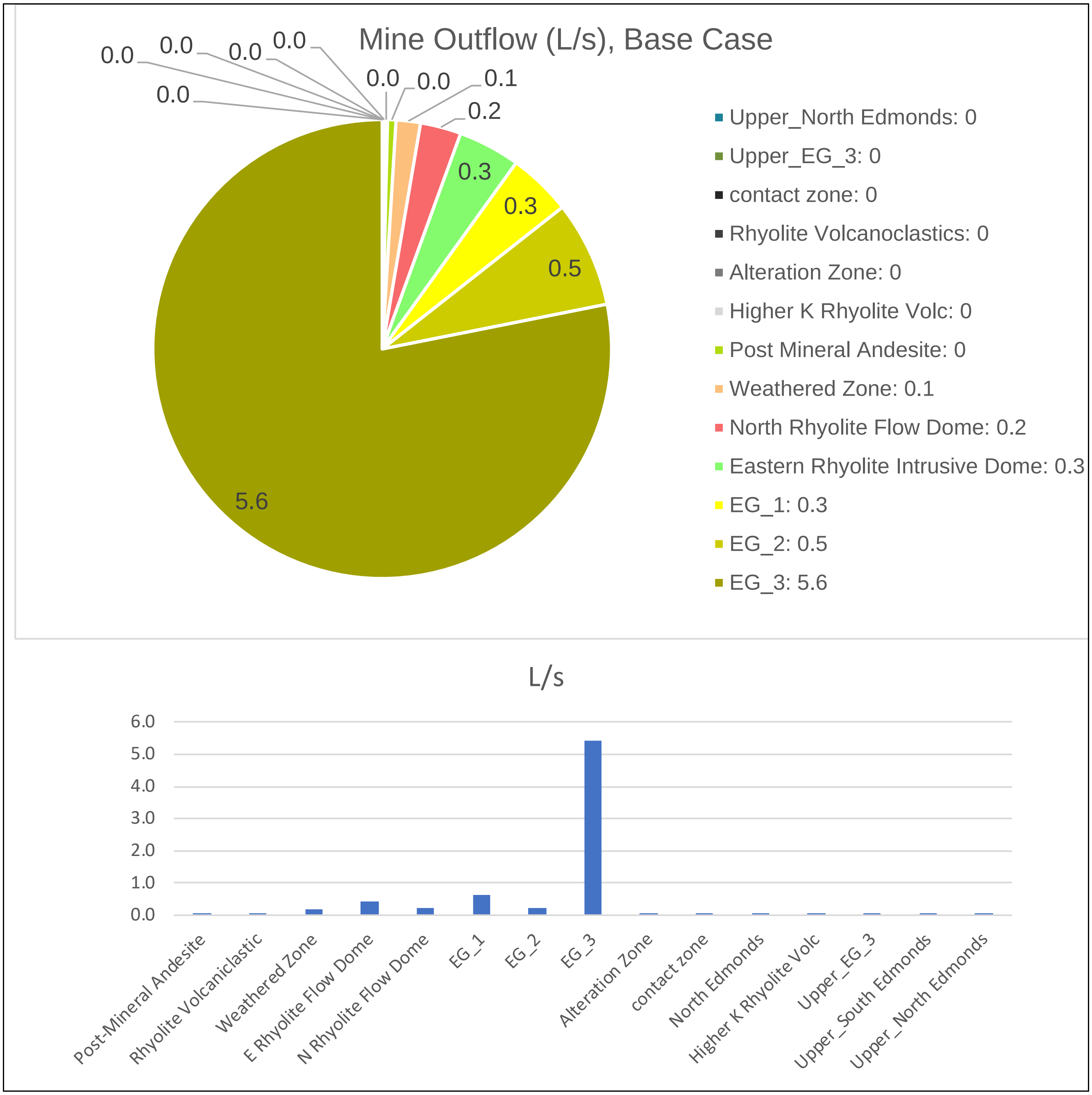


The zone budgets for the EG3 vein are shown in Figure 4.28. There is a large amount of interchange between the cells containing the mine workings and the EG3 vein, due to the three-dimensionality of the proposed mine workings. This can be seen by the 5.6 L/s of outflow from the mine workings to the EG3 vein compared to the 5.4 L/s of inflow from the EG3 vein to other parts of the mine. The primary receptor of groundwater that flows out of the mine workings is the North Edmonds Fault, followed by the north rhyolite flow dome.

Figure 4.28: EG3 Water Budget

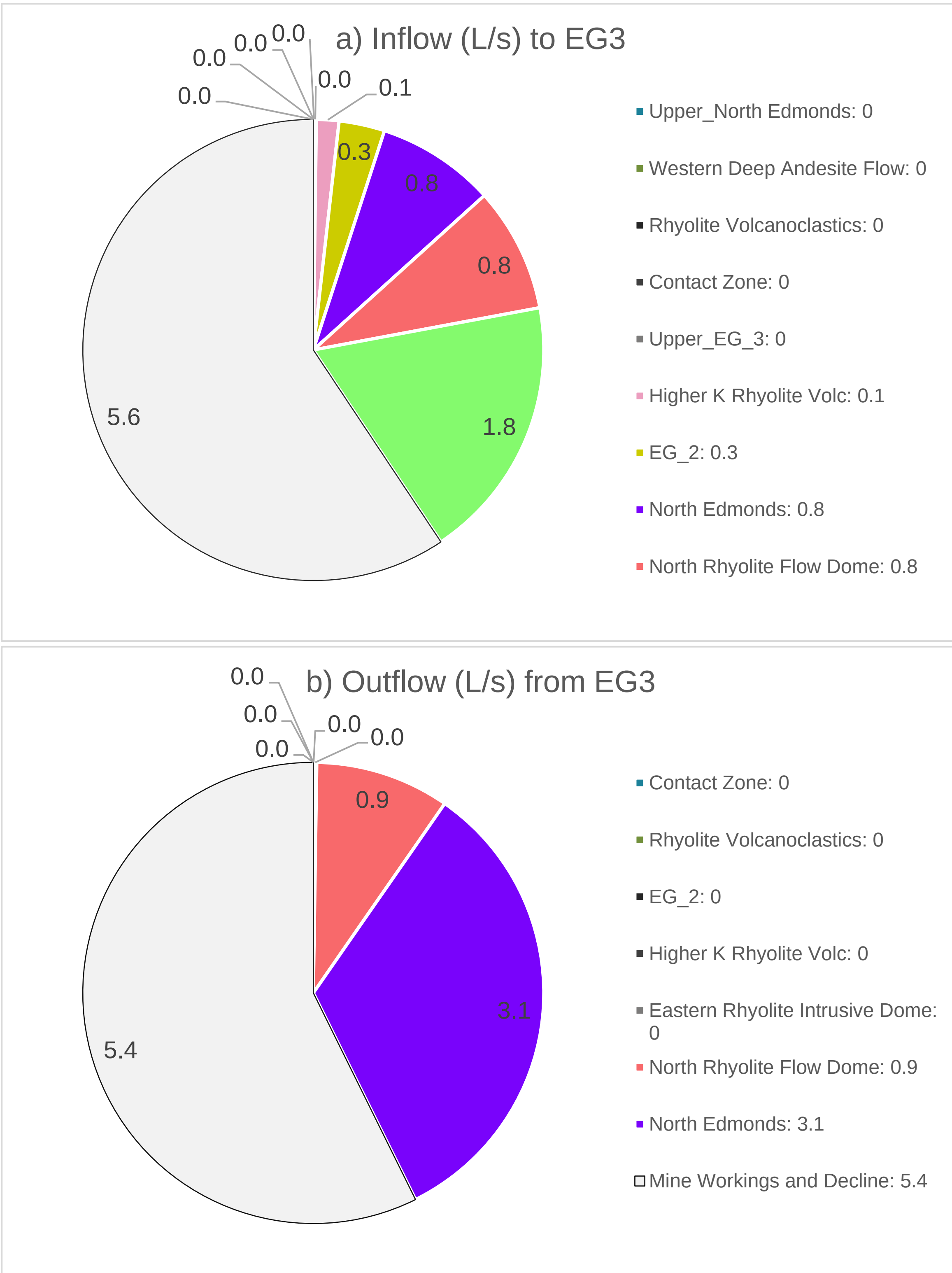

### 4.8.2 Particle Tracking

Predictive particle-tracking scenarios provide a useful means of estimating travel times and directions. The method involves placing particles at locations of interest in the model domain and defining a release time for these particles during the simulation (whenever applicable). The model records the position of the particle at each time step, and the resulting trace defines the particle trajectory through the model domain over time. In the particle-tracking assessment, the effective porosity for groundwater velocity calculations is assumed to be equal to the specific yield values from the transient calibration (Table 4.8). This is because there is some similarity in the definitions of these two properties.

- The effective porosity for solute transport describes the portion of soil pore or bedrock fracture that facilitates solute movement. For example, the effective porosity excludes the volume around the sediment or bedrock surface lining a pore space, because in this part of the void space water molecules have either zero or very low velocity.
- The specific yield, by contrast, describes the portion of the pore or fracture that drains due to the decline of the piezometric head by one unit. The specific yield is lower than the total porosity also partly due to the adhesion between solid and liquid near the solid-liquid interface.

For the purposes of this analysis, these two quantities are assumed to be equivalent.

Particles were inserted at various points in the model to facilitate tracking. Particles were also placed in all drain cells representing mine galleries and released at the same time. The transient model was then calculated using mod-PATH3DU (particle tracking program available for MODFLOW and MODFLOW-USG).

The results are important output for post-mining water quality assessments by giving an idea of general pathways and times that water from underground galleries will reach their endpoints.

Figure 4.29 shows the mine galleries overlapped with the simulated particles. Results of the simulation indicate that most of the particles (92%) will go to Edmonds Fault and then travel downstream to the GHB boundary condition (Table 4.13) (Figure 4.32 shows the particles pathlines after model simulation). This is because particles have a preferential flow pathway along the Edmonds Fault, which has higher permeability than surrounding rocks, to the N/NE portion of the area, where deep groundwater flow leaves the model.

The GHB Boundary Condition is the main particle outlet, which confirms that the Edmonds Fault is controlling the underground flow during the mine simulation (by helping to keep the deep groundwater levels low) and during post mining simulations, by facilitating the underground flux along this regional permeable structure. Considering the importance of the Edmonds Fault structure on regional flow, further field assessment and testing of this structure will be required pre-mining and during mine development.

Approximately 7% of particles will stop at the water table within the workings, during the period where the water table is rising (first 17 years). This is because the mine workings represent a low point in the water table during water level recovery, with radially inward flow. A very small percentage of particles (less than 1%) will be either stagnated or will reach stream reach 9 (Figure 4.30).

Figure 4.29: Mine galleries and particles.

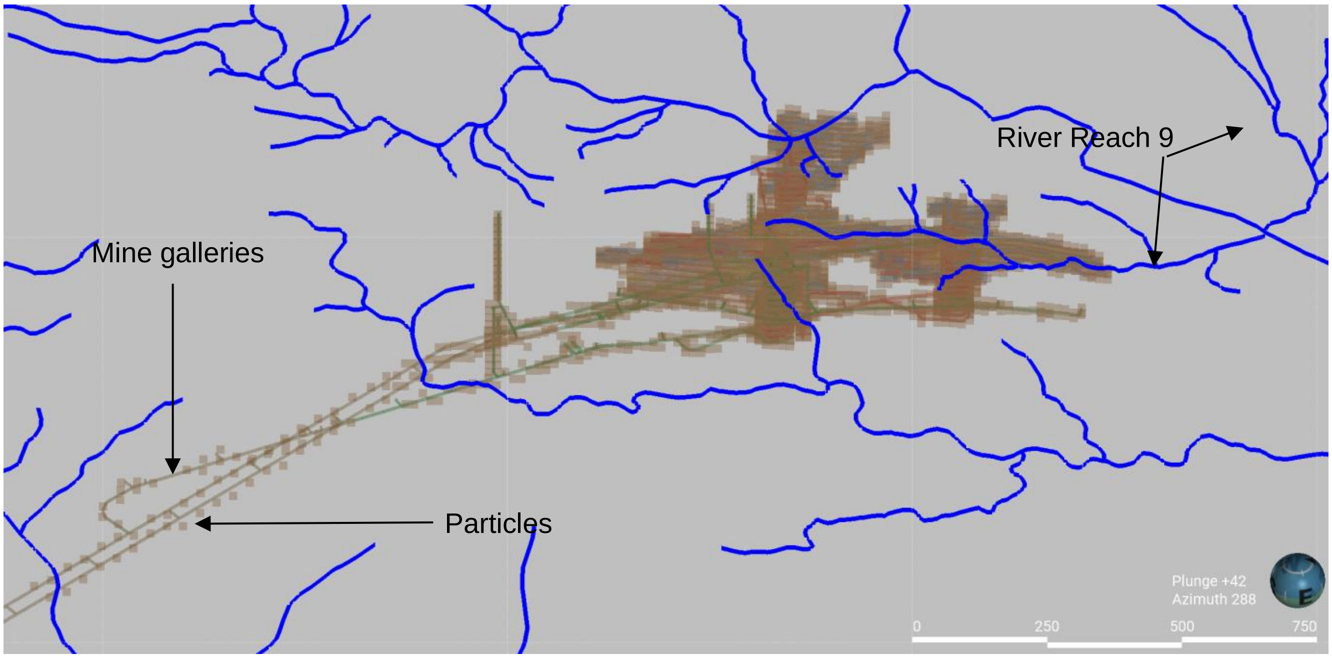

Figure 4.30: Rivers and Reach 9

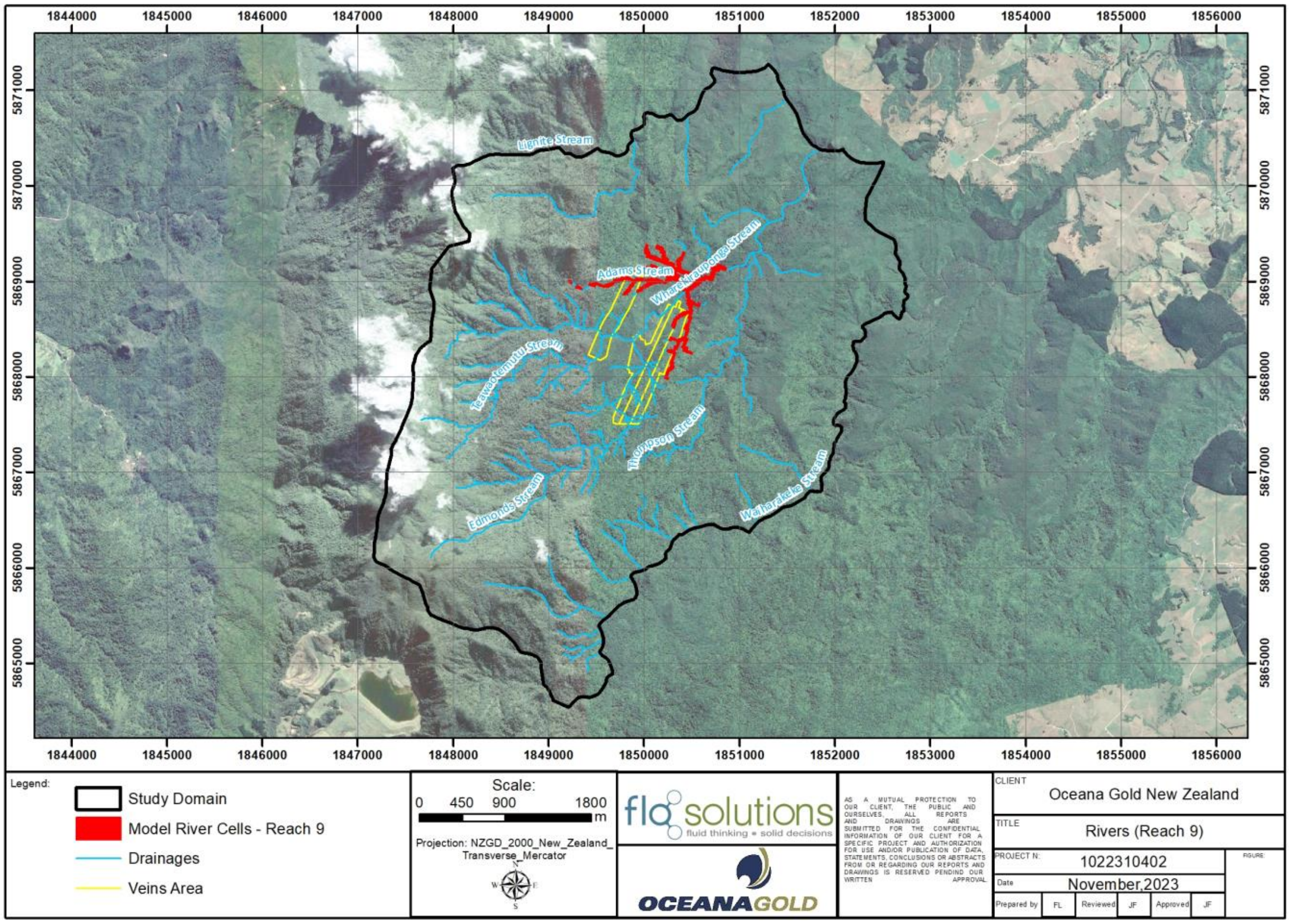


Table 4.13: Particles captured by each different model structures.

| Particle Captured by: | Number of Particles | % |
|---|---|---|
| Edmonds Fault - GHB | 3894 | 92.14% |
| Water Table | 315 | 7.45% |
| Stagnated - DT very small | 13 | 0.31% |
| Streams (Reach 9) | 4 | 0.10% |

Travel times from particle starting locations to the endpoint can be quite variable depending on where the particle has been set (in which geological unit). Travel time in the Edmonds Fault presents median time of 91 years with first arrival in 32 years.

Particles in the EG-Vein and closer to Edmonds fault usually move faster when compared to particles located in the tunnel area where K and porosity are lower.

To help visualize particle travel times in detail, eight (8) groups of particles with similar travel times are defined, as illustrated graphically in Figure 4.31. Groups arranged from particles with the shortest travel times (Group 1) to the longest travel times (Group 8). Travel times for each group are summarized in Table 4.14. Detailed figures for each particle group are contained in Appendix E - below

Figure 4.31: Particle groups

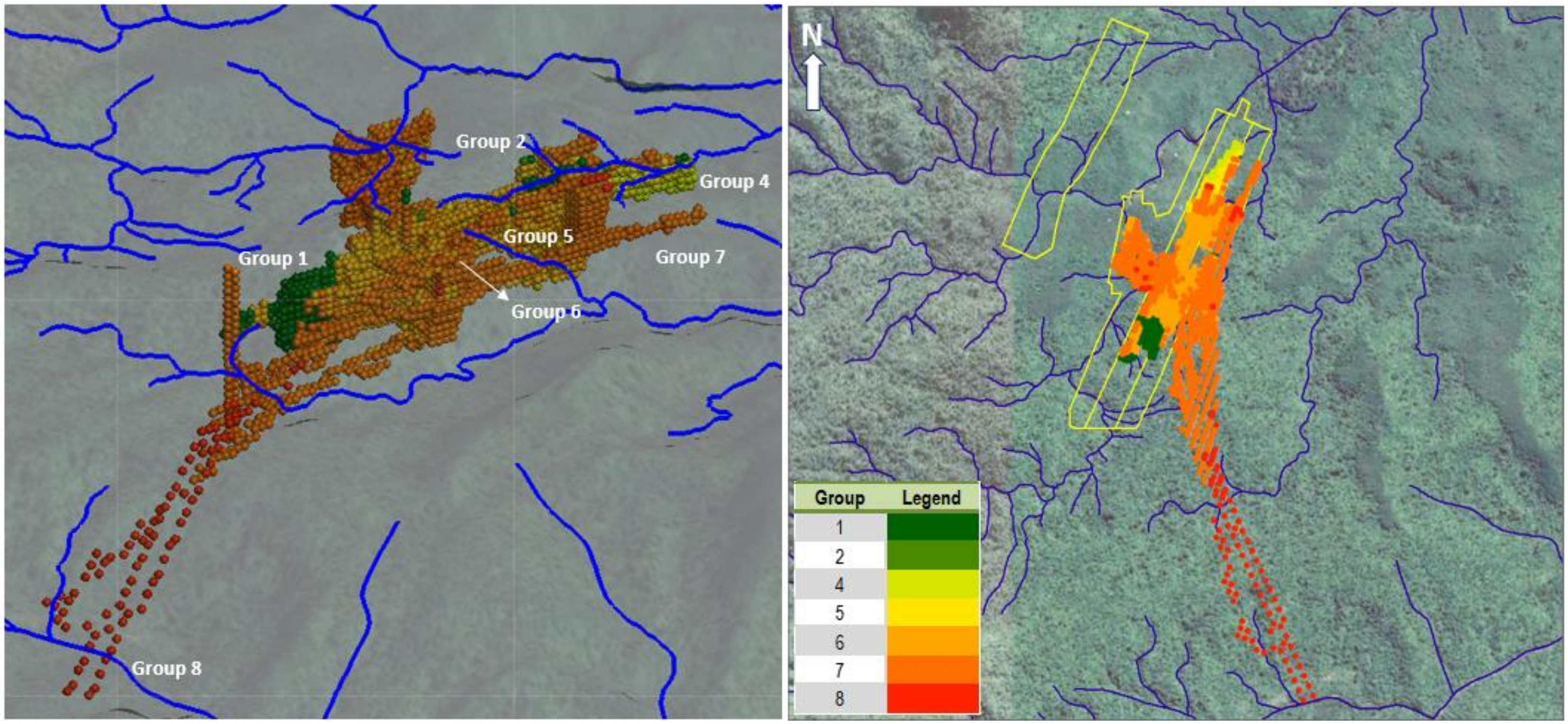

Table 4.14: Travel times calculated for each group of particles.

| Group | Average Travel Time (Years) | Number of Particles | % of total |
|---|---|---|---|
| 1 | 0.1 | 316 | 7.5% |
| 2 | 13.3 | 12 | 0.3% |
| 3 | - | - | - |
| 4 | 36.9 | 82 | 1.9% |
| 5 | 46.1 | 212 | 5.0% |
| 6 | 72.7 | 1851 | 43.8% |
| 7 | 325.7 | 1632 | 38.6% |
| 8 | 27527.4 | 121 | 2.9% |

Figure 4.32 Particles pathlines

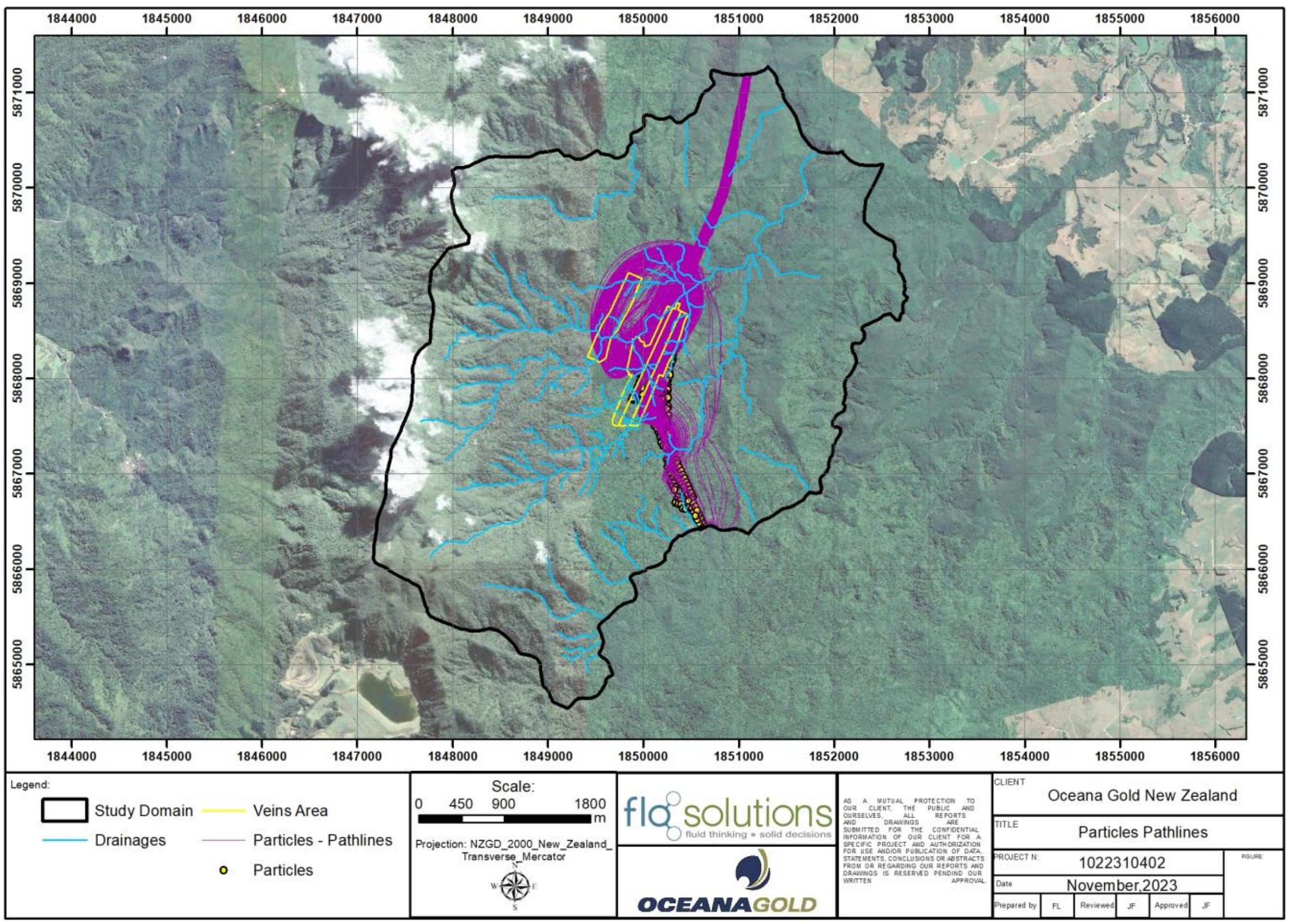

### 4.8.3 Mine Recovery

As previously discussed, the mine recovery simulation consists of extending the transient simulation model by a few decades to allow for the water levels to recover. If a full recovery is not observed from the observation points, more time can be added to the model simulation to allow for a complete water level recovery.

The mine simulation model was adjusted to run an additional 40 years from the end of mining. Drains remained active thorough the mining period up to 2035, at which point they were turned off simultaneously to simulate cessation of dewatering. Recharge was also maintained constant throughout the model simulation.

Results are presented in a series of graphs, Figure 4.33, Figure 4.34, Figure 4.35, Figure 4.36, and Figure 4.37. Water level recovery is shown in Figure 4.33 and Figure 4.34. As can be seen from these figures, the water level rebound is variable depending on the piezometer location and the catchment analysed, but, in general, water level recovery times to pre-mining water levels take approximately 30 to 40 years.

Considering the methodology that the groundwater model uses to calculate the recovery (sudden shut down of all drain cells) sometimes the observation points show a rapid / stronger water level rebound in the first years followed by gradual water level recovery (as can be seen on the calculated heads from points WKP-08D, Edmonds, WKP3 and WKP2).

Base flow recovery is presented in Figure 4.35, Figure 4.36, and Figure 4.37 – which have different scales based on base flow of the relevant sub-catchment.  For most sub-catchments, base flow reductions are less than 1 L/sec, and recovery occurs on the order of ~ 30 years.

Figure 4.33: Water level recovery graphs (WKP04D, WKP07D, WKP06D, WKP03D)

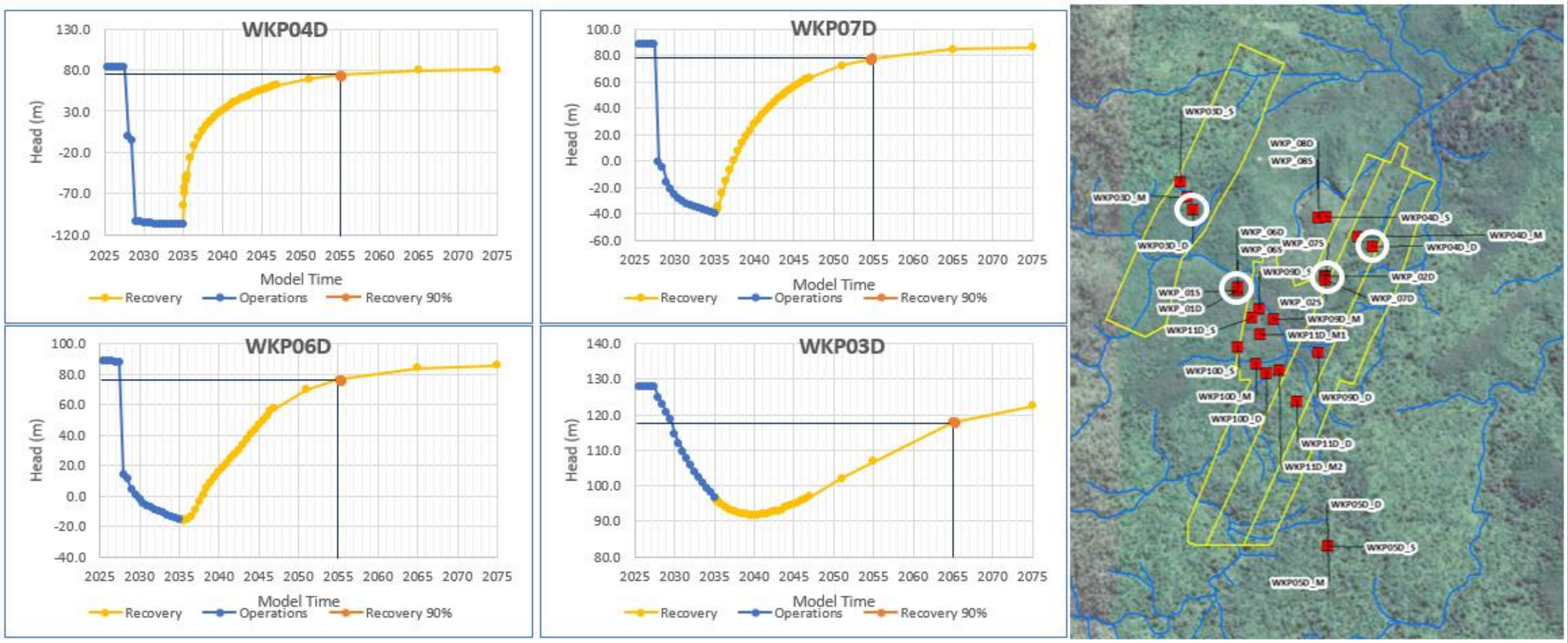


| | | |
|---|---|---|
| PROJECT NO. | 1022310402 | Mine Recovery - Heads |
| PROJECT NAME. | Hydrogeology Support for WUG | |
| DRAWING DATE | Aug-2023 | Client: OCEANAGOLD |
| AUTHORED | Andrea Santos | Figure |
| REVIEWED | Frederico Lemos | |
| APPROVED | John Fortuna | |

Figure 4.34: Water level recovery graphs (WKP09D, WKP11D, WKP08D, WKP05D)

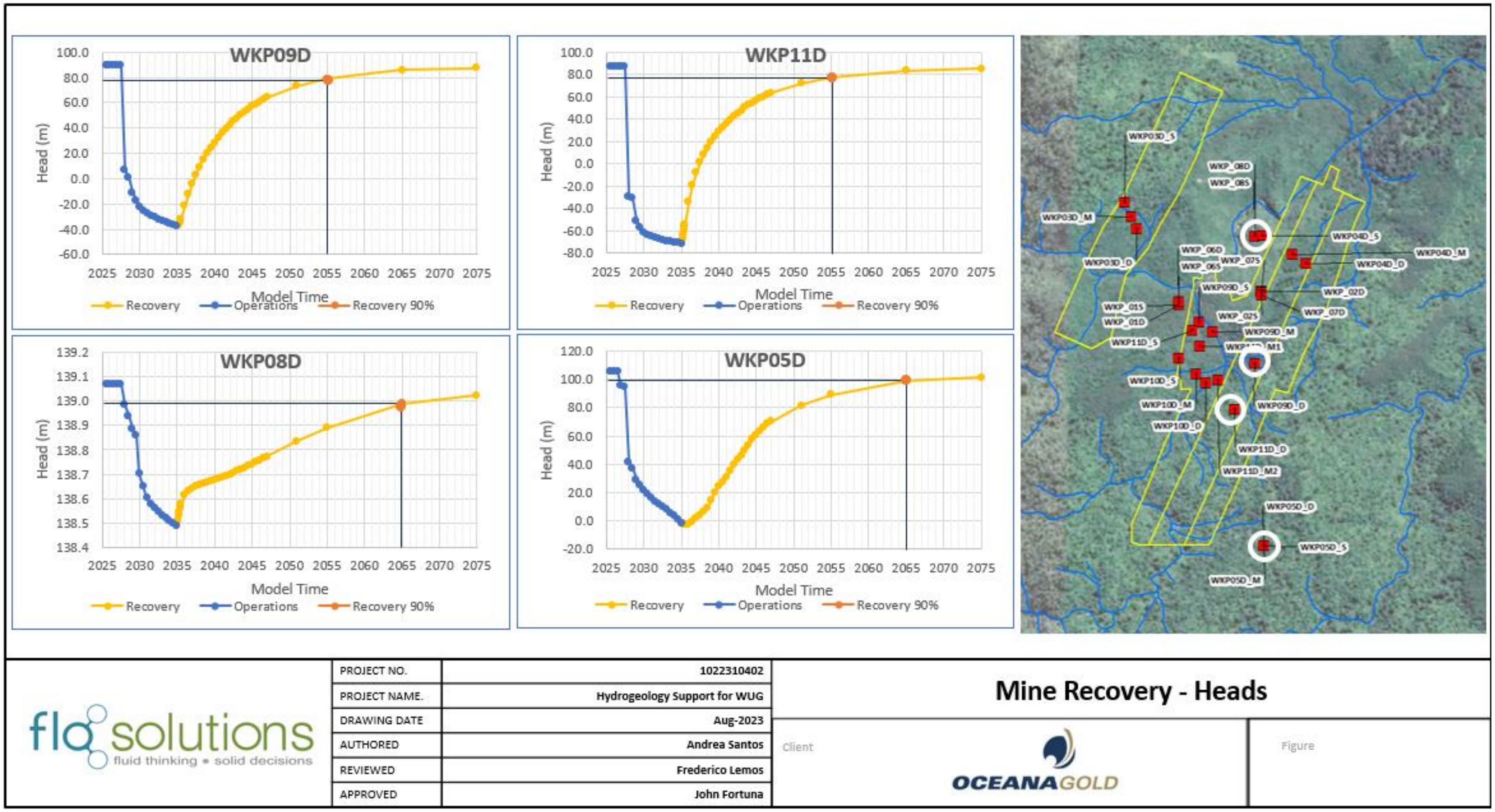

Figure 4.35: Baseflow recovery graphs (Lignite, Waiharakeke, Edmonds and Thompson)

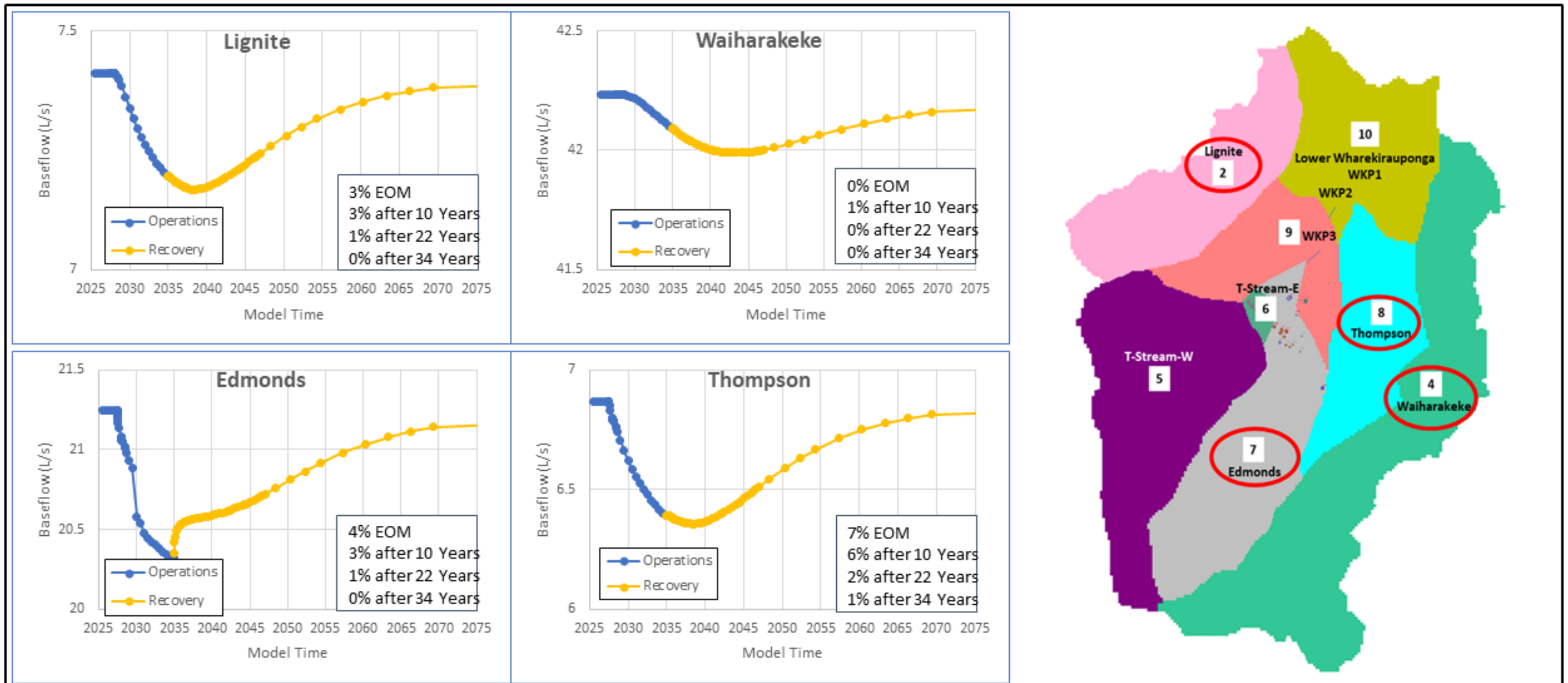


| | |
|---|---|
| PROJECT NO. | 1022310402 |
| PROJECT NAME. | Hydrogeology Support for WUG |
| DRAWING DATE | Aug-2023 |
| AUTHORED | Andrea Santos |
| REVIEWED | Frederico Lemos |
| APPROVED | John Fortuna |

**Mine Recovery - Baseflows**

Client

Figure

Figure 4.36: Baseflow recovery graphs (T-Stream E, T-Stream W, WKP3 and WKP2)

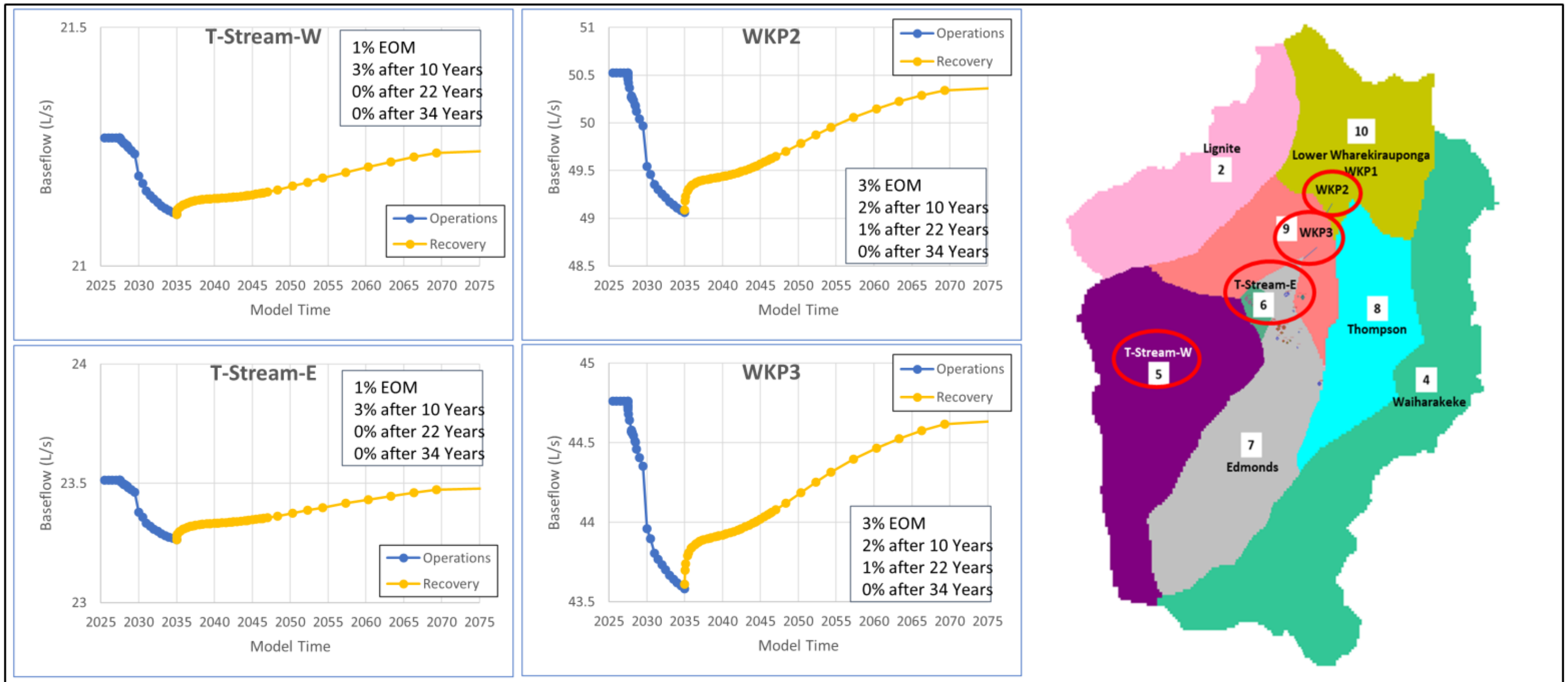


| PROJECT NO. | 1022310402 |
|---|---|
| PROJECT NAME. | Hydrogeology Support for WUG |
| DRAWING DATE | Aug-2023 |
| AUTHORED | Andrea Santos |
| REVIEWED | Frederico Lemos |
| APPROVED | John Fortuna |

flo solutions fluid thinking • solid decisions

**Mine Recovery - Baseflows**

Client OCEANAGOLD

Figure

Figure 4.37: Baseflow recovery graphs (Lower Wharekirauponga)

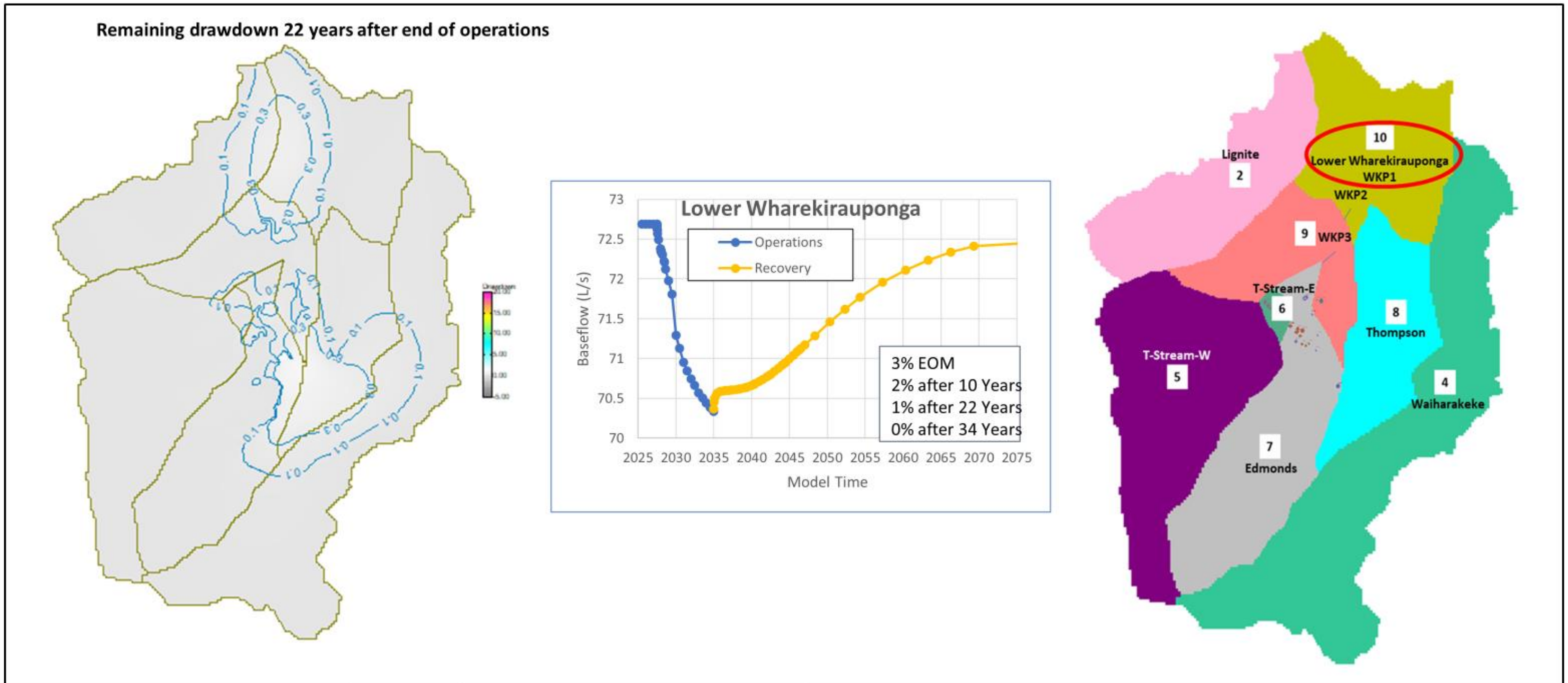


| | |
|---|---|
| PROJECT NO. | 1022310402 |
| PROJECT NAME. | Hydrogeology Support for WUG |
| DRAWING DATE | Aug-2023 |
| AUTHORED | Andrea Santos |
| REVIEWED | Frederico Lemos |
| APPROVED | John Fortuna |

fluid thinking • solid decisions

**Mine Recovery - Baseflows**

Client OCEANAGOLD

Figure

# 5. UNCERTAINTY ANALYSES

A limited Monte Carlo uncertainty analysis was conducted on the WUG numerical groundwater model. This uncertainty analysis is described in detail in Appendix F. In the WUG model, the uncertainty analysis was conducted on the hydraulic conductivity, which is assumed to be lognormally distributed. A second uncertainty analysis was conducted on the recharge rate, using the same hydraulic conductivity for each run, and assuming a normal distribution of the recharge rate. The results of the recharge uncertainty assessment are not shown in this report, as they resulted in calibration statistics and model predictions that were well within the range of outputs for the hydraulic conductivity assessment. Because the uncertainty in the hydraulic conductivity yielded a greater uncertainty range, only the hydraulic conductivity uncertainty analysis is presented here.

In order to facilitate the screening of the Latin Hypercube-derived simulations, the base case model was recalibrated to improve the steady state statistics. One key objective of the LHS uncertainty analysis was to identify any potential issues with the proposed mine design with respect to groundwater discharge to surface water flow (baseflow) in the project area. To this end, a more conservative base model was developed to better simulate shallow piezometric heads and with the intent not to underestimate potential impacts to project-area surface water. This model, called LH0 is described in Appendix F. Table 1.2 in Appendix F - indicates that the match to target baseflows is slightly better than the base case model.

Metrics were defined to evaluate the calibration resulting from the selected parameters and the model output using the selected parameters. The LH0 model was calibrated with a focus on the goodness-of-fit of the numerical groundwater model to the shallow piezometric head values at WKP_02D, WKP_02S, WKP03D_M, and WKP04D_S. So, the goodness-of-fit of the initial, pre-mining steady state heads at these points was given the highest priority in the LHS uncertainty analysis. Two key aspects of the transient calibration were evaluated. Specifically, the parameter combination was expected to simulate the minimal piezometric head fluctuations in the EG vein while also showing some response to hydraulic heads in the shallow piezometers.

In the predictive models, the uncertainty analysis was focused on the distribution of drawdown in Layer 1 of the model and the predicted changes in stream baseflow at the end of operations.

## 5.1 Model Settings

The parameter ranges for the LHS uncertainty analysis described here were derived from the LH0 model as a starting point. Thirty (30) equally likely parameter values were selected assuming a lognormal distribution. The LHS was repeated for the anisotropy ratio of the model hydraulic conductivity values, also assuming a lognormal distribution. In the case of the anisotropy ratio, the distribution was truncated with a lower value of one, so that the vertical hydraulic conductivity was always equal to or less than the horizontal hydraulic conductivity in the model.

The LHS parameter settings are illustrated in Figure 5.1. A table of values can be found in Appendix F. The parameters which had a significant influence on the goodness-of-fit of the model to the shallow heads, such as the upper EG Vein, the Alteration zone, the Weathered zone, and the North Edmonds Fault, have the lowest range of parameter values in the LHS. Hydraulic conductivity values outside of these relatively narrow ranges led to a significant deterioration in the calibration. Conversely, some parameter zones were not found to strongly influence the head in the shallow piezometers, including the T-stream vein, the EG-1 part of the EV-vein, and the South Edmonds fault. For these parameters, the range of simulated hydraulic conductivities spanned up to four orders of magnitude, as seen in Figure 5.1a.

A similar, but slightly different, trend can be seen in the anisotropy ratios (Figure 5.1b). For this parameter, the range of values was constrained by the initial value, with a higher range of anisotropy ratios generally applied in materials with a higher base anisotropy, and a smaller range applied to units that are generally isotropic. As mentioned above, the anisotropy ratio was truncated at a value of 1.

Figure 5.1: Hydraulic Conductivity Ranges in LHS Uncertainty Analysis.

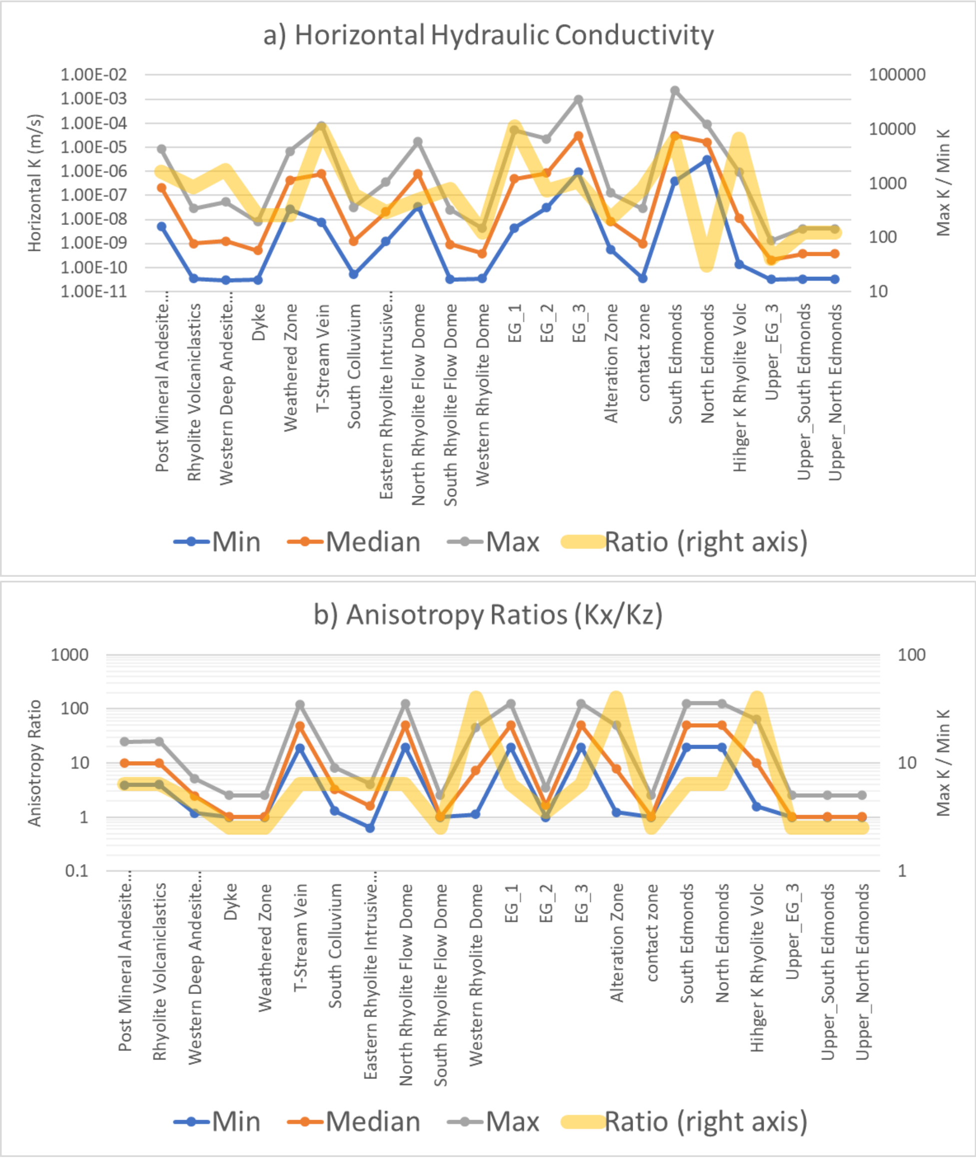


## 5.2 LH0 Scenario (LHS Base Case)

The LH0 calibration results are presented in Appendix F. In general, the LH0 calibration has a better fit to the shallow piezometric heads than the base case model and a higher degree of hydraulic connection between the shallow and deep aquifers than the base case model. The higher shallow-deep connection in the LH0 model results in a higher predicted zone of drawdown in Layer 1 of the model at the end of operations as well as a higher predicted reduction in baseflow at the end of operations (Figure 5.2).

Figure 5.2: Predicted End-of-Mine Drawdown and baseflow Reduction, LH0

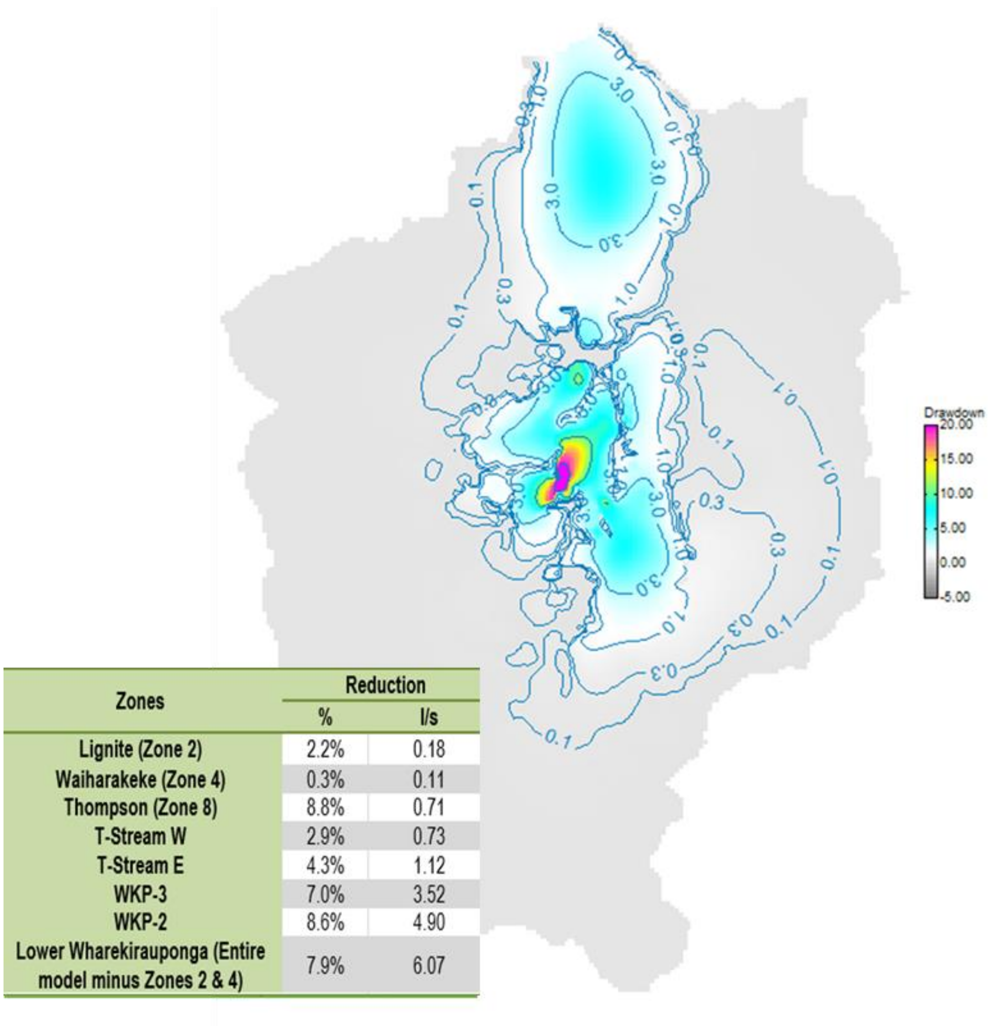


| Zones | Reduction | |
|---|---|---|
| | % | l/s |
| Lignite (Zone 2) | 2.2% | 0.18 |
| Waiharakeke (Zone 4) | 0.3% | 0.11 |
| Thompson (Zone 8) | 8.8% | 0.71 |
| T-Stream W | 2.9% | 0.73 |
| T-Stream E | 4.3% | 1.12 |
| WKP-3 | 7.0% | 3.52 |
| WKP-2 | 8.6% | 4.90 |
| Lower Wharekirauponga (Entire model minus Zones 2 & 4) | 7.9% | 6.07 |

## 5.3 LHS Calibration Summary

An attempt was made to use a broad range of parameter values to bracket the range of possible outputs. Nevertheless, as discussed in Appendix F, seven of the thirty realizations were excluded from further analysis because of high or low values of the hydraulic conductivity of the two most important units: Zone 5, the shallow weathered rock zone, and Zone 7, the alteration zone. This suggests that, despite their initially narrow ranges, the initial range of hydraulic conductivities of these two units was too broad.

A summary of the calibration output for the 23 final uncertainty analysis runs is shown in this section. Figure 5.3 summarizes the steady state calibration statistics. The normalized root mean squared error of the head calibration is in the range of 12% to 39%. The two runs with an NRMSE greater than 30% are S01 and S24, both of which overestimate the head in the model domain. The other outliers in terms of the simulated head are S14 and S15, which have low values of simulated head in the model domain. The simulated versus observed head data for the 23 runs plus LH0 are shown in Appendix F. The range of simulated baseflow values is shown in Figure 5.4. The lowest baseflow is simulated in model S20. The transient calibration output is presented in Appendix F.

Figure 5.3: Steady State Calibration Statistics, Final LHS Runs

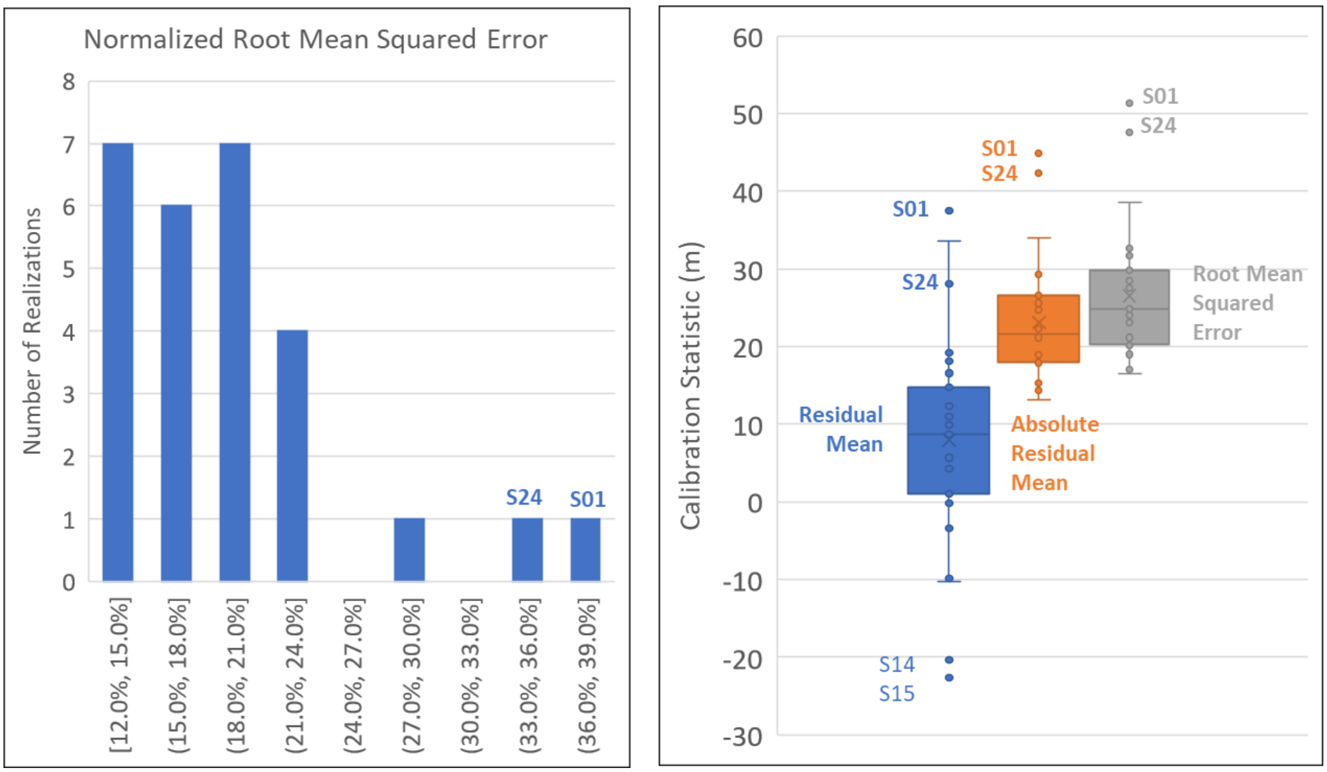

Figure 5.4: Simulated Pre-Mining Baseflow, Final LHS Runs

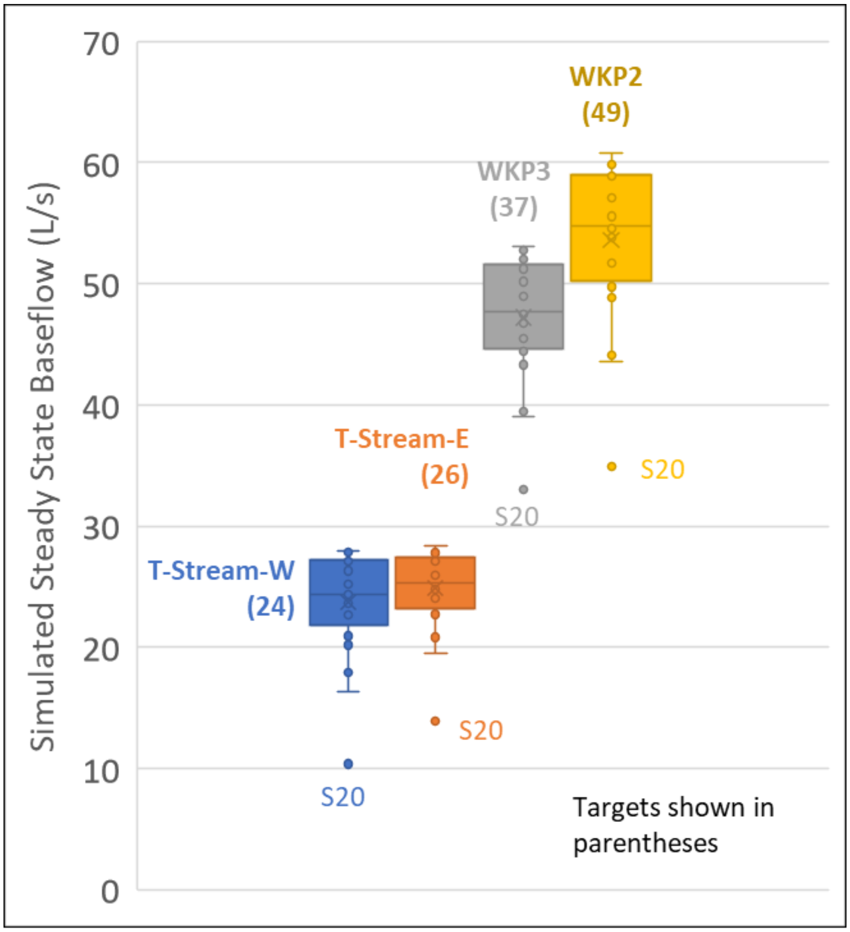


## 5.4 Mine Simulation

Using the 23 parameter sets described in the previous section, the mine predictions to the end of operations were carried out to determine a range of possible outcomes. Overall, the range of predicted mine-life-averaged mine inflows is 13 l/s to 89 L/s, with a median value of 45 L/s (see Appendix F).

The simulated drawdowns for the 23 uncertainty analysis runs are presented in Appendix G. The LHS parameter sets lead to some models with significantly lower drawdown than model LH0, such as S11, S15, S22 and S23. The LHS parameter sets also include models with significantly higher drawdown, such as models S17, S18, S24 and S25. As a result of the variable drawdowns and hydraulic conductivities, the uncertainty analysis yields a range of predicted baseflow reductions, as shown in Table 5.1.

Table 5.1: Summary of Baseflow Reduction Ranges from LHS Uncertainty Analysis.

| Catchment | Lower Quartile | Median | Upper Quartile |
|---|---|---|---|
| Lignite | 3% | 3% | 6% |
| Waiharakeke | 0% | 1% | 2% |
| T-Stream-W | 3% | 3% | 4% |
| T-Stream-E | 4% | 5% | 6% |
| Edmonds | 7% | 10% | 16% |
| Thompson | 6% | 11% | 25% |
| WKP3 | 6% | 7% | 12% |
| WKP2 | 7% | 9% | 14% |
| lower Wharekirauponga | 6% | 9% | 13% |

The majority of LHS parameter sets results in minimal impacts to the baseflow in the Lignite catchment. The outliers are S17 and S20 (see Appendix F). S17 has the highest hydraulic conductivity, 9.9e-4 m/s, in the deep EG vein (EG_3) as well as a high hydraulic conductivity of 2.7e-5 m/s in the North Edmonds fault. S20 has high hydraulic conductivities in the North Edmonds fault (2.1e-5 m/s) and the Weathered Zone (Zone 5), which has a value of 4.2e-6 m/s. In both models, the hydraulic separation between the shallow and deep aquifer systems is underestimated (see Appendix G). Generally small impacts are also predicted for Waiharakeke stream, except for S24, which has the one of the highest values of horizontal hydraulic conductivity (1.2e-7 m/s) for the East Rhyolite Flow Dome. Model S20 has a significantly lower initial baseflow than the other models, with rates that are approximately half of the baseflow target (see Figure 5.4). S24 is one of the two models with the highest steady state calibration error (see Figure 5.3). Therefore, the predictions from these two realizations are less likely than those of the other models.

The LHS uncertainty assessment predicts that Thompson Stream is likely to experience a median baseflow reduction of 11%, with higher reductions predicted in S30, which has the maximum value of hydraulic conductivity, 8.5e-6 m/s, in the post-mineral andesite that is present in this area, and in S24, which as mentioned above has a high hydraulic conductivity for the East Rhyolite Flow Dome. Details can be found in Appendix F.

The median predicted reduction in baseflow above T-Stream-West is 3%, with higher reductions predicted in S18, which has the highest hydraulic conductivity (1.7e-5 m/s) in the North Rhyolite Flow Dome, and in S20 and S24, described above. In T-Stream-East, the median predicted reduction in baseflow at T-Stream-East is 5%, with higher values in the same simulations that predict higher streamflow reductions in T-Stream-West.

Edmonds stream is predicted to experience higher baseflow reductions that T-Stream-West, with a median predicted reduction of 10% (Table 5.1). The primary reason for this is that the tunnel will be advanced in the lower parts of the Edmonds Stream catchment.

At WKP3 and WKP2, the median reduction in groundwater discharge to surface water is predicted to be 7% and 9%, respectively (Table 5.1). The outliers with high baseflow reductions are S20 and S18, discussed previously (also see Appendix F). In the “Lower Wharekirauponga” catchment, defined as the entire model domain minus the portions of the Lignite and Waiharakeke catchments that are within the model domain, the median predicted reduction in baseflow is 9%.

## 5.5 Discussion

A LHS abridged Monte Carlo uncertainty analysis was conducted for the WUG project using the zoned MODFLOW model. For this assessment, the numerical groundwater model was recalibrated to better match the shallow piezometric heads and to create a more conservative nominal model with respect to baseflow reductions. An initial set of 30 realizations was completed. Within that group, 23 realizations were selected to continue to prediction. The seven model runs that were not considered were excluded for the following reasons, which should inform future revisions of the numerical groundwater model. Seven runs were excluded because the hydraulic conductivity of the Weathered zone (Zone 5) and/or the alteration zone (Zone 15) were either too high or too low. These were:

- **S02** was excluded because it had the second lowest hydraulic conductivity (4.4e-8 m/s) for the Weathered rock zone. Similarly, **S14** did not converge because it had the lowest hydraulic conductivity (2.7e-8 m/s) for the Weathered rock zone. This resulted in ponded water at the surface of the numerical model domain in excess of 100 m of standing water and could not be used in the analysis.
- **S06** was excluded because it had excessively low initial baseflow values due to high values of hydraulic conductivity in the Weathered Zone (6.8e-6 m/s) and Alteration Zone (5.6e-8 m/s).
- **S04** was excluded because it had the lower-bound hydraulic conductivity (5.6e-10 m/s) for the alteration rock zone. This led to significant issues with shallow ponding, similar in form to **S02**.
- **S10** was excluded because the piezometric head in the shallow aquifer was approximately equal to that of the deep groundwater system. The reason for this is that the Weathered zone and the Alteration zone had approximately the same horizontal hydraulic conductivity, with values of 6.1e-8 m/s and 4.4e-8 m/s, respectively.
- Although not initially identified during the steady state calibration, **S13** and **S19** were also excluded from the assessment due to an overestimate of the drawdown in intermediate-depth groundwater. These two models had the highest and second highest value of hydraulic conductivity for the Alteration zone, with values of 7.7e-8 m/s and 1.2e-7 m/s, respectively.

With the remaining 23 simulations, ranges of baseflow reduction and drawdown were estimated. The results can be found in Appendices F and G. The uncertainty analysis realizations that predict the highest potential impact are those associated with higher hydraulic conductivities in these units:

- Post-Mineral Andesite
- East Rhyolite Flow Dome
- North Rhyolite Flow Dome
- North Edmonds Fault

The first three units—the post-mineral andesite, east rhyolite flow dome, and north rhyolite flow dome—are relatively poorly characterized units and have a relatively large range of hydraulic conductivity values in the LHS analysis (Figure 5.1). Improving our understanding of the hydraulic properties of these units would reduce the range of probable hydraulic conductivities and consequent impact predictions. Specifically,

- East Rhyolite Flow Dome: S24 has the highest hydraulic conductivity of this unit, with a value of 1.2e-7 m/s, among the 23 model runs. It also has poor steady state calibration statistics, and the upper bound hydraulic conductivity should be lower in future uncertainty assessments. A lower value of this parameter will reduce the maximum predicted impact on Thompson and Waiharakeke Streams
- Post-Mineral Andesite: S30 has the highest hydraulic conductivity of this unit and relatively poor steady state calibration statistics, particularly with respect to the shallow-deep separation (see Appendix F) The upper bound hydraulic conductivity should be lower in future uncertainty assessments.
- The North Rhyolite Flow Dome is in the immediate vicinity of the WUG project. The current upper bound hydraulic conductivity of this unit, used in S18, predicts high impacts to streams above the WUG project. If field data justify the change, the upper bound hydraulic conductivity should be lower than 1.7e-5 m/s in future uncertainty assessments.

In addition, higher values of the North Edmonds Fault hydraulic conductivity led to predictions of baseflow reductions in Lignite stream. This occurs especially in S17 and S20. S20 has an initial baseflow prediction that is approximately half of the baseflow target and is not a probable parameter set. The high impact predicted in S17 is due to a combination of a high North Edmonds Fault hydraulic conductivity and a high deep EG vein hydraulic conductivity. Understanding the extent and properties of the North Edmonds fault will reduce the range of uncertainty in the baseflow reduction predictions from the current values, shown in Table 5.1.

# 6. CONCLUSIONS

The current study assimilates numerous datasets collected during the characterization phase and improves understanding of the hydrogeologic system at WUG. Correspondingly, the model developed is utilized to demonstrate the need for additional information and further understanding of some hydrogeological characteristics.

Principal study findings based on modelling results are summarized below, while recommendations are presented in Section 7:

- The area where OGC intends to develop the underground mine development is in the Wharekirauponga Watershed, a high rainfall zone (2022: 3487 mm/yr – Waitekauri River Station), with a complex drainage system well developed and distributed in many tributaries feeding the main river channel – Wharekirauponga Stream)
- Flows in the principal stream (Wharekirauponga Stream) can vary substantially between different months and years depending on the amount of rainfall. Field information from WKP-01 located in the downstream of the Wharekirauponga Stream shows that in May 2020 river flows were ranging around 68 L/s and in August 2022 they were 669 L/s (almost 10 times greater than the minimum value).
- The geological setting is complex in terms of geological development and structural geology, especially due to the genesis of the geological terrain. The main area of the model is formed by a quartz vein system highly structured and fractured in the deeper portion – footwall, hosted by intrusive domes (North Rhyolite Flow Dome and Eastern Rhyolite Intrusive Dome). This whole core portion of the model is hosted by a greater zone defined as Rhyolite Volcaniclastics. The shallow portion of the geological model is formed by a Post Mineral Colluvium and a more recently interpreted weathered zone.
- Water level information is restricted to the mine area with a total of 25 points (5 pairs of double level standpipe piezometers and 5 groups of VWPs with 3 sensors each). Water levels indicate a shallow groundwater system highly responsive to rainfall / stream variations and a deep groundwater system ranging around elevation 110m that is generally not responsive to shallow variations.
- Radon water analysis had been carried out and reported by (GWS, 2021). The most comprehensive Radon sampling was completed in December 2020 and has shown that downstream of the Wharekirauponga catchment there are more groundwater inputs to surface water and more water mixing, also suggesting that groundwater plays an important role in river and creeks flows in this area.
- The shallow groundwater flow, estimated using measured water levels, indicates a flow direction from SW to NE, consistent with regional surface water drainage patterns. The shallow groundwater has piezometric elevations ranging from 200 to 150m in the mine domain. Deep groundwater levels are mostly restricted to the vein system and show a quite regular heads around 110 to 120 meters.
- Calculated recharge by WGS, 2021 estimates an average of 7% of the AAP as direct infiltration to the groundwater system. This estimation was further reviewed during model calibration under 8 different recharge zones with an average recharge of 21% of the AAP across the model domain.

- The groundwater numerical model was developed encompassing the main vein system in the central portion of the model domain and a total area of 22.1 $Km^2$. The model mesh was refined in the vein zone to better represent the vein system and the planned mine. In total the groundwater model contains 38 layers.
- Hydraulic conductivities had been defined initially from field testing and further adjusted during model calibration. Higher conductivity zones were associated to the vein system (9.1E-4 m/s) and less conductive zones were defined, such as the dike structure which intersects the zone between the T-Stream vein and EG-Vein (2.8E-10 m/s).
- The boundary conditions applied to the model were: no flow, recharge, river, general head and drains (this last BC to represent the underground mine plan). Adjustments on boundary conditions were also carried out during model calibration and further assessed during the sensitivity analysis.
- The steady-state model reached a calibration with an NRMSE of 17.3% with higher residuals in some shallow groundwater instruments (WKP-07S, WKP-02D and WKP-10S).
- The transient model simulates a period from Dec/2018 to April/2023 (53 stress steps). This period was selected considering the availability of groundwater levels from standpipe piezometers and some VWPs. This groundwater data was used to adjust the transient hydraulic parameters (specific storage and specific yield) since no field-derived parameters, such as from a pumping test, are available to be used.
- The mine simulation, as detailed in this report, has been completed using drains cells to represent the planned underground workings. Since the model mesh was initially developed with smaller cells in the mine domain, the discretization of the mine could also be better developed with a total of 4389 drains.
- The hydraulic conductivity used to compute the drain conductance was set equal to the hydraulic conductivity of the model grid cell (i.e., bedrock) in which the drain was contained.
- The findings of model simulation have been used and the starting point for the sensitivity analysis – which has been completed in 2 different parts (sensitivity for the steady state model and sensitivity for the simulation model).
- During the trial-and-error calibration, some geological units were found to be more sensitive to changes to the hydraulic conductivity when compared to others. The units found to be more sensitive in the model were: Rhyolite Volcaniclastics, Alteration Zone and Weathered Zone.
  - Sensitivity in the Rhyolite Volcaniclastics is the most relevant in terms of interactions with the EG-Vein since this unit hosts all rest of geological units, therefore any change in this unit also changes the way the model responds in terms of heads and fluxes.
- Most sensitive scenarios for the simulation analysis were:
  - Scenario SA12: Increasing the hydraulic conductivity of the alteration zone resulted in the highest baseflows reductions. Which suggests, once more, that the Alteration Zone plays an important role in limiting interactions between the deeper groundwater zone and shallow groundwater.

- Scenario SA2: Increase of Rhyolite Volcaniclastic K – Increasing the K of the Rhyolite Volcaniclastics also changes the way the shallow and deep groundwater system interacts, especially in the downstream area.
- Scenario SA4: Higher hydraulic conductivity when applied to the weathered zone makes this zone to be more influenced by recharge (absorbing more water) therefore reducing the impacts of baseflow reduction during mine simulation.
- Scenario SA11: When a lower K is applied to the alteration zone, lower impacts are observed to river and streams due to limitation of the interaction of deep groundwater with shallow groundwater.

- Post mining flow analysis was conducted to get a sense of main mine inflows and outflows after drain cells were deactivated, to calculate particle travel times and trajectories and to calculate recovery times of water heads after the mine galleries are shut down.
  - In terms of mine inflows, almost 90% of mine inflows will be derived from the EG-3 veins plus direct recharge + shallow rock infiltration. The largest inflows to the EG3 vein from a bedrock unit are from the east rhyolite intrusive dome (see Figure 4.28).
  - Mine outflows will mostly likely pass through the EG-3 (almost 75%).
  - Particle tracking assessment has shown that the vast majority of particles will be captured by the GHB boundary condition in the northern portion of the model area, indicating that the Edmonds Fault structure is the main responsible for conducting groundwater flow after mine operations are ceased.
  - Baseflows and water levels, in general, will recover an average of 90% of its initial conditions after 20 to 30 years after mine is deactivated.
- An abridged, Latin Hypercube sampling (LHS)-based uncertainty analysis was carried out. It corroborated the observation from the sensitivity analysis that the Weathered Zone and Alteration Zone are the most important parameters in determining the hydraulic (dis-)connection between shallow and deep groundwater systems. The LHS uncertainty analysis used a revised initial calibration, called LH0. This calibration has an NRMSE of 12.4%. The transient calibration of the LH0 model was different from the base case model and had a better fit in different piezometers than the base case model. The predicted impact to streams in the mine area is higher in the LH0 model than in the base case model.
- Using the LH0 model to define median values of the hydraulic conductivity and anisotropy ratio of the 23 hydrostratigraphic units in the model, a total of 30 uncertainty analysis realizations were completed, using lognormal distributions for these 46 parameters (23 horizontal hydraulic conductivity values and 23 anisotropy ratios). Of the 30 realizations, 23 were considered to have acceptable calibration statistics to carry forward to prediction.
- The 7 rejected realizations are characterised by values of the hydraulic conductivity of the Weathered Zone and/or Alteration Zone at either the upper or lower bound of the range used in the LHS run determination. Future modelling using the hydrostratigraphic units defined in the LHS uncertainty analysis should use revised ranges for these parameters.

- Within the 23 LHS realizations, the median reduction in baseflow to the key mine area streams is predicted to be: 3% at T-Stream-W, 5% at T-Stream-E, 7% at WKP3, and 9% at WKP2. Higher reductions, of 10% and 11%, respectively, are predicted for Edmonds and Thompson streams.
- The LHS analysis identified uncertainty in four key hydrostratigraphic model units. The Post-Mineral Andesite and East Rhyolite Flow Dome are located outside of the WUG area but have a potential influence on projected baseflow reductions in Thompson and Waiharakeke streams. The hydraulic conductivity of the North Rhyolite Flow Dome, and North Edmonds Fault have an influence on the drawdown in the mine area, and higher values of these parameters could lead to baseflow reductions outside of the immediate mine area.

# 7. RECOMMENDATIONS

Based on the current findings and simulations, the following points are recommended for a further improvement of the conceptual and numerical model:

- As described in this report, the interaction between rivers and the shallow groundwater system is still not fully understood. Available shallow groundwater levels show that fluctuations due to high rainfall events are common, but these fluctuations could only be simulated in the model with river variation rather than recharge variation.
    - A further assessment of river morphologies and variations (width and stages) would allow a better representation and discretization in the transient modelling.
    - Installation of additional near stream piezometers would also help to understand water levels along river margins and fluctuations.
- Rhyolite volcaniclastics is the most significant geological unit and one of the most sensitive to model parameter changes. Information received from OGC says that this unit had been used and a “background unit” when the geological model was expanded for hydrogeological modelling purposes. A further understanding of heterogeneity of this zone should also been completed:
    - Representing this zone as a unique Hydraulic Conductivity - K, Specific Storage - Ss and Specific Yield - Sy can lead to overestimating or underestimating of flows and drawdowns.
    - Alterations zones, if properly mapped and represented in the model, could add more heterogeneity to the system and better representation of flows and groundwater levels.
    - There are no transient hydraulic parameters for any geological unit at the site. Rhyolite volcaniclastics should be further assessed to define its real capacity in terms of Sy and Ss (a pumping test should be carried out in this zone).
- The approach of representing the vein system as a unique K zone is based on the water level data (quite regular and constant throughout the vein). Representing this unit as a unique K can lead (during the mine simulation) to a big sink for water, affecting the shallow groundwater system and overall water level reductions.
    - A pumping well should be placed (if possible) in the EG-Vein, and a pumping test conducted, to assess how the drawdown would propagate along the vein and in the surrounding units.
- The calibration of the shallow groundwater system has only been possible due to the representation of a weathered geological zone (briefly defined from core review and geophysics review) in addition to a clay alteration zone underneath. Representing these units in the model is relevant not only for shallow calibration but also for the assessment of impacts on the shallow groundwater system.
    - Additional field investigations (drilling) should be assessed geologically to map these two units (if possible, these zones should also be incorporated in the OGNZL geological model).
    - Shallow drillings outside the vein area should, whenever possible, be completed. Spatial distribution of core logs is a significant limitation of the current study.

- As observed from drawdown maps, the drawdown cone propagates along the Edmonds Fault. This structure was added to the model after a careful review of the GNS database, and, by placing a higher K structure connecting the vein system to the model limit in the northern / northeastern boundary, helped with the calibration of the deep groundwater levels, indicating that some regional feature should be present conceptually to help with the depressurization.
    - Further analysis of geological datasets to verify the existence of such structure should be completed.
- The LHS analysis identified uncertainty in four key hydrostratigraphic model units that have potential influence on projected baseflow reductions, as described above. Additional investigations in these units to characterize hydraulic properties would reduce model uncertainty and improve model predictive capabilities.

# 8. BIBLIOGRAPHY


/1/ Anderson, M. P., Woessner, W. W., & Hunt, R. J. (2015). *Applied Groundwater Modeling - Simulation of Flow and Advective Transport.* Philadelphia: Elsevier Inc.

/2/ Barnett, B., Townley, L. R., Post, V., Evans, R. E., Hunt, R. J., Peeters, L., . . . Boronkay, A. (2012). Australian groundwater modelling guidelines. *Waterlines report*.

/3/ Boffa Miskell. (2021). *Waihi Gold Underground Mine - Potentital Stream Effects.*

/4/ Doherty, J. E., & Hunt, R. J. (2010). *Approaches to Highly Parameterized Inversion: A Guide to Using PEST for Groundwater-Model Calibration.* Reston, VA: U.S. Geological Survey.

/5/ Domenico, P. a. (1965). *Water from low-permeability sediments and land subsidence.* Water Resources Research, vol. 1, no. 4., pp. 563-576.

/6/ Ebel, B. A., Mirus, B. B., Heppner, C. S., VanderKwaak, J. E., & Loague, K. (2009). *First-order exchange coefficient cou-pling for simulating surface water-groundwater interactions: Parameter sensitivity and consistency with a physics-based approach.* Hydrological Processes 23, no.13 - 1949-1959.

/7/ Environment Waikato . (2010). *Significant Natural Areas of the Hauraki District, Terrestrial and Wetland Ecosystems.*

/8/ Flipo, N. (2014). *Continental hydrosystem modelling: the concept of nested stream—aquifer interfaces.* Hydrology and Earth System Sciences,18.

/9/ FloSolutions. (2023). *1022310402-R-01 - Hydrogeological Conceptual Model Report.*

/10/ FloSolutions. (2023). *Clay Alteration Review and Rhyolite Volcaniclastics differentiation - 1022310402-TM-07.*

/11/ FloSolutions. (2023). *Site visit trip report - 1022310402-TM-10_REVB.*

/12/ Furman, A. (2008). *Modeling coupled surface-subsurface flow processes: A review.* Vadose Zone Journel 7, no 2: 741-756.

/13/ Goderniaux, P. (2009). *Large scale surface–subsurface hydrological model to assess climate change impacts on groundwater reserves.*

/14/ GWS. (2021). *Assessment of effects on Groundwater - Draft Report.*

/15/ Heath, R. (1983). *Basic ground-water hydrology.* U.S. Geological Survey Water-Supply Paper 2220, 86p.

/16/ Ling. (2003). *The Groundwater Regime of the Waihi Basin.*

/17/ McDonald, M. G., & Harbaugh, A. W. (1988). *A modular three-dimensional finite-difference ground-water flow model.* USGS.

/18/ MDBC. (2001). Groundwater flow modelling guideline. *Murray–Darling Basin Commission*.

/19/ Middlemis, H., & Peeters, L. (2018). *Information Guidelines Explanatory Note: Uncertainty analysis for groundwater modelling.*

/20/ Morris, D. a. (1967). *Summary of hydrologic and physical properties of rock and soil materials as analyzed by the Hydrologic Laboratory of the U.S. Geological Survey.* U.S. Geological Survey Water-Supply Paper 1839-D, 42p.

/21/ OceanaGold. (2020). *Waihi District Study, Preliminary Economic Assessment.* Waihi.

/22/ OceanaGold. (2021). *Waihi North Project, Project Description.* Waihi.

/23/ Panday, S., Langevin, C. D., Niswonger, R. G., Ibaraki, M., & Hughes, J. D. (2013). MODFLOW-USG version 1: An unstructured grid version of MODFLOW for simulating groundwater flow and tightly coupled processes using a control volume finite-difference formulation: U.S. Geological Survey Techniques and Methods.

/24/ Prickett, T. A. (1971). *Selected digital computer techniques for groundwater resource evaluation.*

/25/ Skinner, D. N. (1986). Neogene volcanism of the Hauraki volcanic region, in Smith, I.E.M. In V. 2. Late Cenozoic Volcanism in New Zealand. Royal Society of New Zealand Bulleting.

/26/ USGS. (1967). *Specific Yield: Compilation of Specific Yields for Various Materials.* doi:DOI: 10.3133/wsp1662d

/27/ Waihi Gold Company. (1985a). *Martha Hill Project: Environmental Impact Report - Waihi Gold Company.*

# Appendix A - Geological Layers - Modflow

## Appendix B - Transient Calibration – Hydrographs

## Appendix C - Mine Simulation – Hydrographs

## Appendix D - Sensitivity Analysis Results

## Appendix E - Particle Tracking - Spatial Analysis

## Appendix F - Latin Hypercube Method

## Appendix G - Latin Hypercube Results